
Southern Ocean and West Antarctic continental shelf biases and future projections in Global Climate Models

A thesis submitted to the School of Environmental Sciences of the University of East Anglia in partial fulfilment of the requirements for the degree of Doctor of Philosophy

Kyriaki M. Lekakou

September 2023

© This copy of the thesis has been supplied on condition that anyone who consults it is understood to recognise that its copyright rests with the author and that use of any information derived there-from must be in accordance with current UK Copyright Law. In addition, any quotation or extract must include full attribution.

Abstract

The proximity of the Antarctic Circumpolar Current to the West Antarctic continental shelf allows for warm water to intrude onto it, reach the base of the ice shelves and cause basal melt. Persistent biases in the Southern Ocean sea ice, circulation, temperature and salinity create uncertainty in our future projections of subsurface temperature on the West Antarctic continental shelf. The ability of climate models to represent Southern Ocean features realistically is crucial for increasing confidence in our future projections.

We assess 4 CMIP6 climate models with different horizontal resolution, from 1° to $1/12^\circ$, and found large differences in their ability to represent Southern Ocean characteristics. The $1/4^\circ$ model has large sea ice, circulation, temperature and salinity biases and a fresh and cold West Antarctic continental shelf with a westward slope current. A link between high sea ice melt rates in West Antarctica and subsurface freshening on the West Antarctic continental shelf is found. The best performing model in our study is the $1/12^\circ$ resolution model with minimal biases in the Southern Ocean. Future projections of subsurface temperature in the Amundsen Sea in the $1/12^\circ$ model demonstrate deep cooling by 2050. On the other hand, future projections of the $1/4^\circ$ model exhibit deep warming in the Amundsen Sea by the end of the century, similar to the 1° models.

Horizontal resolution plays an important role in representing circulation features, such as the slope current. Its presence is linked with changes in subsurface temperature and salinity on the West Antarctic continental shelf. It is possible that the West Antarctic continental shelf can shift from a warm state to a cold one and vice versa. Investigating the mechanisms behind these shifts is critical for future projections of subsurface temperature and ice shelf melt rates.

Access Condition and Agreement

Each deposit in UEA Digital Repository is protected by copyright and other intellectual property rights, and duplication or sale of all or part of any of the Data Collections is not permitted, except that material may be duplicated by you for your research use or for educational purposes in electronic or print form. You must obtain permission from the copyright holder, usually the author, for any other use. Exceptions only apply where a deposit may be explicitly provided under a stated licence, such as a Creative Commons licence or Open Government licence.

Electronic or print copies may not be offered, whether for sale or otherwise to anyone, unless explicitly stated under a Creative Commons or Open Government license. Unauthorised reproduction, editing or reformatting for resale purposes is explicitly prohibited (except where approved by the copyright holder themselves) and UEA reserves the right to take immediate 'take down' action on behalf of the copyright and/or rights holder if this Access condition of the UEA Digital Repository is breached. Any material in this database has been supplied on the understanding that it is copyright material and that no quotation from the material may be published without proper acknowledgement.

Contents

	1
1 Introduction	1
1.1 The role of the West Antarctic Ice Sheet in sea level rise	1
1.2 The Amundsen Sea	5
1.3 The Antarctic Slope Current	11
1.4 Climate Model Intercomparison Project	14
1.5 Biases in climate models and future projections	16
1.6 This thesis overview and aims	19
2 Performance and comparison of the UK family of climate models in the Southern Ocean	20
2.1 Introduction	20
2.2 Mean state of key Southern Ocean properties	24
2.3 Biases in HadGEM3-GC3.1-MM; from the Weddell to the Amund- sen Sea	31
2.4 Conclusions	40
3 In depth analysis of biases in the medium resolution HadGEM- GC3.1 model spin up run	43
3.1 Introduction	43
3.2 Biases evolution and methods	46

3.3	Bias development in early years and freshwater budget	52
3.4	Particle Tracking	59
3.5	Discussion and Conclusions	70
4	Future projections in West Antarctica using the high resolution model HadGEM-HH	72
4.1	Introduction	72
4.2	Changes on the West Antarctic continental shelf	74
4.3	Future projections from other UK climate models	82
4.4	Conclusions and discussion	85
5	Discussion and conclusions	88
5.1	Performance based evaluation and comparison of the 4 models . .	89
5.2	Biases, future projections and the importance of freshwater redistribution in a changing climate	92
5.3	Limitations and future work	97
5.4	Thesis summary	99

List of Figures

1.1	Changes in global mean sea level. (a) Reconstruction of sea-level from ice core oxygen isotope analysis for the last 800 kyr. (b) Reconstructions for the last 2500 years based upon a range of proxy sources with direct instrumental records superposed since the late 19th century. (c) Tide-gauge and, more latterly, altimeter-based estimates since 1850. (d) The most recent period of record from tide-gauge and altimeter-based records (IPCC, 2021).	3
1.2	Change in Antarctic ice-shelves thickness and volume from 1994 to 2012. Thickness change rate coloured from -25 to +10 meters per decade. Percentage of thickness lost (red circles) or gained (blue circles) over 18 years. Timeseries of average volume change (cubic kilometers) for the West (red) and East (blue) Antarctic ice shelves (bottom left) (Paolo et al., 2015).	6
1.3	Ensemble mean trends in horizontal advection of heat, relative to the surface freezing point; X and y components calculated separately using annual means and their magnitude is shaded in red. Vectors plotted where the magnitude exceeds 125 kW/m ² /century. Dotted blue line: 1000 m depth contour on the shelf break (Naughten et al., 2022).	7

1.4	Potential temperature, salinity, and geostrophic velocity sections for across-shelf transects (sections A–E). White contour on the temperature and salinity sections is the 28.00 kg m ⁻³ neutral density surface and on the velocity sections the zero velocity line (Walker et al., 2013)	10
1.5	ASC (red line) and uncertainty in the existence of ASC (red dashed line) (Thompson et al., 2018)	12
1.6	Schematic of water masses, along- and across-slope flows and supporting mechanisms in the (a) Fresh shelf, (b) Dense shelf and (c) Warm shelf in locations corresponding to each Antarctic Slope Current (ASC) regime: the eastern Weddell Sea, the western Weddell Sea and the Bellingshausen Sea. Water masses identified: Antarctic Surface Water (AASW), Circumpolar Deep Water (CDW), Dense Shelf Water (DSW) (Thompson et al., 2018).	13
2.1	Averaged percentage of sea ice concentration over 20 years (1995-2014) (a) NOAA NSIDC, (b) UKESM1, (c) HadGEM3-GC3.1-MM, (d) HadGEM3-GC3.1-LL, (e) HadGEM3-GC3.1-HH	25
2.2	Averaged surface temperature and salinity; (a),(b) UKESM1, (c),(d) HadGEM3-GC3.1-LL, (e),(f) HadGEM3-GC3.1-MM, (g),(h) HadGEM3-GC3.1-HH, (i),(j) WOA18	26
2.3	Averaged bottom temperature and salinity; (a),(b) UKESM1 (c),(d) HadGEM3-GC3.1-LL, (e),(f) HadGEM3-GC3.1-MM, (g),(h) WOA18. The ocean bottom is defined as the bottom-most ocean grid cell	27
2.4	(a) SOSE surface zonal velocity averaged over 2013-2019. Surface zonal velocity averaged over 20 years 1995-2014; (b) UKESM1, (c) HadGEM3-GC3.1-LL, (d) HadGEM3-GC3.1-LL, (e) HadGEM3-GC3.1-HH.	30

-
- 2.5 Averaged over 20 years (1995-2014) (a) cumulative sum of the meridional volume transport in the Weddell Sea (across the 69.61°S zonal section), (b) cumulative sum of the zonal volume transport in Drake Passage (c) annual cycle of the peak integrated meridional volume transport in the Weddell Sea; green line: HadGEM3-GC3.1-MM, blue line: HadGEM3-GC3.1-HH, red line: HadGEM3-GC3.1-LL, orange line: UKESM1, black line: SOSE. 32
- 2.6 September mixed layer depth in the Weddell Sea averaged over 20 years (1995-2014) (a) UKESM1, (b) HadGEM3-GC3.1-LL, (c) HadGEM3-GC3.1-MM, (d) HadGEM3-GC3.1-HH. White contour: sea ice concentration >15%. 33
- 2.7 HadGEM3-GC3.1-MM historical run timeseries of annual mean (a) sea ice area, (b) mixed layer depth and (c) northward volume transport in the Weddell Sea; (d) westward volume transport and (e) total volume transport at Drake Passage; (f) westward volume transport over the continental slope in the Amundsen Sea. 35
- 2.8 Meridional section at 109°W in the Amundsen Sea; x axis latitude; 20 year (1995-2014) averaged zonal velocity (a) SOSE, (b) UKESM1, (c) HadGEM3-GC3.1-LL, (d) HadGEM3-GC3.1-MM, (e) HadGEM3-GC3.1-HH. 36
- 2.9 Amundsen Sea 106° meridional section of 20 year averaged potential temperature (a) WOA18, (b) UKESM1, (c) HadGEM3-GC3.1-LL, (d) HadGEM3-GC3.1-MM, (e) HadGEM3-GC3.1-HH. 38
- 2.10 Timeseries of temperature (a) HadGEM3-GC3.1-LL, (b) UKESM1. White contour line is the 0° C isotherm. Inset map of the Amundsen Sea continental shelf showing the location of the selected grid cell with colour contoured bathymetry. 39

3.1	Subsurface maxima of annual mean temperature and salinity, over depth greater than 69 m, and sea ice concentration of (a),(b),(c) historical run, (d), (e), (f) first year of the spin up run, (g), (h), (i) 15th year of the spin up run, (j), (k), (l) last year of the spin up run. Black contour: 800 m isobath, white contour: annual mean sea ice 15% contour.	47
3.2	Spin up annual mean timeseries of (a) Weddell Sea sea ice concentration %, (b) Weddell Sea mixed layer depth, (c) Weddell Sea northward volume transport, (d) Drake Passage westward volume transport, (e) Drake Passage total volume transport, (f) Amundsen Sea continental shelf slope westward volume transport, (g) Amundsen Sea maximum temperature below 150m, (h) volume transport from the Bellingshausen Sea to the Amundsen Sea	49
3.3	Changes in (a) surface salinity, (b) temperature and (c) subsurface salinity form year 0 to year 3 of the spin up run.	53
3.4	Annual mean sea ice melt in the regions (a) East Bellingshausen Sea, (b) West Antarctic Peninsula, (c) Antarctic Peninsula tip, (d) Bellingshausen Sea; green dots represent 5 annual means from the HadGEM3-GC3.1-HH model historical run, red is their average; blue line is annual means from the spin up run of the HadGEM3-GC3.1-MM	54
3.5	Timeseries of freshwater budget calculated over the closed region between 70° S and the coast. Dark blue line is the rate of change of freshwater volume within the closed area; Light blue line is the total freshwater surface flux including ice shelf melt; Orange line is the meridional freshwater volume transport in the closed area; Green line is the calculated sum of total surface freshwater flux including ice shelf melt and the freshwater volume transport in the closed area.	55

3.6	Timeseries of freshwater budget calculated for the Bellingshausen Sea. (a) As Fig. 3.5 but red line is the total freshwater volume transport in the closed area, (b) as Fig. 3.5 but red line is the meridional freshwater volume transport and orange line is the zonal freshwater volume transport in the closed area.	56
3.7	Schematic of changes in the freshwater volume transport in and out of the Bellingshausen Sea. Green shaded area is the Bellingshausen Sea region mentioned in Fig. 3.6	57
3.8	Annual mean timeseries of westward freshwater volume transport (Sv) through a section between the Bellingshausen and Amundsen Sea (green section) from the coast to (a) the continental slope and (b) the continental shelf break; Green dots represent the same for 5 annual means from the HadGEM3-GC3.1-HH model historical run, red is their average	58
3.9	Weddell Sea particle release in location shaded green at the surface in (a) month 0. Snapshots of location and temperature of particles during (b) month 12, (c) month 24, (d) month 36, (e) month 48, (f) month 60	60
3.10	Temperature and position of particle released at the surface of the West Antarctic Peninsula (purple shaded area) during (a) month 12, (b) month 24, (c) month 36, (d) month 48. (e) Salinity during month 48, (f) depth during month 48.	62
3.11	(a) Bellingshausen Sea particle release in location shaded red at the surface in month 12, (b) position and temperature of the particles in month 0, (c) position and temperature of the particles in month 24, (d) position and salinity of the particles in month 24.	64
3.12	Amundsen Sea particle release in location shaded red at 300m depth (a) in month 48. Snapshots of position and temperature of the particles in (b) month 36, (c) month 24, (d) month 12, (e) month 0.	66

3.13	Amundsen Sea particle release in 2 location shaded in red at 300m depth (a), (b) in month 48 . Snapshots of position and temperature of the particles in (c), (d) month 36; (e), (f) month 24; (g), (h) month 12; (i), (j) month 0.	68
3.14	Amundsen Sea particle release in 2 location shaded in blue at 300m depth (a), (b) in month 48. Snapshots of position and depth of the particles in (c), (d) month 0.	69
4.1	(a),(b),(c) Maximum subsurface temperature , (d),(e),(f) maximum subsurface salinity, (g),(h),(i) sea ice concentration ; black contours indicate the 1000 m isobath; annual mean of the (a),(d),(g) beginning of the spin run, (b),(e),(h) middle of the spin run, (c),(f),(i) end of the spin run.	75
4.2	(a-c) Monthly mean temperature on the Amundsen Sea continental shelf under the SSP585 scenario; (d) difference of the central grid cell temperature between the SSP585 scenario and the equivalent years of the control run.	76
4.3	Monthly mean (a) temperature and (b) salinity on the Amundsen Sea continental shelf under the SSP585 scenario.	78
4.4	Timeseries of volume transport (Sv) in two cross sections on the Amundsen Sea continental slope.	79
4.5	(a) Timeseries of annual mean total volume transport in Drake Passage (Sv), (b) Cumulative sum of total volume transport in Drake Passage (Sv), blue: year 1, green: year 25, red: year 35.	81
4.6	Future projection of temperature on the Amundsen Sea continental shelf under the SSP585 scenario, years 2015-2100 (a) HadGEM-LL, (b) UKESM1, (c) HadGEM-MM.	84

Acknowledgements

I would like to thank the Amar-Franses & Foster-Jenkins trust whose funding supported me throughout my PhD journey. A specific thank you to Richard and Maureen for showing interest in my research and listening carefully when I was presenting my results.

A big thank you to all the researchers from the UK Met Office who exchanged dozens of emails with me, patiently and timely answering all my questions and providing access to data valuable for my research.

A huge thanks to my flatmates Simon and Ellie for not giving up on inviting me to join them to outdoorsy activities, even if I was refusing most of the times, because I was not used to the UK cold and rainy weather. I sincerely thank all of the friends I made during this journey. Nele, Rocio and Stephanos I would be a more miserable person if it was not for you! Of course a big thank you from the bottom of my heart to my partner Flavio for his support, listening to me talking for hours and providing structured and rational advice when I was too stressed. Another big thanks to the people I met during the FDSE 2022 summer school in Paris for being an amazing community of PhD students and make me feel understood.

Finally, the biggest thanks goes to my supervisors, Ben, Karen and Dave, that were present every week for our meetings, providing me with immensely valuable feedback. You were always understanding and encouraging me to go out of my comfort zone and try new things.

Chapter 1

Introduction

1.1 The role of the West Antarctic Ice Sheet in sea level rise

In response to climate change the Global Mean Sea Level (GMSL) has risen. Thermal expansion and the addition of melt water into the ocean, from melting glaciers and mass loss from the Greenland and Antarctic ice sheets, are two of the reasons why GMSL is rising. The magnitude of the sea level rise is not uniform across the globe. Areas with different elevation levels as well as on different latitudes and longitudes will be affected differently. For a lot of coastal regions sea level rise means more frequent and more destructive surge events. Sea level rise will most substantially affect low-lying coastal areas and a proportion of population may be forced to migrate.

The mean sea level during the Last Interglacial (130.000- 115.000 years ago) was

6- 9 metres higher than today, although polar temperatures were only slightly warmer compared to nowadays (DeConto and Pollard, 2016). In the IPCC (2013) report, is mentioned that the GMSL was 6.4 m higher than present, with a 95 % probability, 7.7 m higher with a 67 % probability and more than 8.8 m m higher with a 33 % probability. Another study estimates that the global mean sea level rise was at 5.5 to 9 m (Dutton and Lambeck, 2012). Regarding the more recent past, sea level rise rates for the last 50-100 years, range from 1 to 3 mm per year and uncertainties from 0.15 to 0.90 mm per year (Douglas, 1991). A more recent study suggested a rate of 1.2 mm per year between 1901 and 1990 and a rate of 3.0 ± 0.7 mm per year between 1993 and 2010 (Hay et al., 2015). Lastly, it is stated in the IPCC (2021) report that the 20th century GMSL rise was the fastest in at least 3000 years (Fig. 1.1)

At present, the role of Antarctica is adding a lot of uncertainty to future GMSL rise rates. It is highly likely that the values of sea level projections beyond the year 2100 systematically underestimate Antarctica's future contribution (Church et al., 2013). The largest uncertainty in sea-level projections of this century is the future evolution of the Antarctic Ice Sheet (Feldmann and Levermann, 2015). The West Antarctic Ice Sheet (WAIS) has been characterized as inherently unstable, mainly due to the fact that it is grounded below sea level, and has been described as responding drastically to climate warming (Hughes, 1973). These characteristics form the hypothesis of the marine ice sheet instability (MISI). The MISI hypothesis is suggests that there is the potential for substantial loss of ice-shelves where the bedrock is below sea level or deepening inland (Hanna et al., 2013). This rapid loss will result the grounding line to migrate inland. Because a large portion of the WAIS is grounded below sea level, and many ice sheets are

grounded on retrograde slopes the WAIS is getting a great deal of attention.

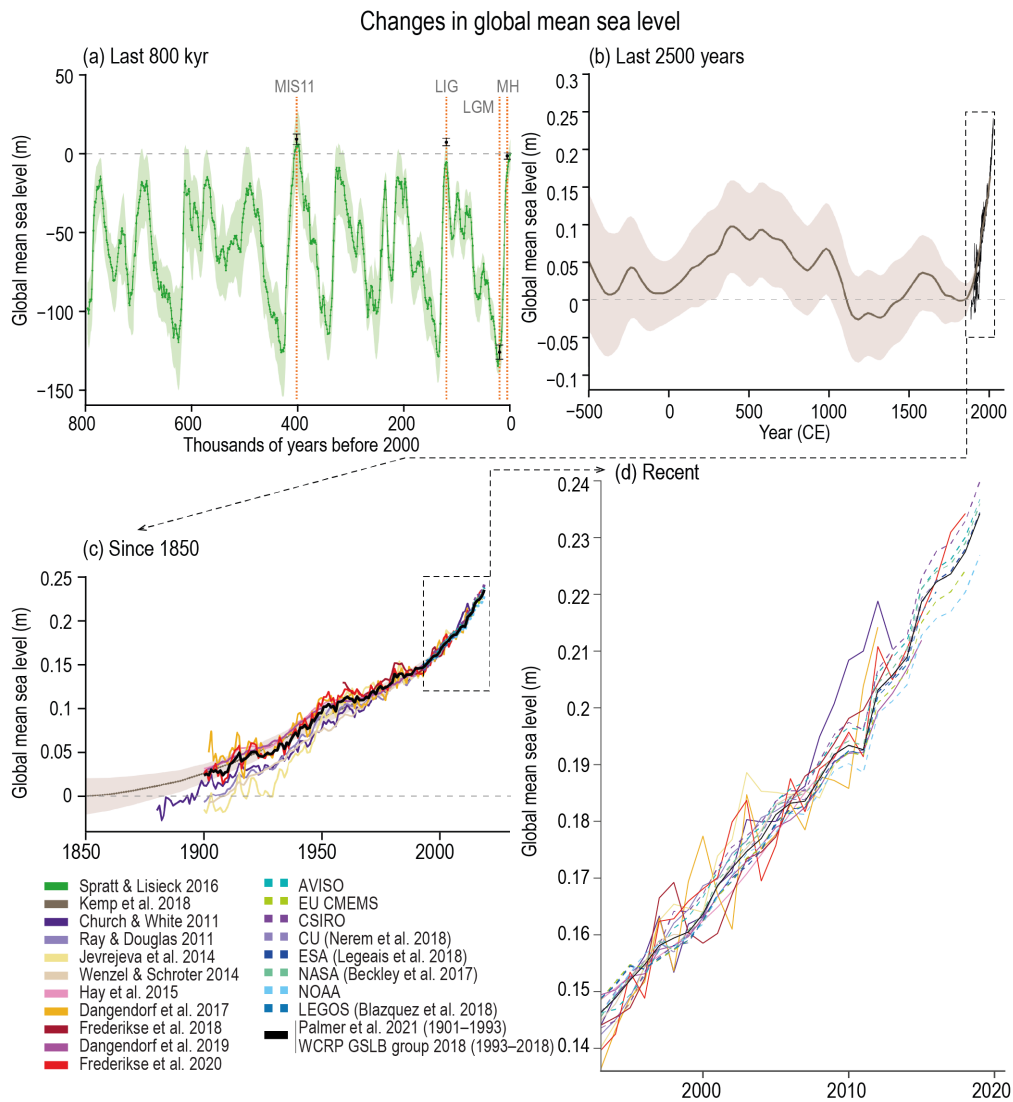


Figure 1.1: Changes in global mean sea level. (a) Reconstruction of sea-level from ice core oxygen isotope analysis for the last 800 kyr. (b) Reconstructions for the last 2500 years based upon a range of proxy sources with direct instrumental records superposed since the late 19th century. (c) Tide-gauge and, more latterly, altimeter-based estimates since 1850. (d) The most recent period of record from tide-gauge and altimeter-based records (IPCC, 2021).

There are a number of studies that estimate the potential GMSL rise from a collapse of the WAIS. The first one to raise the concern on a potential collapse of the

WAIS goes back to 1970s, when [Mercer \(1978\)](#) suggested that a rapid deglaciation of West Antarctica is possible and could lead to 5 m rise in sea level based on climate models calculations. Many years later, using all available data from Antarctica and integrated digital topographical models, the total contribution in sea level rise from the WAIS was calculated again at 5 m ([Lythe and Vaughan, 2001](#)). Taking into consideration the hypothesis of the marine ice sheet instability (MISI), but including only the areas where the bedrock is below sea level, a value of about 3.3 meters sea level rise contribution of the WAIS was obtained ([Bamber et al., 2009](#)).

Records of past WAIS states support the MISI hypothesis. Sediments collected from beneath the WAIS, contain direct evidence that the West Antarctic interior was ice-free, before and after the development of grounded ice sheets ([Scherer, 1991](#)). In addition to this, results from modelled WAIS growth and retreat, for the past 5 million years, show variations that range from present-like states to extension near the continental shelf break and dramatic retreats with only a few ice caps on the islands ([Pollard and DeConto, 2009](#)). From the same study derives an interesting result that is independent of the parameterized temporal variations in long-term forcing, result. Even with a smooth transition in forcing, the WAIS experiences rapid transitions, even in and out of collapse, including full glacial to modern-like ice extents.

We know that the WAIS has shrunk considerably, and sometimes completely collapsed in the past, but we lack the knowledge of precisely when it happened ([Joughin and Alley, 2011](#)) and under which atmospheric and oceanic conditions. [Mercer \(1968\)](#) introduces the idea that with no more than 7-10 °C higher than today's air temperature, the WAIS was completely disintegrated. Records show

that this happened at least once in the past, with evidence indicating a complete collapse of the WAIS in the Last Interglacial period (Mercer and Emiliani, 1970). It can also be speculated that the WAIS disintegration happened during a period when the global mean air temperature was less than 2 °C warmer than present-day conditions (Oppenheimer, 1998). A simulation of the Antarctic Ice Sheet during the last Interglacial indicates that the threshold for a total WAIS collapse is a rise in Southern Ocean's temperature of about 2-3 °C (Sutter et al., 2016). The same methodology was applied under extreme weather projections for the next couple of centuries, where a rise of 2-3 °C in Southern Ocean's temperature together with 6 °C rise in atmospheric temperature eventually lead to WAIS collapse (Oppenheimer, 1998).

A recent study by Golledge et al. (2015), that simulated the ice-sheet evolution, suggests that a sharp decline in the ice-shelves extent will eventually happen with a sustained 1.2 °C above present atmospheric temperature and 0.3 °C above present oceanic temperature. The same study suggests the complete disappearance of 80 - 85 % of the floating ice, if the atmospheric and oceanic temperature rise more than 2 °C and 0.5 °C respectively, compared to the present day. The long-term response to global warming depends on the individual ice shelves, but a rise in atmospheric temperature between 2 and 2.7 °C will probably trigger a WAIS response that will have an unstoppable contribution to sea level rise (Pattyn et al., 2018).

1.2 The Amundsen Sea

Based on observations, the Antarctic Ice Sheet lost approximately 40 Gt/y in 1979–1990 (West Antarctica was responsible for almost a quarter of this), while

the total mass loss for the period of 2009–2017 was 252 Gt/y (West Antarctica was responsible for more than half of this number), mainly at the Amundsen and Bellingshausen sea sections (Rignot et al., 2019). Overall, the average ice-shelf volume loss of West Antarctica has increased by 70 % during the last decade (Fig. 1.2) (Paolo et al., 2015). Ice sheets that rest on bedrock below sea level are sensitive to changes in their surrounding oceans and the loss of the ice shelves that buttress these ice sheets could impact sea level and large scale ocean circulation (Schoof, 2007)

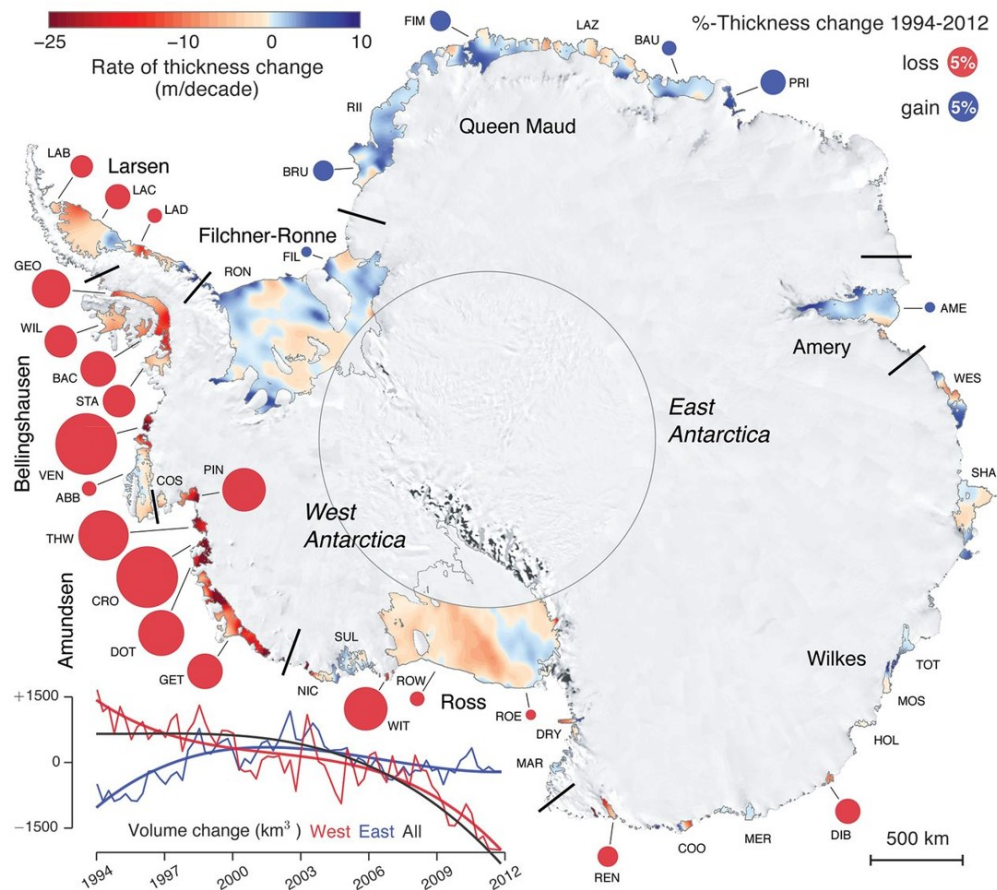


Figure 1.2: Change in Antarctic ice-shelves thickness and volume from 1994 to 2012. Thickness change rate coloured from -25 to +10 meters per decade. Percentage of thickness lost (red circles) or gained (blue circles) over 18 years. Timeseries of average volume change (cubic kilometers) for the West (red) and East (blue) Antarctic ice shelves (bottom left) (Paolo et al., 2015).

The regional thinning in AS cannot be explained just by negative surface mass balance, retreating ice-shelf fronts or by reduced glacier influx (Pritchard et al., 2012). We have to conclude that it is caused by increased basal melting from ocean interactions (Paolo et al., 2015; Pritchard et al., 2012). The greatest thinning is happening where warm water is able to flow towards the ice shelves through bathymetric troughs extending from the shelf break and onto the Amundsen Sea continental shelf and thus melts the ice shelves from below (Turner et al., 2017). The source of this relatively warm water has been identified as Circumpolar Deep Water (CDW), and once on the shelf, many refer to this as modified CDW.

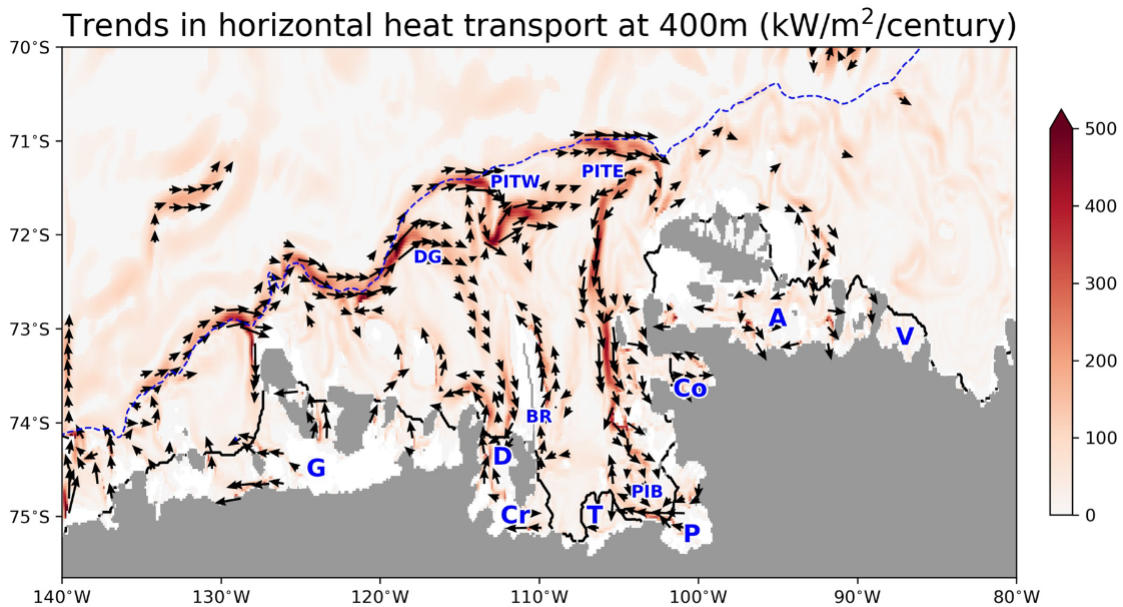


Figure 1.3: Ensemble mean trends in horizontal advection of heat, relative to the surface freezing point; X and y components calculated separately using annual means and their magnitude is shaded in red. Vectors plotted where the magnitude exceeds $125 \text{ kW/m}^2/\text{century}$. Dotted blue line: 1000 m depth contour on the shelf break (Naughten et al., 2022).

The Amundsen Sea continental shelf was relatively unexplored until the late 1980s, and the bathymetric data for a detailed regional map was not obtained until the

last couple of decades (Nitsche et al., 2007). The first oceanographic surveys did not happen until the 1990s. Deep troughs on the continental shelf are present and provide evidence that the ice shelf once extended across the continental shelf (Anderson et al., 2002). These deep troughs allow the deep warm water to penetrate across the shelf into the ice shelf cavities (Fig. 1.3). Relatively recent bathymetry representations (ETOPO2 (2001), BEDMAP (2001), ETOPO2v2 (2006)) did not include in detail or at all these deep troughs that facilitate warm CDW to enter beneath the Ice Shelves.

The three main water masses in the Amundsen Sea are Antarctic Surface Water, Winter Water and CDW. The CDW is a mixture of the world's deep waters and it is a component of the Antarctic Circumpolar Current (ACC) (Dinniman et al., 2012). In 1994, the vertical temperature profile of an oceanographic survey at the Pine Island Glacier calving front revealed a layer deeper than 600 with temperature above 1 °C and more than 2 °C warmer than at most other locations on the Antarctic continental shelf Jacobs et al. (1996). CDW is 3-4 °C warmer than the in situ freezing point (Jenkins et al., 2010), it dominates the Amundsen Sea continental shelf and it plays a key role in ocean driven melting (Walker et al., 2013). The relatively dense CDW is modified as it moves southwards and intrudes across the shelf break (Ribeiro et al., 2021). This modification is the result of mixing with the cooler Antarctic Surface Water once it has entered the continental shelf, resulting in a fresher and cooler water mass called modified CDW (mCDW) (Wåhlin et al., 2010). The mCDW is the warmest mass on the continental shelf since it originates from CDW mixed with shelf waters (Wang et al., 2023) with temperatures approximately 3 °C above freezing (Wåhlin et al., 2010). The processes that allow CDW to reach the continental shelf and the

current system on the continental slope are not yet fully understood but they are believed to be partially related to wind forcing, Ekman transport and a slope undercurrent (Heywood et al., 2016). A weakened front associated with a weak slope current could lead to subsurface warming (Spence et al., 2014).

A complete analysis of CTD data carried by Walker et al. (2013), suggests that the two ways the troughs promote the on shelf flow of CDW are by the deeper topography relative to the off-shelf thermocline and the interaction that the shelf-break currents have with the topography. These currents combine a barotropic and a baroclinic component; it is not clear which component is most important for the supply of heat onto the continental shelf. Webber et al. (2019) suggests that CDW and heat transport at the shelf break (ET) is predominantly barotropic, similar to Schodlok et al. (2012), while further south is baroclinic, and suggests that the split between baroclinic and barotropic temperature transport is sensitive to the choice of section. Both studies are referring to the Eastern Trough (ET) (Fig. 1.4).

The water properties over the shelf break and continental slope suggest that the currents associated with the sloping isopycnals surfaces have a significant baroclinic structure (Walker et al., 2013). By analysing CTD data from 5 different sections, Walker et al. (2013) present an upward slope of the isopycnals towards the south, below the level of the shelf break in most sections, that is associated with the shoaling of the temperature maximum. Above this layer there are downward sloping isopycnals related to the southward deepening of Winter Water. The result is a horizontal density gradient, that could be described as a weak Antarctic Slope Front (ASF) (Fig. 1.4). Underneath the surface westward flow there is an eastward undercurrent transports CDW that turns onto the shelf when it

encounters the continental slope.

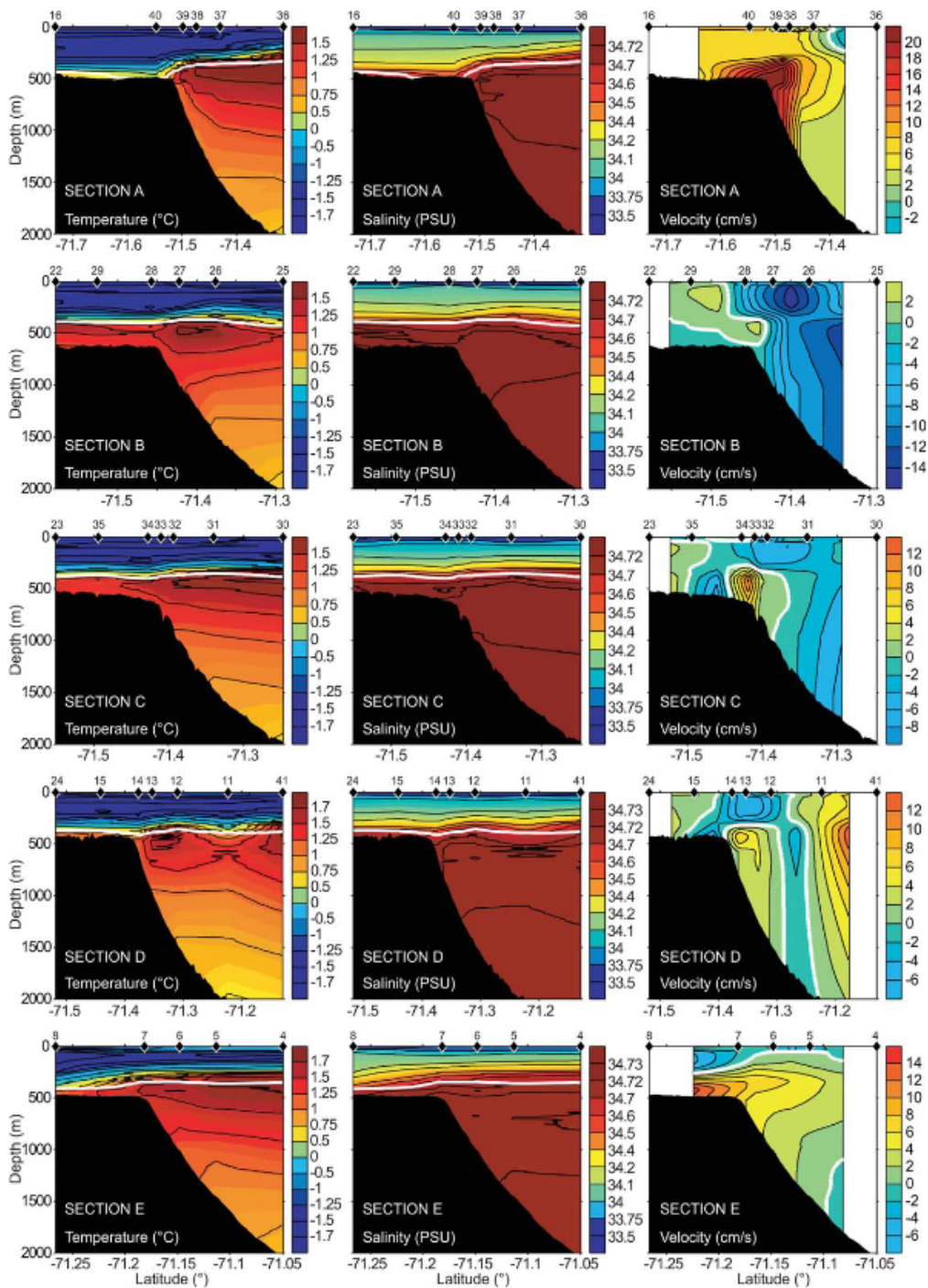


Figure 1.4: Potential temperature, salinity, and geostrophic velocity sections for across-shelf transects (sections A–E). White contour on the temperature and salinity sections is the 28.00 kg m⁻³ neutral density surface and on the velocity sections the zero velocity line (Walker et al., 2013)

The variability of the heat flux crossing the shelf break is difficult to estimate with current observations (Heywood et al., 2016). Overall there is a significant lack of observations and little is known about CDW spatial and temporal variability, especially seasonally (Mallett et al., 2018). Long term observations are required in order to distinguish trends with decadal variability of the CDW (Heywood et al., 2016). Moreover, there is the need for high grid resolution models if we want to represent sufficiently the ACC and the continental shelf break dynamics that are fundamental to the mechanism of subsurface ocean warming (Spence et al., 2014).

1.3 The Antarctic Slope Current

The Antarctic slope current is a westward and persistent circulation feature present around Antarctica, with the exclusion of West Antarctica where the ACC is dominant at the continental shelf break (Fig. 1.5) (Thompson et al., 2020). The slope front associated with the Antarctic slope current, is described as the deepening of the isopycnals on the continental slope and acts as a barrier for heat transport onto the continental shelf (Jacobs, 1991; Spence et al., 2014). That is why an absent or weakened Antarctic slope front could lead to subsurface warming on the continental shelf (Spence et al., 2014). Even though the Antarctic slope current plays a major and important role in regulating the flow of warm water towards the south, it is relatively understudied (Thompson et al., 2018).

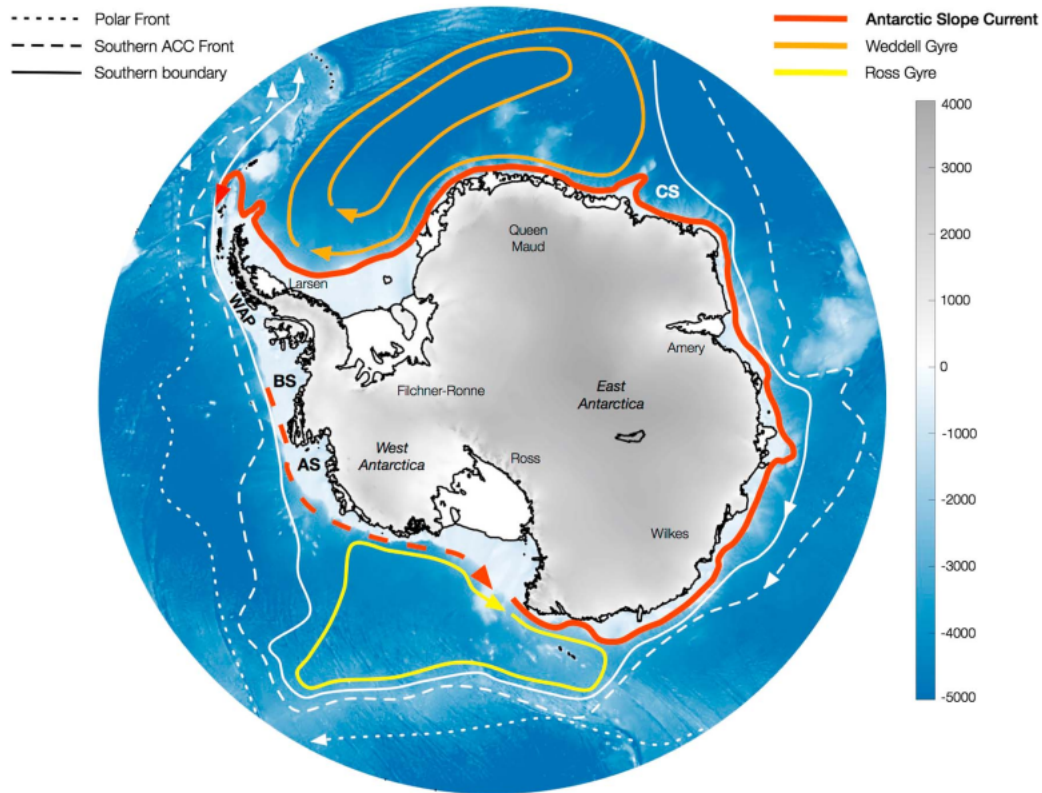


Figure 1.5: ASC (red line) and uncertainty in the existence of ASC (red dashed line) (Thompson et al., 2018)

In the Amundsen Sea some observations point to a westward slope current that is surface intensified, however an eastward undercurrent facilitates warm water intrusion southwards (Walker et al., 2013). Some observations at the Bellingshausen Sea shelf break support a westward flow (Zhang et al., 2016), however this flow has not been related to the Antarctic slope current (Thompson et al., 2020). A potential genesis of the Antarctic slope current in West Antarctica could change the large scale ocean circulation, and interrupt CDW intrusion on the West Antarctic continental shelf leading to dramatic changes (Thompson et al., 2020).

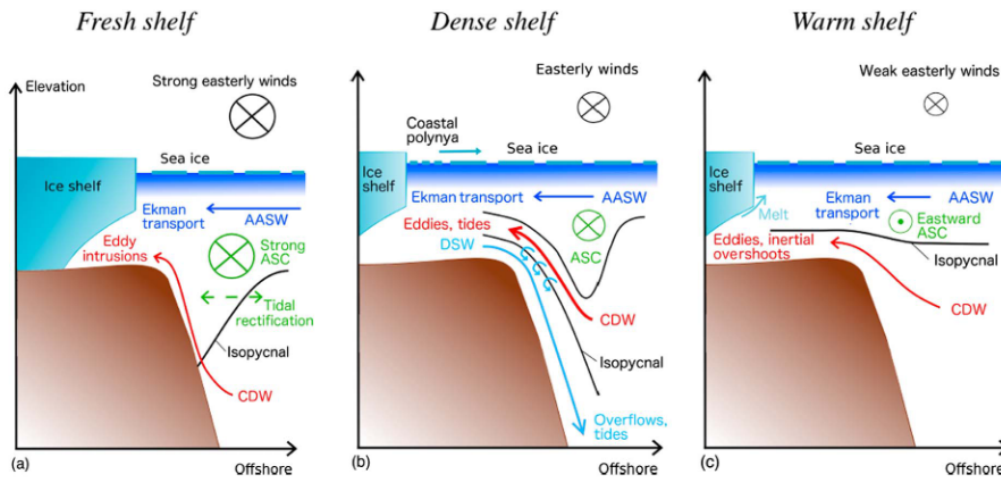


Figure 1.6: Schematic of water masses, along- and across-slope flows and supporting mechanisms in the (a) Fresh shelf, (b) Dense shelf and (c) Warm shelf in locations corresponding to each Antarctic Slope Current (ASC) regime: the eastern Weddell Sea, the western Weddell Sea and the Bellingshausen Sea. Water masses identified: Antarctic Surface Water (AASW), Circumpolar Deep Water (CDW), Dense Shelf Water (DSW) (Thompson et al., 2018).

In the Weddell Sea, dense shelf waters flow westward on the continental shelf break, tilts the warm water down and impacts the Antarctic slope current (Fig. 1.6) (Thompson et al., 2018). The Antarctic slope current mass transport there has been found to be mostly controlled by the strength of easterly winds (Mathiot et al., 2011; Núñez-Riboni and Fahrbach, 2009). However, while wind stress could be playing a major role in the strength of the Antarctic slope current, the formation of dense water and the resulting density contrast on the continental shelf break can be sensitive to the location and rate of sea ice production as well (Goddard et al., 2017). By extension, shelf freshening could further tilt the isopycnals and strengthen the Antarctic slope current. Large surface freshening anomalies can isolate heat offshore of the continental shelf (Goddard et al., 2017). Stewart et al. (2019) found that the circulation of the Antarctic Slope current is essentially dependent on sea ice and mesoscale eddies present over the continental slope.

The West Antarctic Peninsula extends from the eastern limit of the Bellingshausen Sea to the tip of the Antarctic Peninsula, a region where the ACC warm water and westward cold flows from the Weddell Sea meet (Moffat and Meredith, 2018). Observations from Drake Passage revealed an extension of the Antarctic slope current from the Weddell Sea (Meijers et al., 2016), however there is no evidence that it reaches the West Antarctic Peninsula slope in the South (Moffat and Meredith, 2018). Instead, on the central West Antarctic Peninsula slope there is northeast transport, related to the southern boundary of the ACC, and near the coast a fresh southwestward current, the Antarctic coastal current (Moffat and Meredith, 2018). The Antarctic coastal current is present during months with no sea ice and transports freshwater, but disappears when there is no freshwater input and sea ice presence (Moffat et al., 2008).

1.4 Climate Model Intercomparison Project

The Coupled Model Intercomparison Project (CMIP) is currently on its 6th phase (CMIP6). It is responsible for producing outputs from coupled global climate models with common sets of simulations, and it is the result of international collaboration. The Intergovernmental Panel on Climate Change (IPCC) assessments are taking into consideration CMIP output in order to produce reports that inform policy makers about the current and future state of our climate.

Different CMIP6 experiments include among others an initial climate spin up run, and after that a pre-industrial control simulation (piControl run), and a historical run (1850-2014) (Eyring et al., 2015). In this thesis we will use output from the historical run in order to assess the models ability to represent the present state of

the climate (Chapter 2) and the spin up run in order to investigate the origin of biases present (Chapter 3). Additionally, a new scenario framework, the Shared Socioeconomic Pathways (SSP), is part of CMIP6 and its role is to integrate future environmental changes. We will be using data from the SSP585 (Chapter 4) which represents a future with high emissions and radiative forcing similar to its predecessor RCP8.5 (Riahi et al., 2017).

A new feature applied in CMIP6 is the High Resolution Model Intercomparison Project (HighResMIP), which allows for the first time the systematic investigation of how the horizontal resolution of models impact their performance (Haarsma et al., 2016). Ocean horizontal resolutions as low as $1/4^\circ$ and higher are run until 2050, with a possible extension to 2100, with the goal to further understand the implications of systematic model biases (Haarsma et al., 2016).

Here we use the HadGEM3-GC3.1 family of models (Williams et al., 2018), consisting of 3 coupled models with an ocean horizontal resolution of 1° , $1/4^\circ$ and $1/12^\circ$, and the UKESM1 model (Sellar et al., 2019) with a 1° horizontal resolution. The UKESM1 is an earth system model and for its physical core the coupled climate model HadGEM3-GC3.1 is used (Sellar et al., 2019). All 4 models in our study have the same ocean component, Nucleus for European Modelling of the Ocean (NEMO), with a tripolar grid and 75 ocean levels (Roberts et al., 2019). One of our aims here is to investigate how these 4 models that belong to the same family perform in representing realistically the current state of the Southern Ocean (Chapter 2). It is argued that usually models are more accurate when they have higher horizontal resolutions and are eddy permitting ($1/4^\circ$ and higher) than the relatively lower resolution models that are eddy parameterised (1°) (Flato et al., 2014).

1.5 Biases in climate models and future projections

Warm SST biases in the Southern Ocean have been persistent throughout generations of CMIP models and are considered one of the most prominent biases in global models (Wang et al., 2014). These biases are very important because they negatively impact the reliability of model projections for future climate change (Kajtar et al., 2021), yet their origins are still controversial. One possible cause for warm SST bias in CMIP5 models has been found to be a weak Atlantic Meridional Overturning Circulation (AMOC) strength (Wang et al., 2014). However, this was contrasted by another study that found extremely weak correlation between the AMOC strength and SST biases (Hyder et al., 2018), and instead proposed that the warm SST bias in the Southern Ocean is caused by the overestimation of cloud-related shortwave radiation (Furtado and Field, 2017; Hyder et al., 2018). The warm SST bias in the Southern Ocean remains unchanged in the CMIP6 models (Wang et al., 2014), despite their higher horizontal resolution and better physical parameterizations (Eyring et al., 2016). Lastly, Luo et al. (2023) considered a remote factor, the warm bias in the North Atlantic deep ocean, to be responsible for the warm SST bias in the Southern Ocean. Another cause of the persistent warm SST bias in the Southern Ocean could be the coarse spatial resolution that leads to incorrect representation of the ocean eddy fluxes in the eddy-rich Southern Ocean Luo et al. (2023).

Antarctic sea ice can influence the Southern Ocean circulation (Pellichero et al., 2018) and the ice sheet response to the ocean (Massom et al., 2018). Biases in sea ice are extremely important because they can further influence biases in internal

ocean properties and circulation (Beadling et al., 2020). Despite the importance of sea ice, the IPCC report shows low confidence in sea ice projections in the Southern Ocean due to poor representation in key Southern Ocean properties (Meredith et al., 2019). Sea ice biases are large in CMIP6 and this has not improved since the previous phase (CMIP5) (Beadling et al., 2020; Shu et al., 2020). The majority of global coupled climate models have warm sea surface temperature biases that are connected with the sea ice biases (Hyder et al., 2018). Additionally, in the historical run, most CMIP models have negative sea ice trends (Roach et al., 2020) that do not reflect reality. Non eddy permitting horizontal resolution could be one of the causes of widespread sea ice biases (Roach et al., 2020).

The Antarctic circumpolar transport can be influenced by mesoscale eddies and internal mixing among other things (Beadling et al., 2020). It has been proven to be really challenging for global climate models to accurately represent the strength of the ACC (Beadling et al., 2019; Meijers et al., 2012). While its representation has been improved from CMIP3 to CMIP5 (Meijers et al., 2012) and the multi model mean has been reduced from CMIP5 to CMIP6, many CMIP6 models severely underestimate the strength of the ACC (Beadling et al., 2020). It is worth mentioning here that the weak representation in some CMIP6 models is related to an increase in ocean horizontal resolution, from 1° to $1/4^\circ$, since it is mostly the $1/4^\circ$ models that have weak transport, while the 1° versions of the same models perform better (Beadling et al., 2020). Adding to that, models with a horizontal resolution of $1/2^\circ$ and higher display westward flows in Drake Passage, much stronger than observed (Beadling et al., 2020).

Low resolution models cannot resolve eddies that are responsible for controlling warm water intrusion onto the continental shelf (Dinniman et al., 2016). A key

element to future uncertainty about ice shelf melt rates is whether the horizontal resolution of a model allows it to resolve the Antarctic slope current (Beadling et al., 2022). Changes in the ACC strength under a changing climate will also be influenced by models horizontal resolution (Hewitt et al., 2020). Models with horizontal resolution between 10-100km, like $1/4^\circ$ models, are eddy permitting because mesoscale eddies are present, however the dynamics are not resolved well (Chen et al., 2018). These models are 'awkward' in their ability to realistically represent eddies in high latitudes (Held et al., 2019), and there is plenty of room for improvement (Adcroft et al., 2019). Studying the emerging biases in these models can provide a more holistic understanding of the current and future state of the performance of models.

While many of the global climate models still have biases in Southern Ocean circulation features, the topic of increased freshwater in Antarctica and its impact on circulation is very relevant today. It might already be contributing to observed changes in salinity and temperature (Bronseleer et al., 2020). However, models' predictions are divided on the impact of freshwater input on subsurface temperature and salinity on the West Antarctic continental shelf. Eddy permitting models suggest that freshwater input eventually leads to subsurface freshening and cooling of the West Antarctic continental shelf, with a westward slope current present (Beadling et al., 2022; Moorman et al., 2020). Studies using low resolution models point to a subsurface warming response (Bintanja et al., 2013; Bronseleer et al., 2018), even though one recent study using a low resolution model found subsurface cooling and freshening as a response to freshwater forcing (Thomas et al., 2023). This division in models' responses creates large uncertainties in our understanding of the future basal melt rates.

1.6 This thesis overview and aims

Most global climate models struggle to realistically represent key Southern Ocean features such as sea ice concentration and circulation, as well as surface and sub-surface temperature and salinity in regions where ice shelves that are sensitive to changes in the ocean are present. This adds to the uncertainty of our future projections of ice shelf basal melt in a changing climate. A goal of this thesis is to investigate differences between 4 climate models that share the same physical components and differ in ocean horizontal resolution, from 1° to $1/12^\circ$, and evaluate their historical performance and differences (Chapter 2). Biases found in one of the models, the $1/4^\circ$ resolution model, are further investigated in order to establish their time evolution and assess how they are related to each other (Chapter 3). In addition to that, we use a particle tracking software with the aim of understanding the redistribution of large freshwater anomalies on the West Antarctic continental shelf in an eddy permitting model (Chapter 3). Lastly, we are showing future projections in West Antarctica and the Weddell Sea in the best performing model in our study, and discuss how they are different from the projections of the rest of the models here and which new uncertainties arise from them (Chapter 4).

Chapter 2

Performance and comparison of the UK family of climate models in the Southern Ocean

2.1 Introduction

In order to understand ocean-driven Antarctic ice shelf melt and its future projections, models need to represent the Southern Ocean sea ice, SST, mixed layer depth and circulation as realistically as possible and in line with our current understanding. Historically, coupled global climate models are often in disagreement when it comes to representing the key Southern Ocean processes and properties (Beadling et al., 2019; Heuzé et al., 2013; Hyder et al., 2018; Russell et al., 2018). This disagreement causes us to have low confidence in the future projections of the models.

Deficiencies in cloud processes can lead to warm SST biases (Hyder et al., 2018; Meijers, 2014; Sallée et al., 2013). These SST biases in return can be linked to a number of other biases in the Southern Ocean. An example of these biases is the sea ice. The sea ice extent intermodel spread in CMIP6 models has been reduced in comparison to the CMIP5 models, but the biases remain large and poorly represented (Shu et al., 2020). Antarctic sea ice biases are a persistent issue within coupled global climate models and they contribute a lot to our uncertainty in the Southern Ocean. These biases usually are linked to other important biases such as temperature, salinity and geostrophic circulation in the Southern Ocean, but it is challenging to determine the causal links between biases and identify the root causes (Beadling et al., 2020).

Temperature, salinity and circulation biases are also persistent in CMIP6 models. There has been no improvement to the upper ocean's fresh and warm biases, and while the strength of the ACC has been improved, there are still many models that simulate an ACC transport that is too weak (Beadling et al., 2020). Another circulation feature that has been challenging to model until recently, due to the coarse resolution of global climate models, is the Antarctic Slope Current (Dinniman et al., 2016). The ASC so far is relatively understudied compared with the ACC, but has the capacity to change continental shelf waters with its presence or absence and strength, and has a density structure that can potentially be remotely influenced (Thompson et al., 2018).

In this chapter we assess the UK family of climate models (Table 2.1) based on their performance and ability to realistically capture Southern Ocean features. Even though these models use the same atmospheric and oceanic components with the primary difference being the horizontal resolution, they do exhibit large

contrasts between them. Our selection of 4 models allows us to have a variety of different horizontal resolutions. The most common horizontal resolution in CMIP5 and CMIP6 is 1° . In the latest phase CMIP6 we are seeing an increasing number of $1/4^\circ$ models that are considered eddy permitting, so we would expect them to be able to represent circulation features such as the ASC with better fidelity. Lastly, the high resolution $1/12^\circ$ model in our study has the highest resolution among CMIP6 models and it is considered an eddy rich model.

The key differences between the low resolution models and the medium and high resolution models are the deactivation of the ocean eddy flux parameterisation (Gent and McWilliams, 1990) and the reduction of explicit dissipation parameters (Roberts et al., 2019). Moreover, the snow on sea ice albedo is lower in the low resolution model (Kuhlbrodt et al., 2018). We will explore how these differences in resolution and eddy parameterisation are expressed in the historical run of each model and how the differences between the models influence the representation of CDW intrusion on the West Antarctic continental shelf. This chapter will provide the background for the next two chapters that will focus on bias development in the spin up run and future projections.

Model	Ocean resolution	Atmospheric resolution	References
UKESM1-0-LL	100km (1°)	250km	(Sellar et al., 2019)
HadGEM3-GC31-LL	100km (1°)	250km	(Roberts et al., 2019)
HadGEM3-GC31-MM	25km ($1/4^\circ$)	100km	(Roberts et al., 2019)
HadGEM3-GC31-HH	8km ($1/12^\circ$)	50km	(Roberts et al., 2019)

Table 2.1: The 4 CMIP6 models used in this study; ocean resolution; atmospheric resolution; references. The vertical ocean resolution is 75 levels in all 4 models.

We have used monthly and annual mean data output from the first available en-

semble member of each model. A caveat to this is the different internal variability between ensemble members. Further discussion on that can be found at the conclusions section of this chapter. We used data from the World Ocean Atlas 2018 (WOA18) observational climatology ([Locarnini et al., 2018](#)) in order to compare the models temperature and salinity with. For the sea ice concentration we used historical data from the National Snow and Ice Data Center (NSIDC).

The C-gridded dataset at $1/6^\circ$ horizontal resolution Southern Ocean State Estimate (SOSE) was used for the velocity comparison. It has 42 depth levels and uses the K-Profile Parameterization (KPP). In situ measurements include those available from the National Oceanographic Data Center (NODC) which included shipboard CTD measurements, instrument-mounted elephant seal profiles (MEOP) and Argo float profiles. Process study field program data was also used and included measurements from the Diapycnal and Isopycnal Mixing Experiment in the Southern Ocean (DIMES), a mooring array in Drake Passage from the cDrake program, and shipboard and mooring data in the Amundsen Sea from the Oden expeditions. Satellite measurements included sea surface height measurements obtained from the Radar Altimetry Database System (RADS) and sea ice concentrations from the National Snow and Ice Data Center. The velocity structure in Drake Passage is compared to observations in [Firing et al. \(2011\)](#).

SOSE is an eddy-permitting Southern Ocean state estimate, constructed using the machinery developed by the consortium for Estimating the Circulation and Climate of the Ocean (ECCO) [Mazloff et al. \(2010\)](#). The basic ECCO Global Ocean Data Assimilation Experiment (ECCO-GODAE) approach is described in ([Wunsch and Heimbach, 2007](#)) and involves obtaining a least squares fit of an oceanic GCM to the majority of ocean observations, over a finite time interval

[Mazloff et al. \(2010\)](#). The end goal of SOSE is a time-evolving exact solution to the known equations of the GCM that are simultaneously consistent with the observations [Mazloff et al. \(2010\)](#). SOSE is most reliable in regions and for variables with good observational coverage, and more uncertain in regions and for variables with fewer observational constraints. SOSE has some inconsistencies with the observations, however a mean bias is not present in the Antarctic Circumpolar Current, which is the main reason it has been used in this study.

2.2 Mean state of key Southern Ocean properties

The models sea ice concentration has been averaged over the last 2 decades of the historical run (1995-2014) and compared with the equivalent 20-year averaged data from NSIDC (Fig. 2.1) in order to assess the models' present day representation of sea ice in the Southern Ocean (Fig. 2). The high resolution model (Fig. 2.1e) shows a realistic concentration throughout the whole Southern Ocean, with slightly less sea ice over the West Antarctic continental shelf, but it is performing the best out of all 4 models. It is followed by the two low resolution models (Fig. 2.1b,c), UKESM and HadGEM-LL respectively. Comparing the two low resolution models with each other, the low resolution HadGEM3 has less sea ice in West Antarctica and east of the Weddell Sea. However, they both perform relatively well considering the performance of other CMIP6 low resolution models ([Beadling et al., 2020](#)). The medium resolution model exhibits a large sea ice bias in the East Antarctic sector and the Weddell Sea, where there is no sea ice formation at all and most of the sea ice is concentrated above the Weddell Sea continental shelf (Fig. 2.1d).

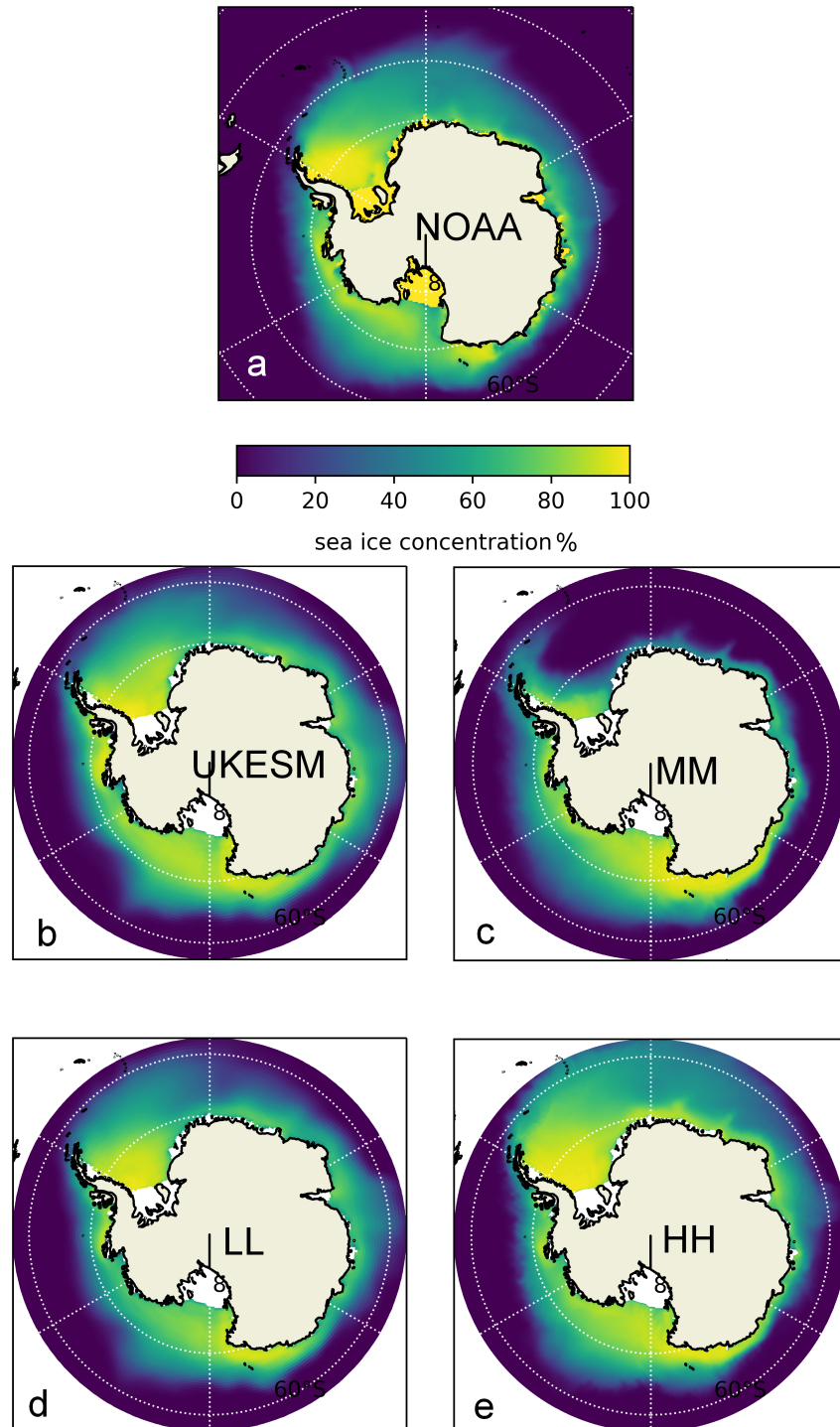


Figure 2.1: Averaged percentage of sea ice concentration over 20 years (1995-2014) (a) NOAA NSIDC, (b) UKESM1, (c) HadGEM3-GC3.1-MM, (d) HadGEM3-GC3.1-LL, (e) HadGEM3-GC3.1-HH

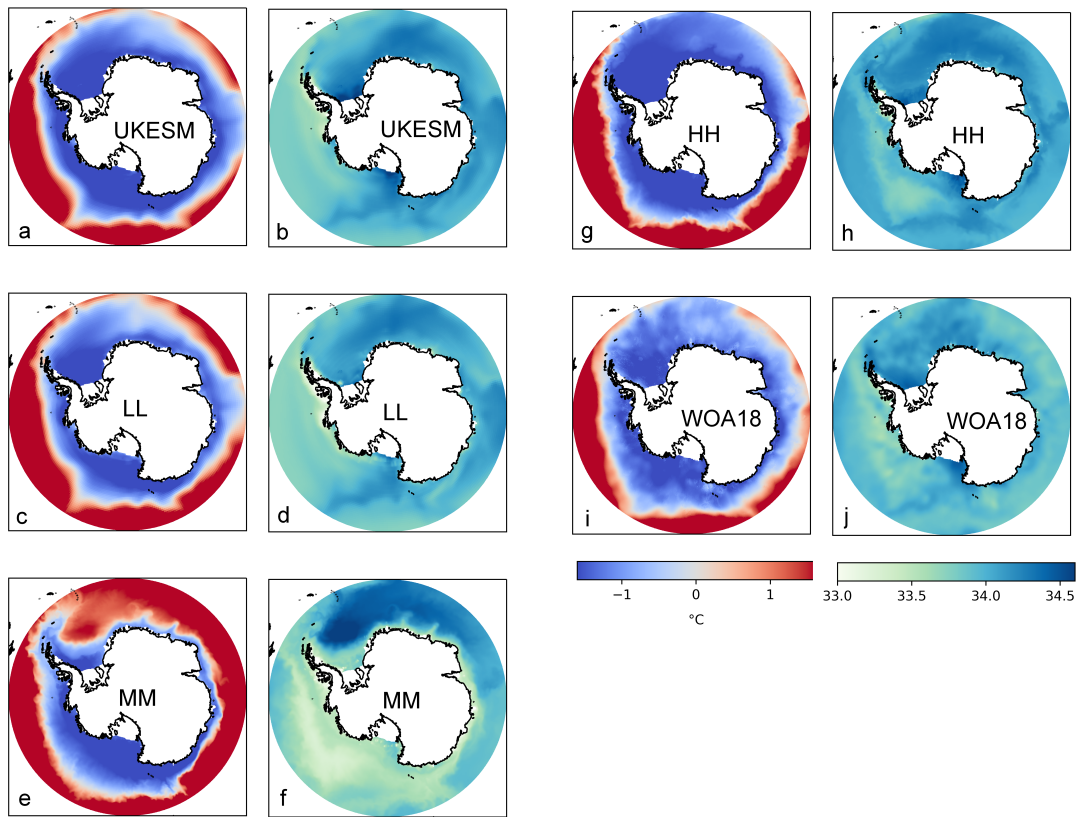


Figure 2.2: Averaged surface temperature and salinity; (a),(b) UKESM1, (c),(d) HadGEM3-GC3.1-LL, (e),(f) HadGEM3-GC3.1-MM, (g),(h) HadGEM3-GC3.1-HH, (i),(j) WOA18

The sea surface temperatures of the medium resolution model (HadGEM3-MM; Fig. 2.2e) are considerably warmer than the observations (WOA18; Fig. 2.2i) in the eastern Weddell Sea and much of the East Antarctic sector, where modelled temperatures are widely warmer than 1°C , compared with observed temperatures around -1°C in these regions, corresponding to a warm bias often exceeding 2°C .

This explains why in these regions the mean sea ice concentration is considerably lower than the observed mean state and the mean state of the other three models (Fig. 2.1d). The surface salinity in the medium resolution model is biased both

in the Weddell Sea, where the salinity has the highest values, and in the West Antarctic sector, where it is considerably fresher than the rest of the models and the observations. The high resolution HadGEM3 has the most realistic surface temperature (Fig. 2.2d) and surface salinity (Fig. 2.2n) and it performs the best out of all the models. The two low resolution models are also performing relatively well. The 1° HadGEM3 model (Fig. 2.2b) is slightly warmer compared with the UKESM1 model east of the Weddell Sea (Fig. 2.2a) and they both have a surface salinity bias throughout the Southern Ocean (Fig. 2.2k,l). Overall, the medium resolution model is the one with the biggest temperature and salinity biases in the Southern Ocean, and they are likely related to the sea ice biases noted previously.

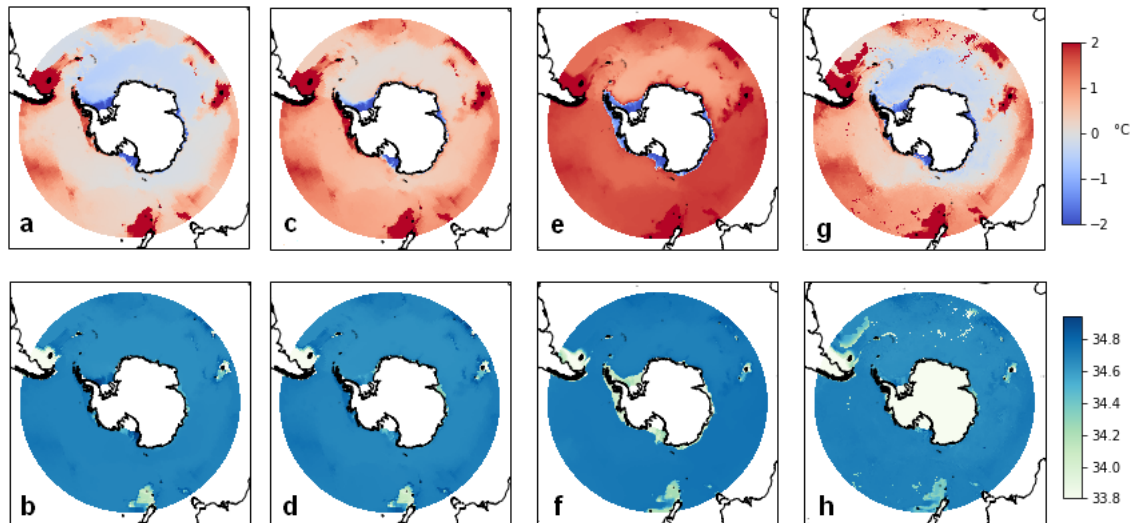


Figure 2.3: Averaged bottom temperature and salinity; (a),(b) UKESM1 (c),(d) HadGEM3-GC3.1-LL, (e),(f) HadGEM3-GC3.1-MM, (g),(h) WOA18. The ocean bottom is defined as the bottom-most ocean grid cell

WOA18 bottom temperature and salinity (Fig. 2.3g,h) should be considered invalid south of the shelf break due to the lack of realistic bathymetry in their dataset. Regarding the bottom properties, bottom temperature and salinity fol-

lows a similar pattern, with the medium resolution model being the most different from the observations. The medium resolution model has a fresh bottom water bias all around the Antarctic continental shelf (Fig. 2.3e) and a cold bottom water bias in the continental shelf in West Antarctica (Fig. 2.3e). Additionally, bottom water further north of the antarctic continental shelf is relatively warm in this model (Fig. 2.3e) which could be a sign of reduced AABW formation or descent (Heuzé et al., 2013). Comparing the two low resolution models we found that the UKESM1 (Fig. 2.3a) has a colder West Antarctic continental shelf than the low resolution HadGEM3 (Fig. 2.3c) and overall the bottom temperature in the UKESM1 model is more realistic (Fig. 2.3a,g).

Surface currents transport heat and fresh water and could link biases in East and West Antarctica. Using the zonal component of the surface velocity, we show here how the models velocity compares to Southern Ocean State Estimate (SOSE) (Fig. 2.4). All 4 models underestimate the strength of the ACC compared with SOSE. The two low resolution models do not have substantial differences between them (Fig. 2.4b,c). They exhibit a typical circulation for coarse resolution models, where there is not a westward flow at Drake Passage, even though it is generally believed that some slightly westward flow is present there (Firing et al., 2011);(Donohue et al., 2016). The low resolution HadGEM3 (Fig. 2.4c) has a slightly stronger westward velocity near the coast over the East Antarctic sector.

The higher resolution models have a richer eddy activity because of their finer resolution and are able to represent in more detail the circulation features of Southern Ocean. The medium resolution model (Fig. 2.4d) shows a striking difference from the rest of the models and the SOSE climate estimate. It has a very strong westward slope current that circulates all around Antarctica, meaning

that it is present in the West Antarctic sector as well. In the estimated velocities (Fig. 2.4a) that is not the case, but this feature can explain the cold and fresh West Antarctic shelf we see in this model (Fig. 2.3e,f) since the front that accompanies this strong slope current can prohibit CDW intrusion on the continental shelf. The zonal velocity of the high resolution model (Fig. 2.4e) exhibits a more realistic Antarctic slope current, present over the East Antarctic sector only, and possibly an underestimated ACC strength, but overall it has the best performance out of all the models in terms of surface zonal velocity.

By examining how the main Southern Ocean characteristics (temperature, salinity, circulation and sea ice) are represented by the models, we found large biases in all of the above properties in the medium resolution model that will be examined in more detail in the next section of this chapter. The medium resolution HadGEM3 has a cold and fresh West Antarctic continental shelf that is consistent with the westward slope current's presence there. We hypothesise that the westward slope current in the model prohibits warm water intrusion to the continental shelf, while that is not the case in the real world. The two low resolution models do not have a lot of differences, but the UKESM1 model is slightly more realistic in representing bottom water temperature and salinity. The high resolution model is the best performing model of all in the metrics assessed so far.

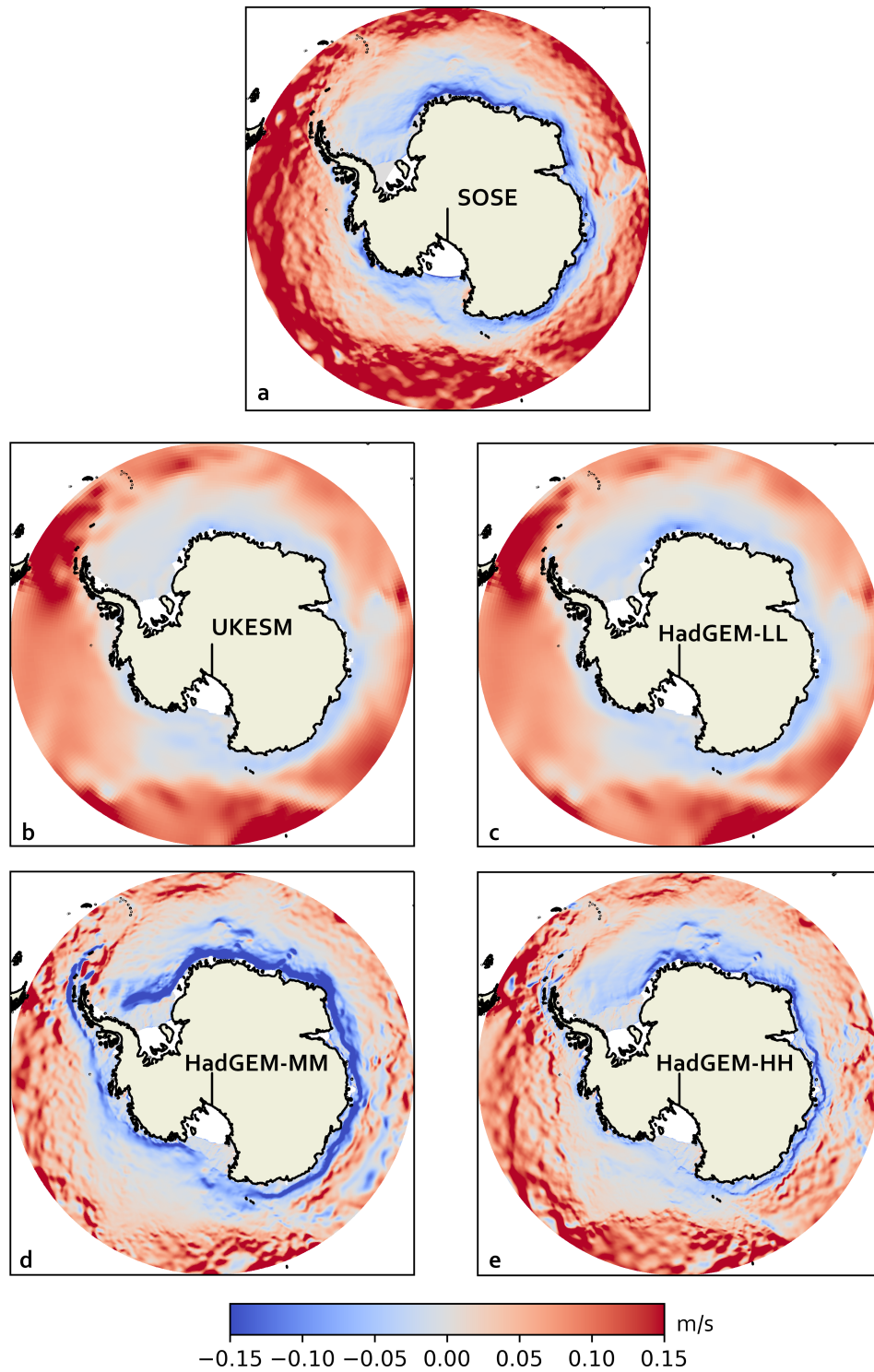


Figure 2.4: (a) SOSE surface zonal velocity averaged over 2013-2019. Surface zonal velocity averaged over 20 years 1995-2014; (b) UKESM1, (c) HadGEM3-GC3.1-LL, (d) HadGEM3-GC3.1-MM, (e) HadGEM3-GC3.1-HH.

2.3 Biases in HadGEM3-GC3.1-MM; from the Weddell to the Amundsen Sea

In this section we will examine in more detail the ACC strength in each model, some of the biased characteristics in the medium resolution model, together with timeseries of their evolution and finally the representation of warm water intrusion on the West Antarctic continental shelf in each model, using meridional sections of the Amundsen Sea continental shelf. The motivation behind this is to link the biases mentioned in the previous section with the ability of this model to represent subsurface water properties such as temperature and salinity on the West Antarctic continental shelf.

The Weddell Sea is a region that exhibits many biases in the medium resolution model as we show in the previous section. The depth integrated cumulative sum of meridional volume transport through a zonal section in the Weddell Sea shows the magnitude of the circulation bias in that area. While the maximum SOSE value is roughly 30 Sv, the medium resolution model's maximum value is almost 3 times higher (Fig. 2.5a). The high resolution model has a stronger than SOSE northward volume transport in the Weddell Sea (Fig. 2.5a), but remains less than half the magnitude of the medium resolution model (Fig. 2.5a). The two low resolution models both underestimate the northward volume transport in the Weddell Sea. However, They seem to capture the depth integrated total volume transport in Drake Passage more realistically (Fig. 2.5b), without the presence of westward transport. The low resolution HadGEM3 is slightly under performing compared to UKESM1.

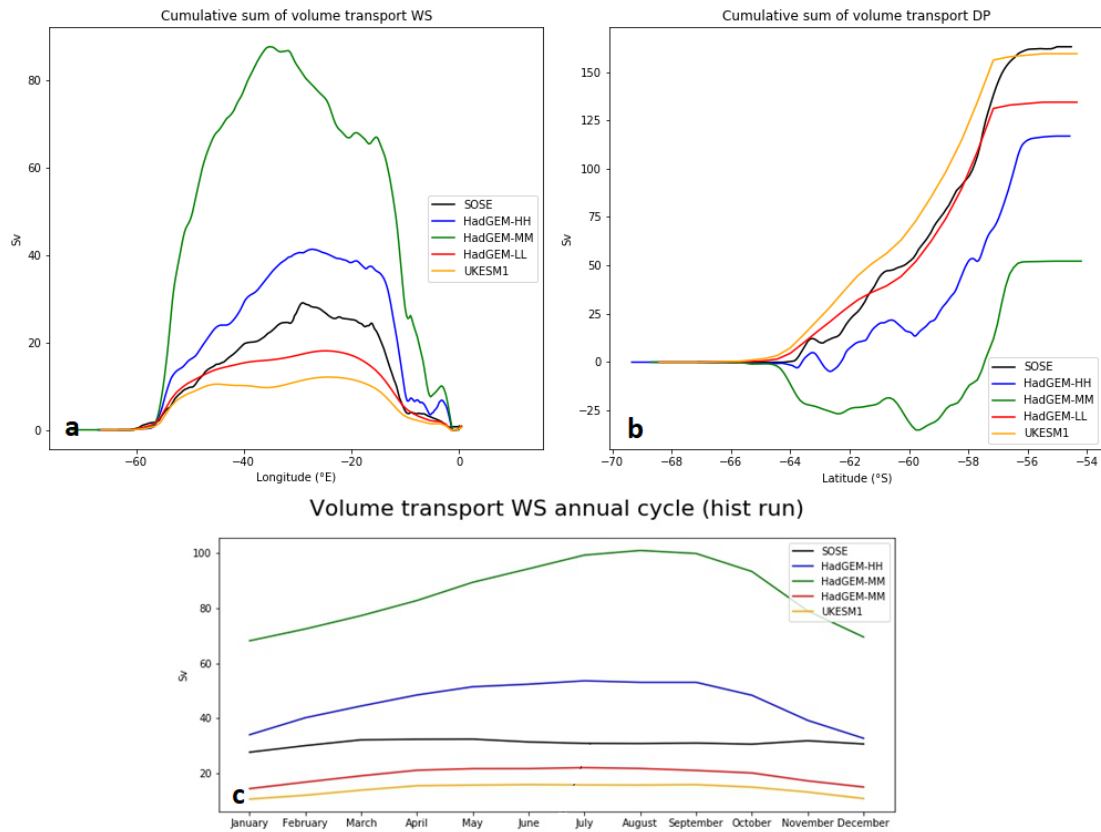


Figure 2.5: Averaged over 20 years (1995-2014) (a) cumulative sum of the meridional volume transport in the Weddell Sea (across the 69.61°S zonal section), (b) cumulative sum of the zonal volume transport in Drake Passage (c) annual cycle of the peak integrated meridional volume transport in the Weddell Sea; green line: HadGEM3-GC3.1-MM, blue line: HadGEM3-GC3.1-HH, red line: HadGEM3-GC3.1-LL, orange line: UKESM1, black line: SOSE.

The previous figure of surface zonal velocity (Fig. 2.4) shows that the low resolution models are not able to represent the observed counter-current in Drake Passage, and that could explain why they are able to represent better the overall circulation and the strength of the ACC, even compared with the high resolution model. On that note, the high resolution HadGEM3 slightly underestimates the total volume transport in Drake Passage compared with SOSE (Fig. 2.5b), partly because of the presence of a small westward current that is not present in SOSE, but it is present in observations. The medium resolution HadGEM3 model is un-

derestimating the total volume transport in Drake Passage, its strength is almost 1/3 of the SOSE value and it has an extremely (more than 25 Sv) strong westward current (Fig. 2.5b). The strong annual cycle of meridional volume transport in the Weddell Sea in the medium resolution model suggests that the biases in circulation might be linked to processes such as sea ice formation and the deepening of the mixed layer depth that also have a strong annual cycle.

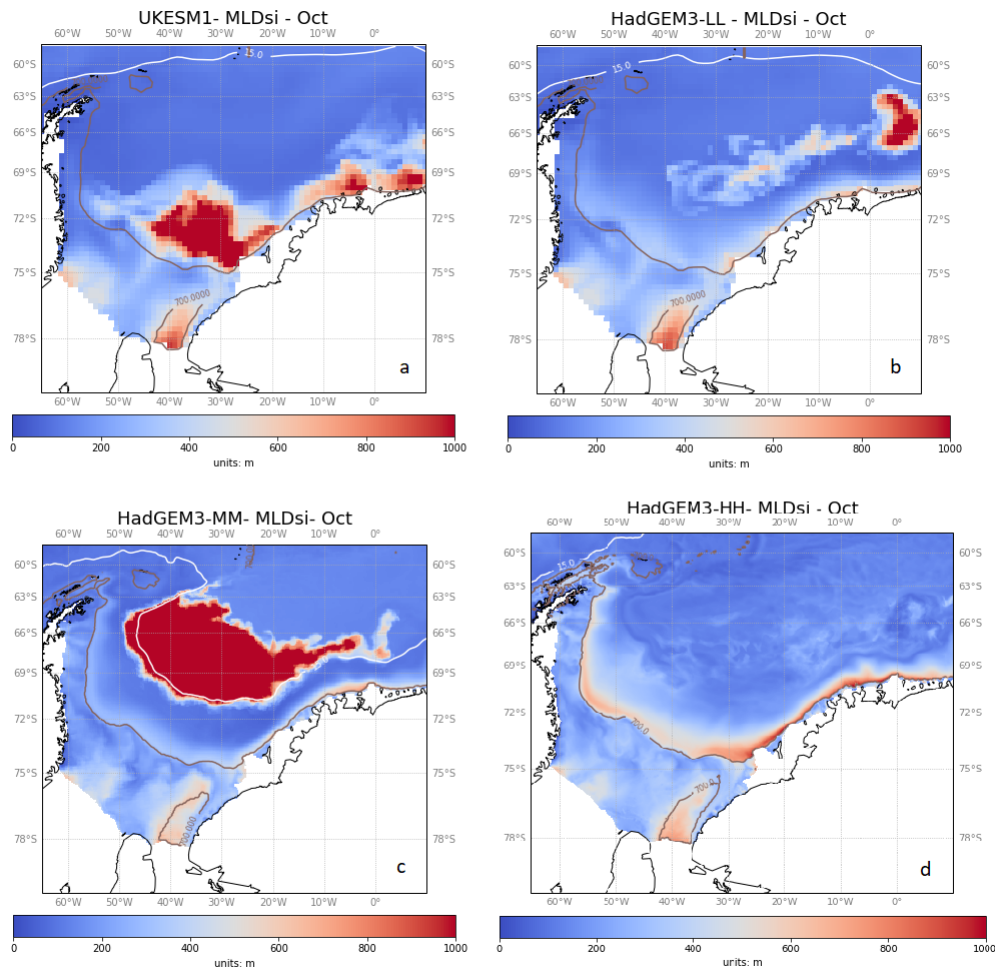


Figure 2.6: September mixed layer depth in the Weddell Sea averaged over 20 years (1995-2014) (a) UKESM1, (b) HadGEM3-GC3.1-LL, (c) HadGEM3-GC3.1-MM, (d) HadGEM3-GC3.1-HH. White contour: sea ice concentration >15%.

We hypothesise that the strength of the Weddell Sea gyre in the medium resolution model is linked to deep convection, where the sea ice is almost absent in the interior of the Weddell Sea. The sea ice concentration in the Weddell Sea is strikingly different between the 4 models (Fig.2.6). The annual cycle of the mixed layer depth is believed to be strongly influenced by the sea ice melt and freeze, with a fresher and lighter mixed layer during the summer and a denser and deeper mixed layer during the winter (Barthélemy et al., 2015; Pellichero et al., 2017; Petty et al., 2014; Ren et al., 2011). Here we show the mixed layer depth in the Weddell Sea as it is represented by each model (Fig. 2.6). The four climate models exhibit a wide variation in their ability to represent the mixed layer depth in the Weddell Sea. The mixed layer depth has a strong seasonal cycle in all four models. The medium resolution model exhibits most of its deep convection in the Weddell gyre region, where there is minimal to no sea ice coverage (Fig. 2.6c). The lack of sea ice in the MM model allows for stronger atmosphere forcing compared to the other models, that results in deep ocean convection. The depth of the mixed layer in the medium resolution model can be more than 3000 m, and is surrounded by an equally unrealistically strong Weddell Sea gyre as shown before (Fig. 2.4; Fig. 2.5).

In order to gain a better understanding of the biases time evolution in the medium resolution HadGEM3 we show timeseries of biased features throughout the entire historical run (Fig. 2.7). The historical run extends from 1850 to 2014, a total of 164 years. Here we evaluate the temporal relationship of annual mean timeseries of sea ice, mixed layer depth and integrated meridional volume transport in the Weddell Sea, as well as integrated zonal volume transport in Drake Passage and along the shelf break in the Amundsen Sea (Fig. 2.7). There is a decreasing trend

in the sea ice concentration in the Weddell Sea between the years 100 and 150 (1950-2000) (Fig. 2.7a), while the mixed layer depth and Weddell gyre volume transport show a positive trend during the same period (Fig. 2.7b,c). During that time, there is also an increase in the total volume transport through Drake Passage (Fig. 2.7d) that can be attributed to the decrease in westward volume transport (Fig. 2.7e).

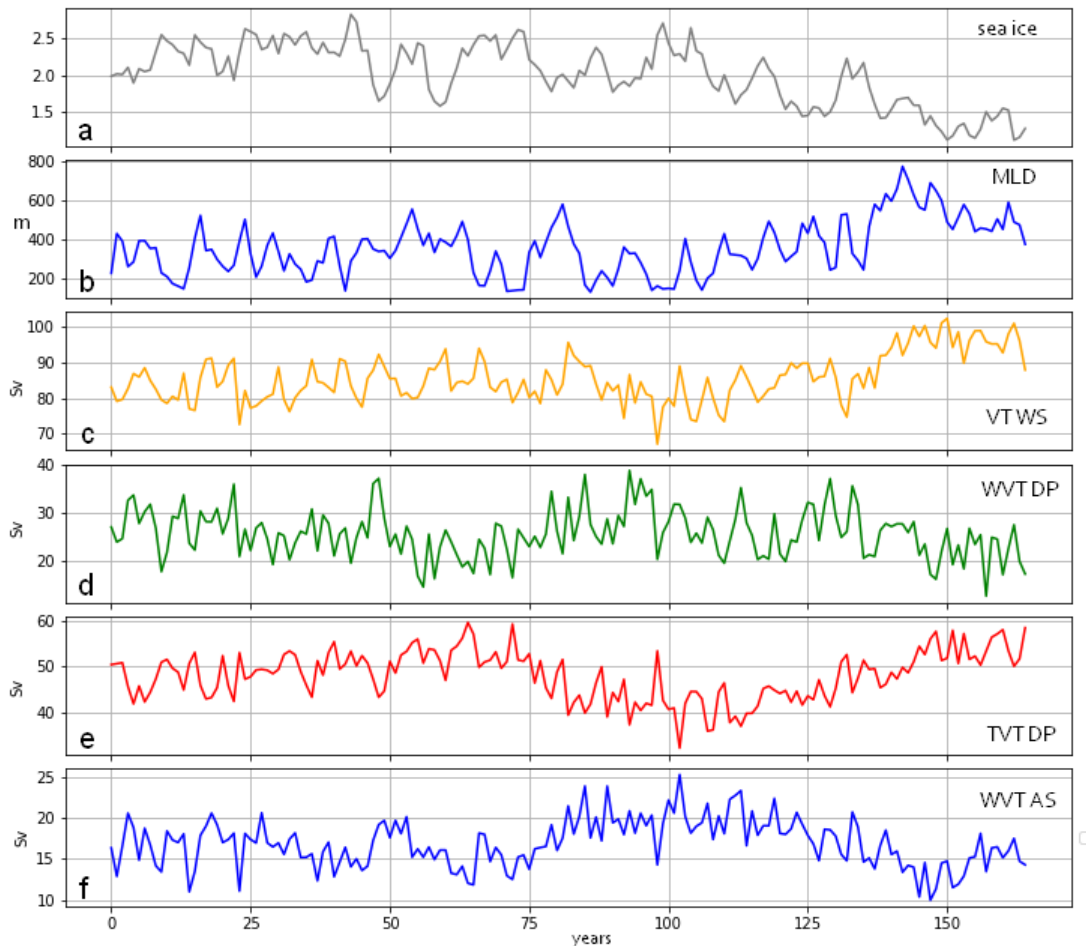


Figure 2.7: HadGEM3-GC3.1-MM historical run timeseries of annual mean (a) sea ice area, (b) mixed layer depth and (c) northward volume transport in the Weddell Sea; (d) westward volume transport and (e) total volume transport at Drake Passage; (f) westward volume transport over the continental slope in the Amundsen Sea.

The changes in volume transport in Drake Passage and the Weddell Sea seem to be linked, and an increase in the latest might influence the former. It is difficult to separate the influence of both an increase in the Weddell gyre and the eastward core of ACC on the westward transport in Drake’s Passage. The westward volume transport over the Amundsen Sea continental shelf break (Fig. 2.7f) decreases during the same period (100-150 year), which correlates relatively well with the increase of the ACC strength. It is not possible to disentangle the feedbacks and determine the root cause without analysing the spin up run to assess which biases develop first. Further analysis is needed in order to understand the origins of all these biases, this will be addressed in Chapter 3.

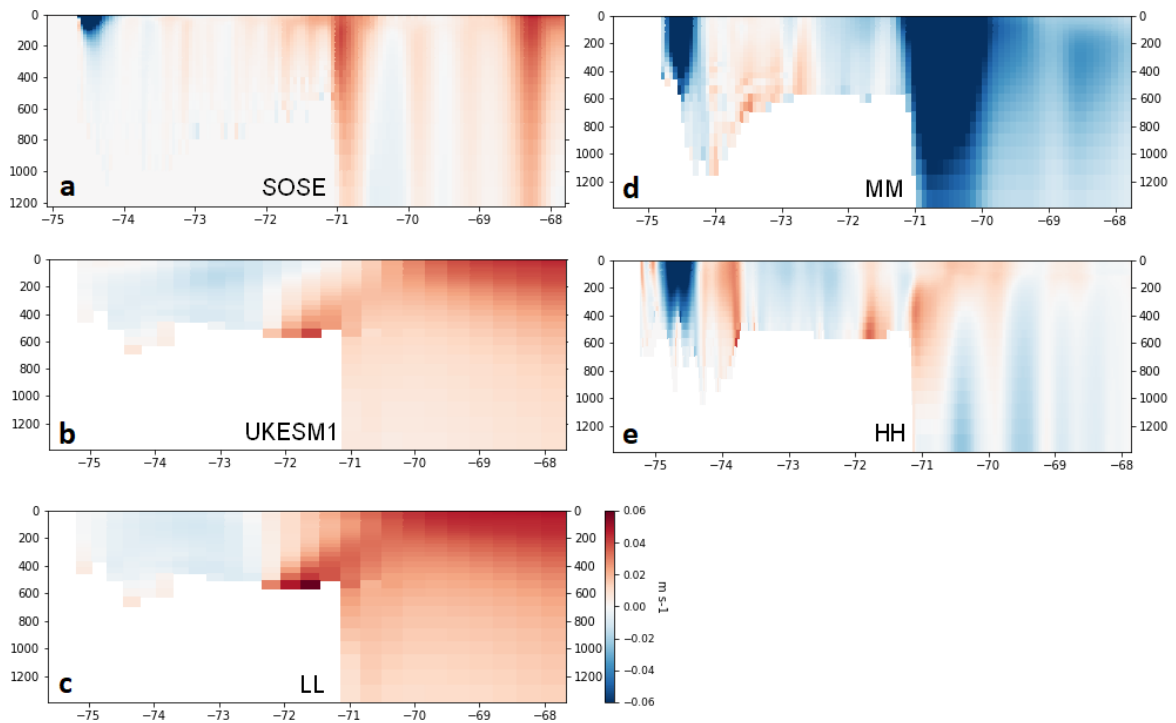


Figure 2.8: Meridional section at 109°W in the Amundsen Sea; x axis latitude; 20 year (1995-2014) averaged zonal velocity (a) SOSE, (b) UKESM1, (c) HadGEM3-GC3.1-LL, (d) HadGEM3-GC3.1-MM, (e) HadGEM3-GC3.1-HH.

We have shown already that the ACC is underestimated in the medium and high

resolution models, while the medium resolution model exhibits the biggest deviation from the state estimate, together with other strong biases in sea ice, mixed layer depth, temperature and salinity. However, as we show in Figures 2.4 and 2.5, the most striking difference is that it represents a very strong westward slope current, that extends in West Antarctica. The medium resolution model has a very strong westward slope current present (Fig. 2.7d) that creates a front that prohibits warm water intrusion on the continental shelf, resulting in a very cold and fresh shelf (Fig. 2.8d). Both the medium and high resolution models manage to capture a westward coastal current that agrees with SOSE (Fig. 2.8d,e). However, the high resolution HadGEM3 does a good job in representing the eastward slope current that is present in SOSE (Fig. 2.8a,e) and is able to represent warm water intrusion on the continental shelf (Fig. 2.8e). The two low resolution models do not have major differences in representing zonal velocities. There is a slightly stronger eastward flow in the low resolution HadGEM3 (Fig. 2.8b-c). The eastward flow at the continental shelf break could be associated with an overall warmer continental shelf (Fig. 2.9b-c), an uninterrupted mechanism in these low resolution models, due to their lack of ability to represent small scale circulation features.

One of the causes of ice shelf melt is warm water intruding onto the continental shelf, and through a number of different pathways, the base of the ice shelves. The Amundsen Sea continental shelf can be used as a great example of CDW intrusion in order to evaluate how the four climate models represent this warm water intrusion on the West Antarctic continental shelf. The bathymetry in WOA18 (Fig. 2.9a) is not realistic south of the continental shelf break (Fig. 2.8a), but its purpose here is to show the temperature stratification at the continental shelf

break and slope. Comparing the UKESM1 with the low resolution HadGEM3 and WOA18 we find that the UKESM1 does a better job in representing the temperature at the continental shelf and has a less warm bias at the surface layer (Fig. 2.9a-c), and we can see that the medium resolution model has an unrealistic temperature (Fig. 2.9d).

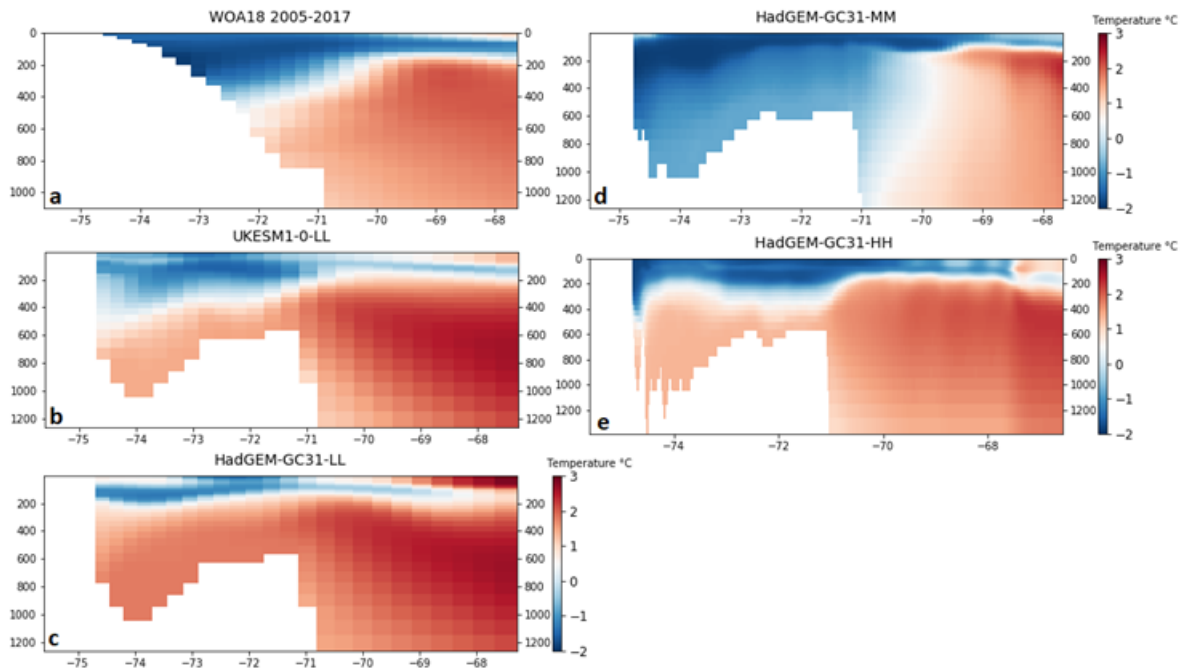


Figure 2.9: Amundsen Sea 106° meridional section of 20 year averaged potential temperature (a) WOA18, (b) UKESM1, (c) HadGEM3-GC3.1-LL, (d) HadGEM3-GC3.1-MM, (e) HadGEM3-GC3.1-HH.

Another noteworthy difference between the two models is the decadal variability of temperature on the Amundsen Sea continental shelf (Fig. 2.10). Timeseries of a grid point near the eastern trough show that the UKESM1 has a greater inter-annual and even decadal variability compared with the low resolution HadGEM3 (Fig. 2.9). Atmospheric teleconnection patterns can influence SST in the Southern Ocean and drive decadal variability (Ferster et al., 2018). This affects the heat content variability and results in a less stratified water column. Surface heat loss

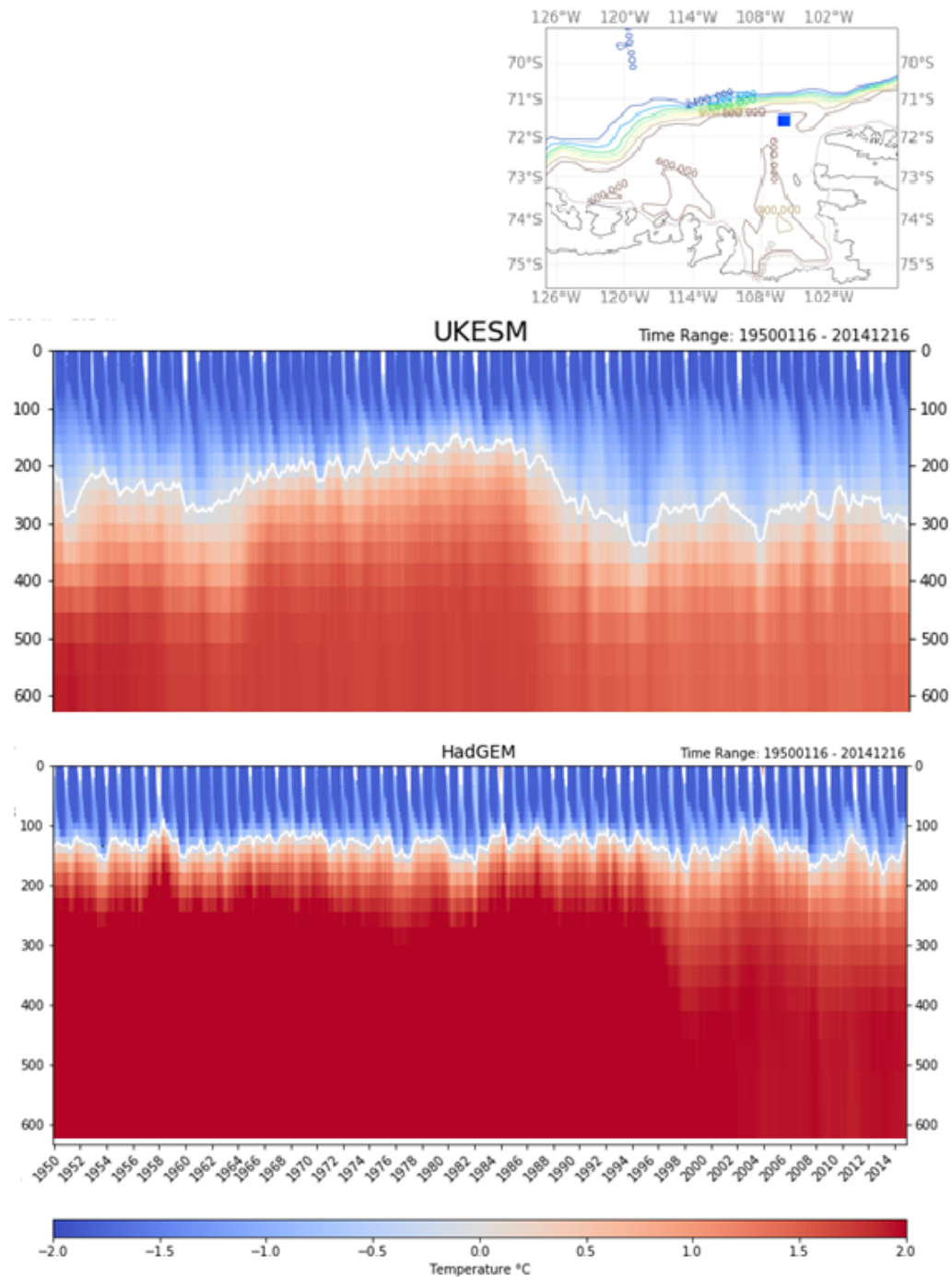


Figure 2.10: Timeseries of temperature (a) HadGEM3-GC3.1-LL, (b) UKESM1. White contour line is the 0° C isotherm. Inset map of the Amundsen Sea continental shelf showing the location of the selected grid cell with colour contoured bathymetry.

and increased sea ice production drive deeper convection and the thermocline deepens resulting in less CDW advection on the continental shelf (Webber et al., 2017). Decadal variability driven by this mechanism is present in the UKESM1 model, while the low resolution HadGEM has an overly stratified water column (Fig. 2.10). Previous studies have shown that inter-annual and decadal variability of the temperature stratification is to be expected on the continental shelf (Thoma et al., 2008);(Dutrieux et al., 2014);(Webber et al., 2019). Overall, the UKESM1 model seems to be more realistic compared with the low resolution HadGEM.

2.4 Conclusions

In this chapter we evaluated the performance of the historical runs of four models, part of CMIP6, that belong to the same family but differ in horizontal resolution. We found large differences between them, with one model, the 1/4°HadGEM3-MM, showing particularly large biases in several ocean features. Our primary focus is the ability of the models to represent realistic warm water intrusion on the West Antarctic continental shelf and the mechanisms related to that.

The two 1°resolution models, UKESM1 and HadGEM-LL, show similar results. The UKESM1 represents slightly better the sea ice concentration, bottom temperature, volume transport in Drake Passage and temperature stratification over the continental shelf break and has a smaller SST bias in the Amundsen Sea. It also has bigger inter-annual and decadal variability of temperature on the Amundsen Sea continental shelf. Overall, UKESM1 performs slightly better compared to the low resolution HadGEM3.

The medium resolution HadGEM3 model has many substantial biases in the

Southern Ocean properties that would drastically impact West Antarctic ice shelf melt rates. However, we consider this an excellent opportunity that allows us to study how the different biases are related and to identify the potential contributors to unrealistic warm water intrusion on the West Antarctic continental shelf. We show that the sea ice concentration is poorly represented and in some cases not present at all, in the East Antarctic sector and in the Weddell Sea. There is a strong westward slope current present all around Antarctica, even in the west sector, which is not realistic. The slope current and its associated front are related to the prohibited warm water intrusion on the West Antarctic continental shelf.

Interestingly, the medium resolution HadGEM3 is not the only $1/4^\circ$ CMIP6 model that has these biases. Other $1/4^\circ$ models have a stronger than observed westward slope current ([Beadling et al., 2020](#)). The increasing number of models from CMIP5 to CMIP6 that represent a strong westward slope current could possibly be explained by the increasing number of $1/4^\circ$ horizontal resolution models that are eddy permitting. This seemingly small detail is of great importance because we can now study the impact of a westward slope current in West Antarctica on present day warm water intrusion, future projections and how this circulation feature is developed. The historical run in its entirety has a circumpolar westward slope current, large sea ice biases in the Weddell Sea and east Antarctica and a cold West Antarctic continental shelf. We hypothesise that large scale fresh water flux from sea ice melt is the cause of the circumpolar circulation and cold bias in this model and we will test this in the next chapter, investigating the development of these biases in the spin up run of the medium resolution HadGEM3.

Regarding the high resolution HadGEM3 model, we show here that it can rep-

resent almost every Southern Ocean characteristic in a realistic way. It has a weaker than observed ACC strength, but it does not have a westward slope current in West Antarctica, like the medium resolution model. Since it is the best performing model in our analysis and has a realistically relatively warm Amundsen Sea continental shelf, we will use data from its future projections run in order to investigate future warm water intrusion on the West Antarctic continental shelf (Chapter 4).

Here we used one ensemble member for each model. Ensemble members evolve independently and each one has a different internal variability. This could pose as a limitation to our approach because the Southern Ocean is strongly influenced by modes of variability. An ensemble of more than one member for each model could help mitigate the impact of model internal variability when analysing the ensemble mean fields ([Andrews et al., 2020](#)). However, considering the scope of our research and the size of the biases presented here, our results are fundamentally robust. Similar results were presented by [Andrews et al. \(2020\)](#), where the sea ice in the medium resolution HadGEM is under extensive due to a warm bias, and the sea ice extend timeseries is comparable to the one presented here (Fig. 2.7). [Andrews et al. \(2020\)](#) used an ensemble of 4 members for each model to assess historical simulations of two different HadGEM3-GC3.1 resolutions.

Chapter 3

In depth analysis of biases in the medium resolution

HadGEM-GC3.1 model spin up run

3.1 Introduction

In the previous chapter we evaluated data from the historical run of the medium resolution HadGEM3 and found a large fresh and cold bias, combined with a strong westward slope current, present on the West Antarctic continental shelf. The tilting of the isopycnals related to this slope current is responsible for prohibiting warm water intrusion on the continental shelf. However, it was not possible to investigate the origins of this circulation feature in the West Antarctic continental

shelf in the model using data from the historical run.

In this chapter we will track the evolution of the biases, starting from the first year of the spin up run, in order to identify the mechanisms that initiated them in the model. We chose two areas of interest, that displayed the largest sea ice, velocity and salinity biases in our previous chapter, the Weddell Sea and West Antarctica. We investigate whether the biases in Weddell Sea sea ice and velocity develop prior to the West Antarctic continental shelf salinity bias and try to establish a time frame in which these potential biases in Weddell Sea can have an impact on the Amundsen Sea continental shelf. We focus on changes in the West Antarctic sector that are developing prior to or simultaneously with the deep freshening in the Amundsen Sea, during the first few years of the run.

A model study by [Flexas et al. \(2022\)](#) showed that freshwater anomalies can be transported from the West Antarctic Peninsula and Bellingshausen Sea to the Amundsen Sea within a couple of years via the coastal current, which as a response to the freshwater anomalies becomes stronger. While the freshening follows a mostly coastal path on the Bellingshausen continental shelf, in the Amundsen Sea it is not constrained near the coast and extends to the continental shelf break. In this study ([Flexas et al., 2022](#)) the freshwater anomaly was released at the surface and near the coast of the West Antarctic Peninsula.

Here, we use a particle tracking software (Ariane) to identify the pathway of water masses. Ariane is an off-line diagnostic tool that can be used on any C-grid to compute 3D streamlines in a given velocity field. It also allows for backward integration of the trajectories, by multiplying the velocity outputs by -1 and reversing their chronological order. We used the latest 2019 version. Sensitivity

tests we carried out by changing the time step, depth and size of the areas where the particles were released. In the case of the Weddell Sea, choosing a larger area for particle release, and not just a small subarea, allowed for more particles to advect west of the Antarctic Peninsula. This resulted in capturing in better detail the link between the Weddell Sea and Amundsen Sea, making our results more robust. No significant differences were present with changes in the depth of the released particles within this region, or any other region. Changing the time step and the size of the initialisation areas did not make a difference in any other region. In the case of the Amundsen Sea, where we tracked the particles backwards, the areas of choice were small sub-regions of the Amundsen Sea, but this did not hinder our ability to locate the particles source.

The spin-up experiment for the medium ocean resolution model was performed only with one atmosphere resolution (MM), the 100km atmosphere (Roberts et al., 2019). The initial conditions for the atmosphere were derived from ERA-20C (Poli et al., 2016) the first day of January 1950. Initial conditions for ocean temperature and salinity were derived from the 1950-1954 mean of the EN4 ocean analysis (Good et al., 2013), which was interpolated to the model ocean grid. For the medium resolution model a multi-day simulation with a very short ocean time step was performed in order to remove small-scale instabilities introduced by the interpolation. The model was then restarted at the first day of year 1950 with these derived ocean initial conditions (Roberts et al., 2019). Sea ice initial conditions were taken from previous ocean-sea ice simulations at the same resolution that were valid around 1979 (Roberts et al., 2019).

3.2 Biases evolution and methods

The historical run of the HadGEM3 medium resolution model has large biases in the Southern Ocean (Chapter 2). For the purpose of this chapter, which is to establish the evolution of the biases in this model, we will be using the mean state of the historical run as a reference point in which the biases are already developed (as shown in Chapter 2). We will be using and referring to mean temperature, salinity, sea ice, volume transport and MLD from the historical run of the model to compare with and evaluate the performance and progression of the spin up run. The annual mean of the first year of the spin up run is considered unbiased and realistic for the purpose of this chapter, because it has a warm and saline west continental shelf and sufficient sea ice in the Weddell Sea (Fig. 3.1d,e,f), and will be referred to as the beginning of the spin up run or year 0.

There are big differences between the annual mean temperature, sea ice and salinity of the historical mean of the model (Fig. 3.1a,b,c) and the first year of the spin up run (Fig. 3.1d,e,f). In the historical run, the West Antarctic continental shelf is considerably less warm than the beginning of the spin up run and the salinity is much lower, meaning that the mean state of the continental shelf is unrealistically fresh and somewhat cold. Moreover, in the historical run, the sea ice concentration in the Weddell Sea is substantially underestimated (Fig. 3.1c). In contrast, in the beginning of the spin up run, warm water is present in the entirety of the west continental shelf (Fig. 3.1d) which is noticeably less fresh (Fig. 3.1e) and the annual mean sea ice in the Weddell Sea has a realistic extent (Fig. 3.1f).

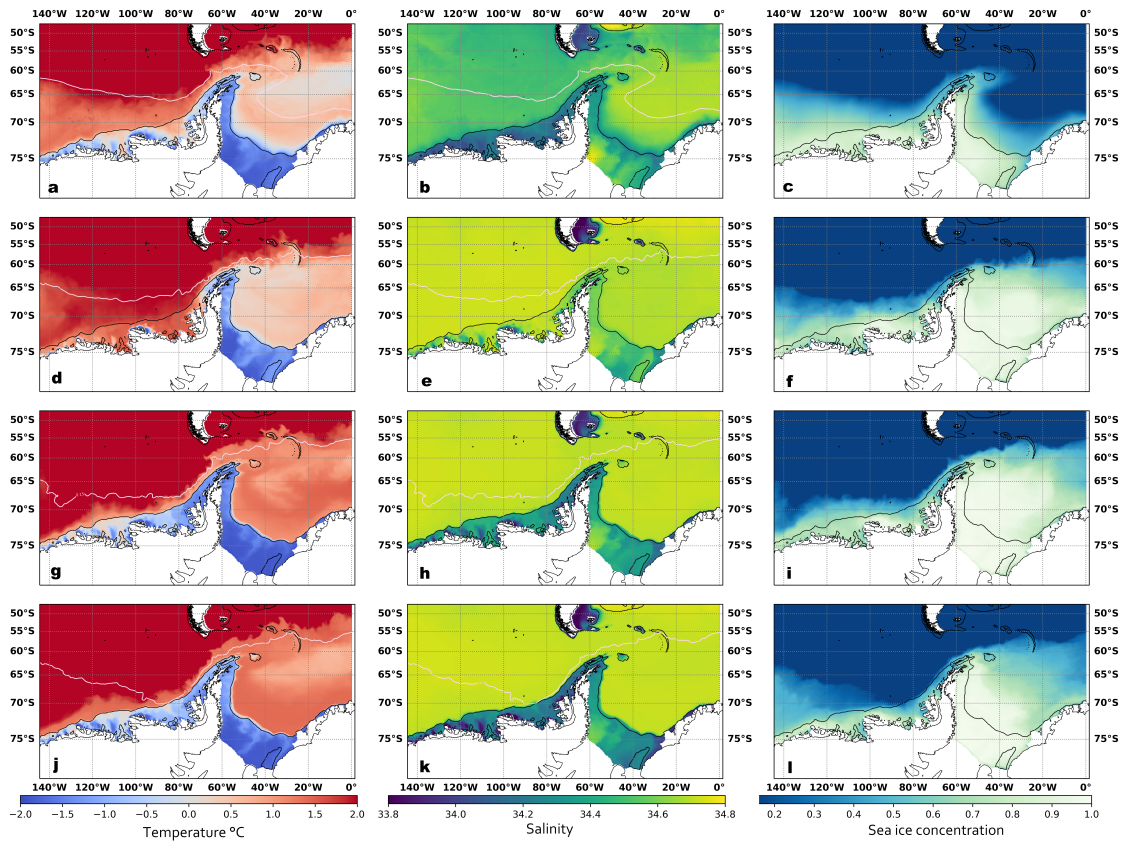


Figure 3.1: Subsurface maxima of annual mean temperature and salinity, over depth greater than 69 m, and sea ice concentration of (a),(b),(c) historical run, (d), (e), (f) first year of the spin up run, (g), (h), (i) 15th year of the spin up run, (j), (k), (l) last year of the spin up run. Black contour: 800 m isobath, white contour: annual mean sea ice 15% contour.

There are no obvious biases present in the beginning of the spin up run (Fig. 3.1d,e,f), since the West Antarctic continental shelf is reasonably warm and the sea ice in Weddell Sea has not disappeared yet. However, comparing the beginning of the spin up run (Fig. 3.1d,e,f) with the middle (Fig. 3.1g,h,i) and the end of it (Fig. 3.1j,k,l), the biases on the West Antarctic continental shelf have already developed at year 15 and are still present and have grown bigger by year 30. The West Antarctic continental shelf has become cold and and fresh (Fig. 3.1g,h) and the sea ice has been slightly decreased (Fig. 3.1i). The Weddell Sea sea ice in

the middle of the run (Fig. 3.1i) does not show any notable biases yet. By the end of the run, the West Antarctic continental shelf has shifted fully to a cold and fresh state (Fig. 3.1j,k) and the sea ice extends mostly as far north as the continental shelf break (Fig. 3.1l). The sea ice in the Weddell Sea is slightly decreased (Fig. 3.1l), but it does not yet show the same magnitude of bias as we see in the historical run (Fig. 3.1c). Overall, at the end of the spin up run the biases on the West Antarctic continental shelf have been developed, but the Weddell Sea biases are not fully developed yet.

In the historical run of the medium resolution model the three regions with the most striking biases were the Weddell Sea, with a significant lack of sea ice, Drake Passage with reduced ACC transport and a strong westward current and the cold West Antarctic continental shelf with a fresh westward slope current (Chapter 2). We have selected the main ocean features that exhibit large biases and significant trends in the historical run (Fig. 2.6, Chapter 2), such as sea ice, mixed layer depth, circulation and temperature, in the 3 key Antarctic regions, the Weddell Sea, Drake Passage and Amundsen Sea. Here, we establish the time evolution of these biases in the spin up run and their corresponding connections (Fig. 3.2).

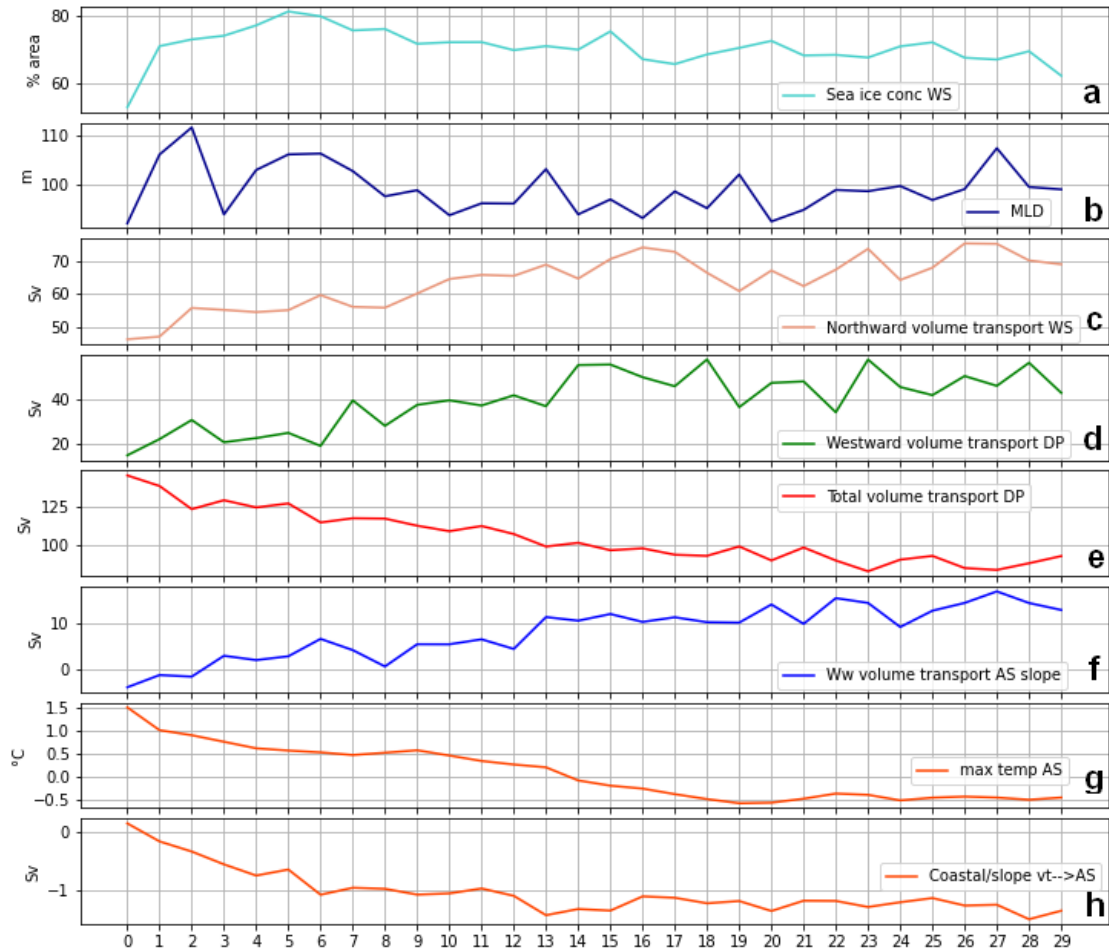


Figure 3.2: Spin up annual mean timeseries of (a) Weddell Sea sea ice concentration %, (b) Weddell Sea mixed layer depth, (c) Weddell Sea northward volume transport, (d) Drake Passage westward volume transport, (e) Drake Passage total volume transport, (f) Amundsen Sea continental shelf slope westward volume transport, (g) Amundsen Sea maximum temperature below 150m, (h) volume transport from the Bellingshausen Sea to the Amundsen Sea

In the Weddell Sea the sea ice and mixed layer depth do not display any large changes or trends throughout the whole spin up run (Fig. 3.2a,b). The northward volume transport in the Weddell Sea (Fig. 3.2c), calculated as the maximum value of the depth integrated cumulative sum in the zonal direction, shows an overall positive trend and grows from 50 Sv to 70 Sv by the end of the run. The westward component of the volume transport through Drake Passage shows a similar trend

and doubles in size, from 20 Sv to 40 Sv by the end of the run. This positive trend seems to take effect after the sixth year (Fig. 3.2d). The total volume transport at Drake Passage is decreasing from 150 Sv to less than 100 Sv by the end of the run (Fig. 3.2e), 20 Sv of this decrease in eastward volume transport can be accounted for by the spinning up westward volume transport.

The westward volume transport along the Amundsen Sea continental shelf slope (Figure 3.2f) is calculated as the depth integrated net volume transport (positive westward) of a cross section above the continental shelf break and slope at 105.8°W, located slightly on the west of the east Amundsen Sea trough. The first 3 annual means of the flow are eastward (negative values), meaning that the observed eastward flow is still present at the continental shelf break, but we do see a positive trend right from the start. After year 3, the volume transport at the AS continental shelf break is westward (positive), hinting at the initiation of the fresh westward slope current that is present later in the spin up run and the historical run. The maximum temperature along the water column on the Amundsen Sea continental shelf decreases by 0.5°C during only the first couple of years and by nearly 1°C during the first 4 years of the run (Figure 3.2g).

We have demonstrated that a substantial freshening trend is present across the West Antarctic continental shelf, already by year 15 (Figure 3.1h). We will show in the next section that this freshening is particularly strong and develops earlier in the Bellingshausen Sea and West Antarctic peninsula (Figure 3.3a). For this reason we hypothesize that part of the freshening in the Amundsen Sea is contributed by freshwater advection from the Bellingshausen Sea and West Antarctic Peninsula. We quantified the depth integrated total volume transport from a cross

section starting on the continental shelf up to the continental slope, between the Bellingshausen and the Amundsen Sea. There is a negative trend (westward transport) present that is linked to the decreasing temperature on the Amundsen Sea continental shelf (Figure 3.2g,h). This negative trend is the strongest between year 0 and 6 (Figure 3.2h).

We found that while some biases in the Weddell Sea sea ice are present by the end of the run (Figure 3.1l), they are not nearly as fully developed as in the historical run (Figure 3.1c). In contrast, biases in circulation are present early on, within the first 3 years of the run the total volume transport at Drake Passage has decreased by 25 Sv (Figure 3.1e), even though the strength of the westward volume transport remains unchanged until year 6. Moreover, the temperature on the Amundsen Sea continental shelf and the transport on the continental shelf slope experience fast changes within the first 5 years, where the westward slope current develops (Figure 3.1f) and the temperature decreases by 1°C (Figure 3.1g). The temperature and salinity biases in the Amundsen Sea develop within the first three to five years, and that implies that a local or nearby source might be responsible for the initiation of them. We will conduct further regional analysis in the next section in order to investigate any local freshwater sources via a freshwater budget and remote sources via particle tracking. We will focus mostly on the short timescale of just the first 5 years of the run, since the biases in the Amundsen Sea have already developed during that time, and examine the timescale in which the Weddell Sea could play a role in these.

3.3 Bias development in early years and fresh-water budget

It was demonstrated in the previous section that while in the first year of the spin up there is no fresh bias in the West Antarctic continental shelf and Weddell Sea, that is not the case for the years to follow. In particular, timeseries revealed that on the Amundsen Sea continental slope the volume transport reversed from eastward to westward during the first 4 years (Fig. 3.2f) and the maximum temperature on the continental shelf decreased by nearly 1°C within this time frame (Fig. 3.2g). Surface salinity differences from year 0 to year 3 indicate that there is freshening near the coast of the West Antarctic peninsula and Bellingshausen Sea, while that is not the case for the Weddell Sea (Fig. 3.3a). Both salinity and temperature changes have started to unfold below the surface in the Amundsen Sea, where temperature has decreased by up to 2°C at depth greater than 200m (Fig. 3.3b), and the salinity that corresponds to the same depth has also decreased noticeably (Fig. 3.3c). Since these large changes in salinity develop in such a short time frame of just 4 years, we consider a nearby source of freshwater responsible for them. Next we investigate sea ice melt rates in West Antarctic peninsula and Bellingshausen Sea where we find the surface freshening.

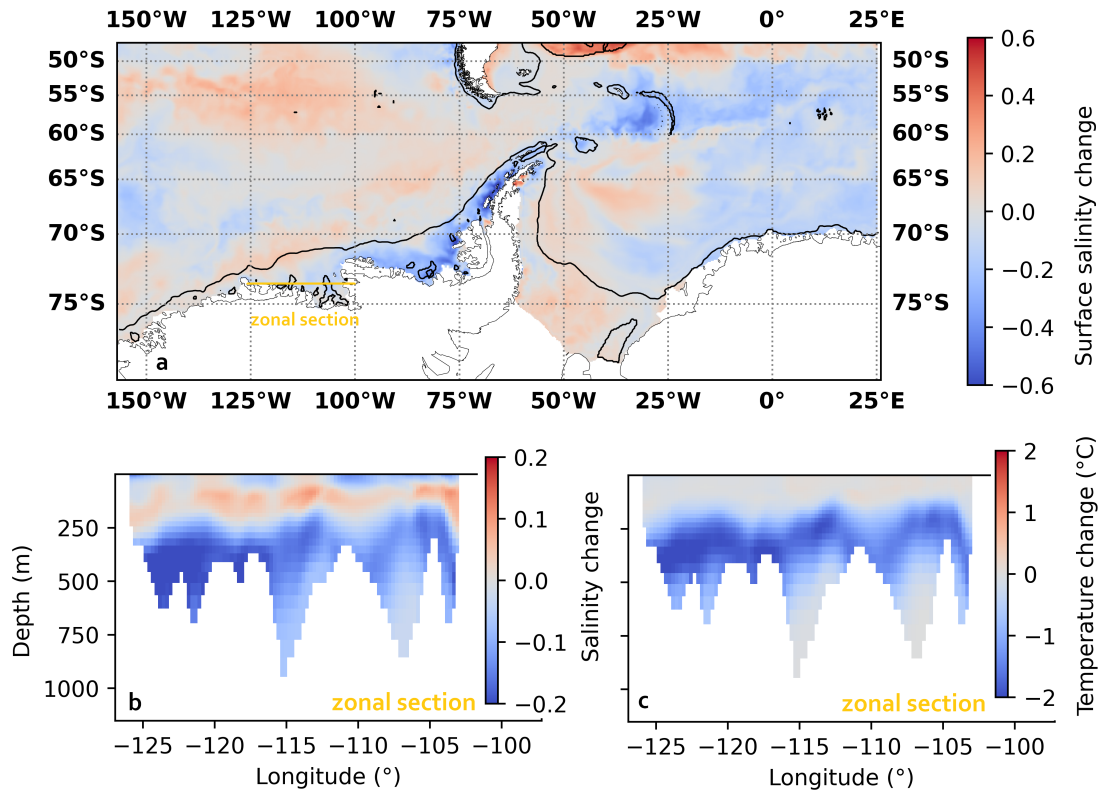


Figure 3.3: Changes in (a) surface salinity, (b) temperature and (c) subsurface salinity form year 0 to year 3 of the spin up run.

The sea ice in the West Antarctic sector reduces and by the end of the run does not extend further north the continental shelf break (figure 3.11). We examine if there is sufficient sea ice melt in the Amundsen Sea nearby regions that could contribute to the freshening trend, specifically in the West Antarctic peninsula and Bellingshausen Sea. We show annual mean values of sea ice melt, in comparison with a sample of 5 years from the high resolution model historical run, that is adequately realistic as we show in Chapter 2, in order to contrast their magnitude (Fig. 3.4). In the medium resolution spin up run there is large inter-annual variability in all the regions (Fig. 3.4). Comparing sea ice melt values between the high and medium resolution model, we demonstrate that in the medium resolution

model there is a substantial amount of freshwater input that within the first 5 years is between 2 to 4 times the amount of freshwater input there is in the high resolution model. This difference in magnitude of freshwater release between the two models is even larger later in the spin up run. Freshwater input from sea ice melt could be responsible for the freshening signal we see over the West Antarctic continental shelf.

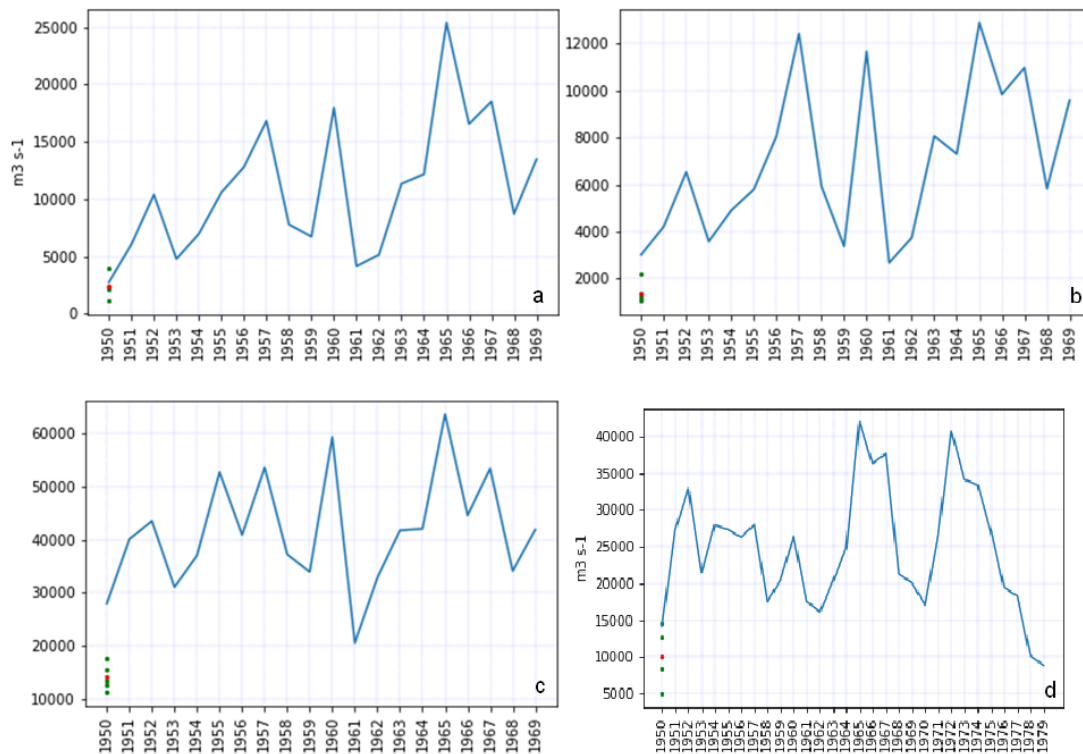


Figure 3.4: Annual mean sea ice melt in the regions (a) East Bellingshausen Sea, (b) West Antarctic Peninsula, (c) Antarctic Peninsula tip, (d) Bellingshausen Sea; green dots represent 5 annual means from the HadGEM3-GC3.1-HH model historical run, red is their average; blue line is annual means from the spin up run of the HadGEM3-GC3.1-MM

We calculated the fresh water budget in the Bellingshausen Sea and in the West Antarctic sector south of 70°S in order to identify the local freshwater sources

and the freshwater volume transport in each area. The surface freshwater flux is negative south of 70 °S and it is mostly driven by sea ice freeze (Fig.3.5). However, the total freshwater volume in the area is increasing, the driver of that being southward meridional transport. We hypothesise that there is a freshwater source north of that section and the meridional volume transport is driving the freshening south of 70 °S.

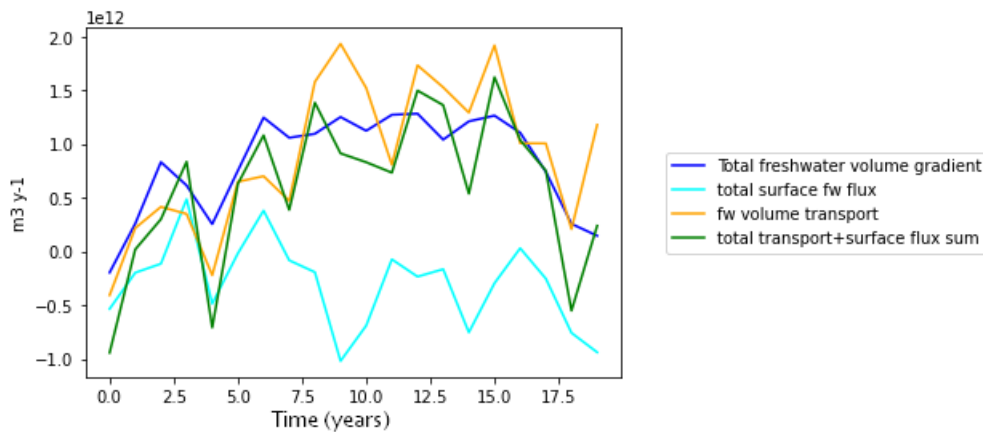


Figure 3.5: Timeseries of freshwater budget calculated over the closed region between 70° S and the coast. Dark blue line is the rate of change of freshwater volume within the closed area; Light blue line is the total freshwater surface flux including ice shelf melt; Orange line is the meridional freshwater volume transport in the closed area; Green line is the calculated sum of total surface freshwater flux including ice shelf melt and the freshwater volume transport in the closed area.

In the Bellingshausen Sea, the total surface freshwater flux is positive (Fig.3.6a) primarily due to ice shelf melt. The total freshwater volume transport is split into the meridional and zonal component (Fig.3.6b). The zonal volume transport is positive in the beginning of the run, but is decreasing, meaning that there is a decreasing trend in freshening sourced from the west, while the meridional transport is negative in the beginning of the run, but is increasing, so the freshening trend within the area is increased from the north. After year 13, the volume transport regime reverses and the Bellingshausen Sea is exporting freshwater to-

wards the west, while there is southward fresh water volume transport into the area (Fig.3.7).

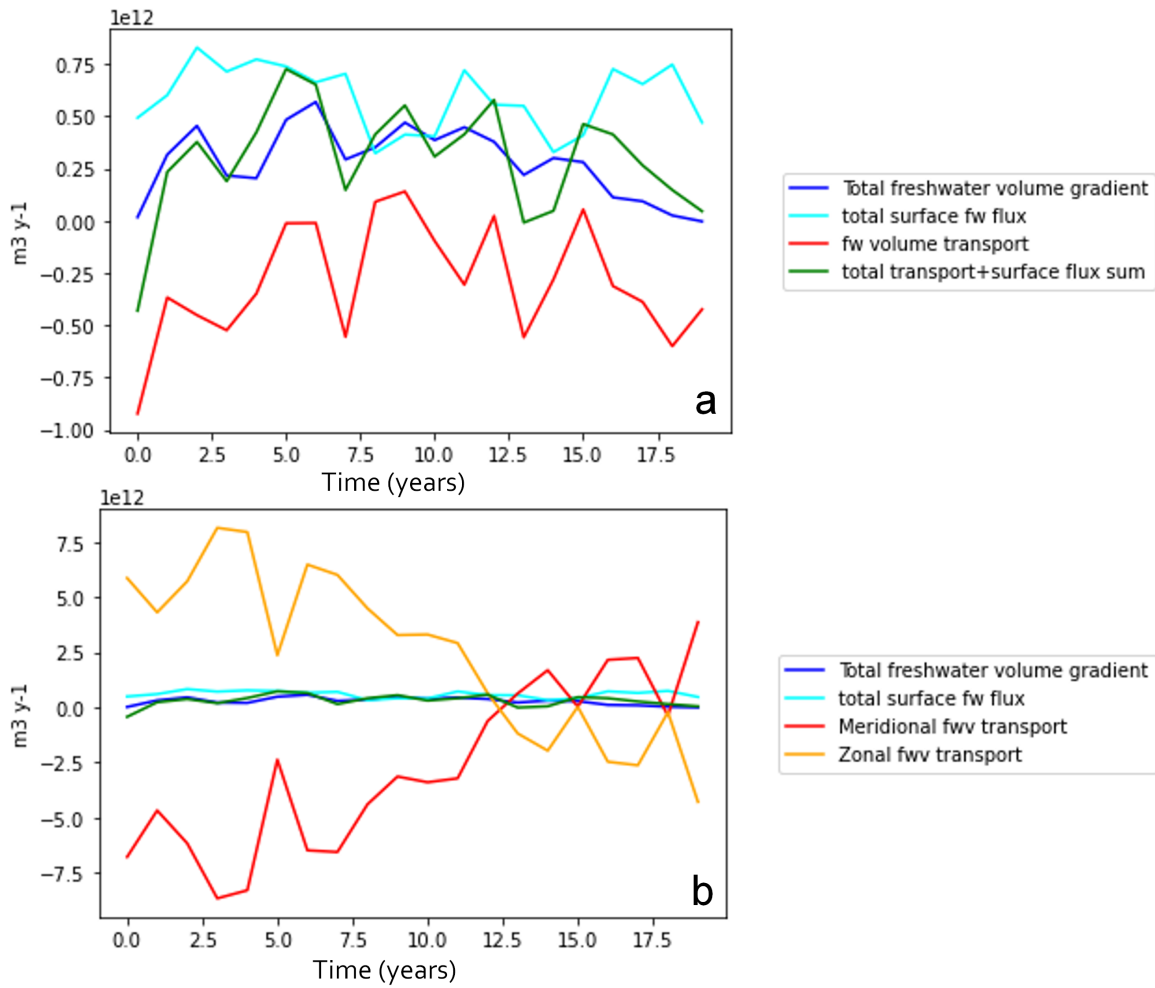


Figure 3.6: Timeseries of freshwater budget calculated for the Bellingshausen Sea. (a) As Fig. 3.5 but red line is the total freshwater volume transport in the closed area, (b) as Fig. 3.5 but red line is the meridional freshwater volume transport and orange line is the zonal freshwater volume transport in the closed area.

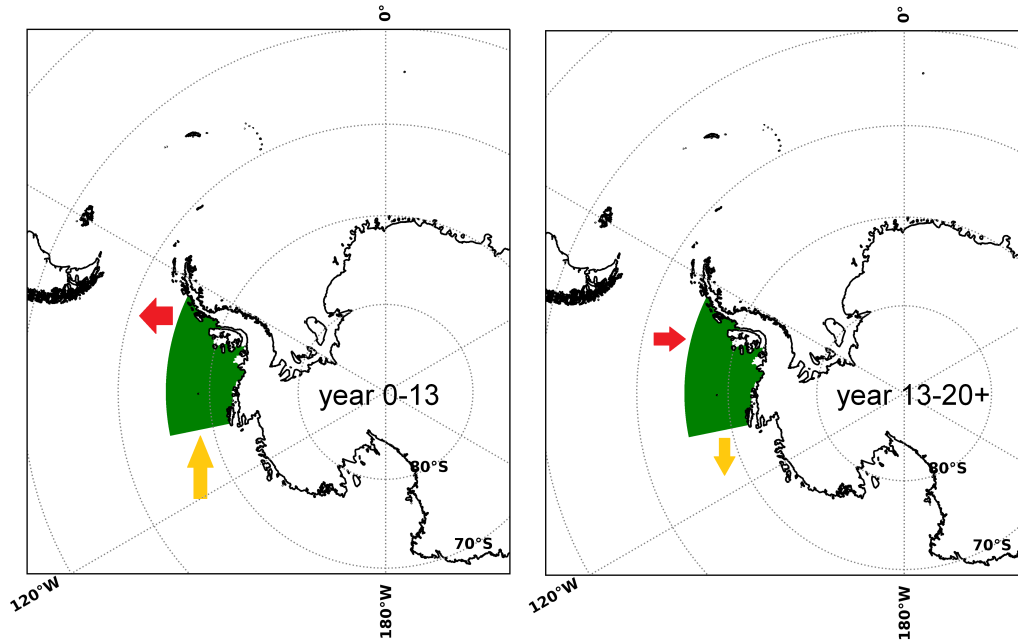


Figure 3.7: Schematic of changes in the freshwater volume transport in and out of the Bellingshausen Sea. Green shaded area is the Bellingshausen Sea region mentioned in Fig. 3.6

We hypothesise that there is a link between freshwater and circulation biases in the Amundsen and Bellingshausen Sea, and that freshwater advecting from the Bellingshausen Sea is prohibiting warm water intrusion on the Amundsen Sea continental shelf. In order to explore this further, we calculated the westward depth integrated freshwater volume transport from the Bellingshausen Sea to the Amundsen Sea continental shelf, and used 5 annual means from the historical run of the high resolution model for comparison (Fig. 3.8). There is a strong positive trend in the medium resolution model freshwater volume transport. The freshwater westward volume transport quadruples in the first 20 years of the spin up run and doubles in the first five years.

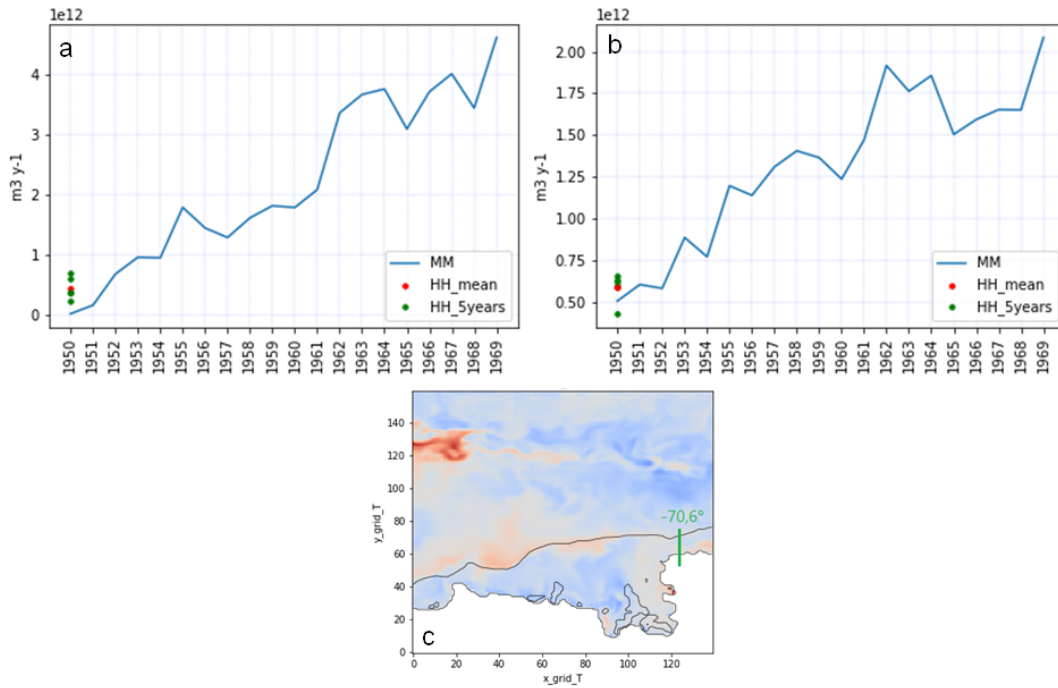


Figure 3.8: Annual mean timeseries of westward freshwater volume transport (Sv) through a section between the Bellingshausen and Amundsen Sea (green section) from the coast to (a) the continental slope and (b) the continental shelf break; Green dots represent the same for 5 annual means from the HadGEM3-GC3.1-HH model historical run, red is their average

Freshwater transport towards the Amundsen Sea is getting progressively stronger, and combined with the very high sea ice melt rates in Bellingshausen Sea and West Antarctic Peninsula (Fig. 3.4) we hypothesise that the West Antarctic continental shelf is entering in a cold and fresh state linked with the development of a westward slope current.

3.4 Particle Tracking

In this section we track particles released in different regions. We have performed experiments including backward and forward integrations with a monthly step, in 3 different regions and 2 different depths in the Amundsen Sea, 1 surface release in each of the Weddell Sea, Bellingshausen Sea and West Antarctic Peninsula (west of Drake Passage). Our motivation is to identify whether and how freshwater can be transported from these regions to the Amundsen Sea and how much time it takes. In the previous sections we showed that there is an extensive amount of sea ice melting in the Bellingshausen Sea and West Antarctic Peninsula (Fig. 3.4). The freshening trend in the Amundsen Sea appears during the first couple of years of the spin up run (Fig. 3.3) and by year 5 the biases have already become large enough to justify the claim that the model unrealistically represents the water masses on the West Antarctic continental shelf. For this reason we are choosing to track particles within a timescale of ≤ 5 years, during which freshwater from areas with extensive sea ice melt should already be advected in the Amundsen Sea, otherwise these regions could not be responsible for the freshening we observe in the Amundsen Sea. We will also test the hypothesis that the Weddell Sea could play a role in the Amundsen Sea freshening.

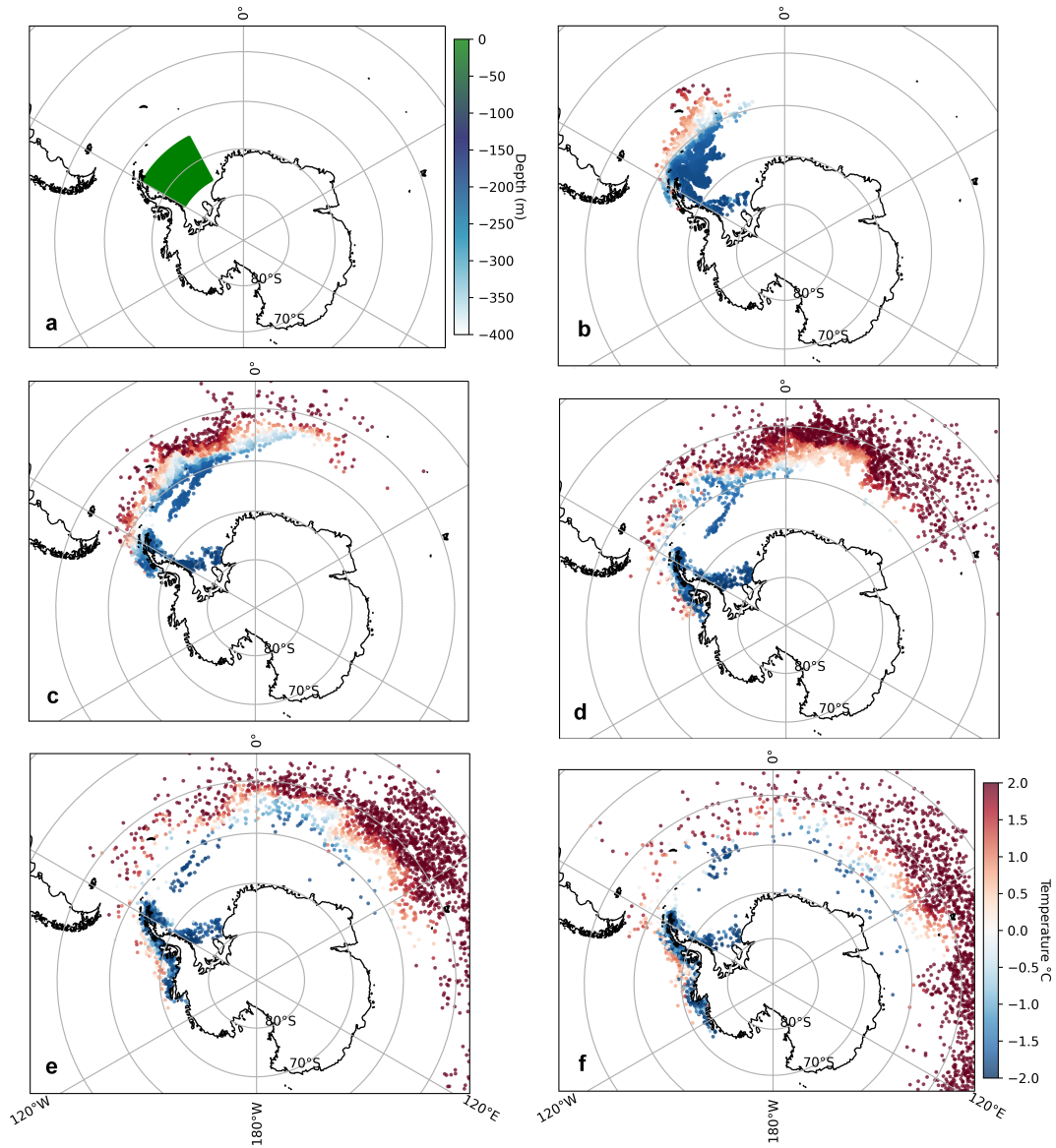


Figure 3.9: Weddell Sea particle release in location shaded green at the surface in (a) month 0. Snapshots of location and temperature of particles during (b) month 12, (c) month 24, (d) month 36, (e) month 48, (f) month 60

For the Weddell Sea experiment we released particles at the surface (Fig.3.9a) during the first month of the spin up and run it for 60 months (5 years). The majority of the particles follow the Weddell Sea gyre circulation, but some of them go around the tip of the Antarctic Peninsula onto the West Antarctic Peninsula

continental shelf, which is consistent with previous studies [Renner et al. \(2012\)](#). The particles going west at Drake Passage stay mostly on the West Antarctic continental shelf with temperature near -2°C . The end of year 4 is shown as a snapshot of month 48 (Fig. 3.9e), where only an insignificant amount of particles (0.0025%) reaches the Amundsen Sea. Within this time frame, the sea ice concentration in the Weddell Sea does not decline, on the contrary the sea ice area is slightly growing (Fig. 3.2a). By the end of year 5, there are particles present on the West Antarctic continental shelf originated from the Weddell Sea surface (Fig.3.9d) . However, this cannot explain the substantial Amundsen Sea temperature and salinity decline (Fig. 3.3) that predates the particles' arrival. We therefore conclude that the Weddell Sea is not initiating the changes we see in the Amundsen Sea in the first 4 years of the spin up run and another region must be responsible for that, possibly the Bellingshausen Sea which is the nearest and has the most sea ice melt.

We released particles at the surface of the purple shaded area in West Antarctic Peninsula, which has high sea ice melt rates (Fig. 3.4b), and track the particles for 48 months (Fig. 3.10). Some of the particles are getting advected by the ACC and move eastwards at Drake Passage, with a relatively warm temperature. At the end of year 3 (Fig. 3.10c) some particles have reached the east side of Amundsen Sea embayment in a formation that resembles the coastal current. At the end of year 4 (Fig. 3.10d) particles have travelled to the Amundsen Sea embayment. In contrast with the previous release in the Weddell Sea (Fig. 3.9e,f), these particles stay on the West Antarctic continental shelf and are positioned closer to the coast, remaining exclusively on the continental shelf and seemingly following the coastal current in the Bellingshausen and Amundsen Sea. The particles that made

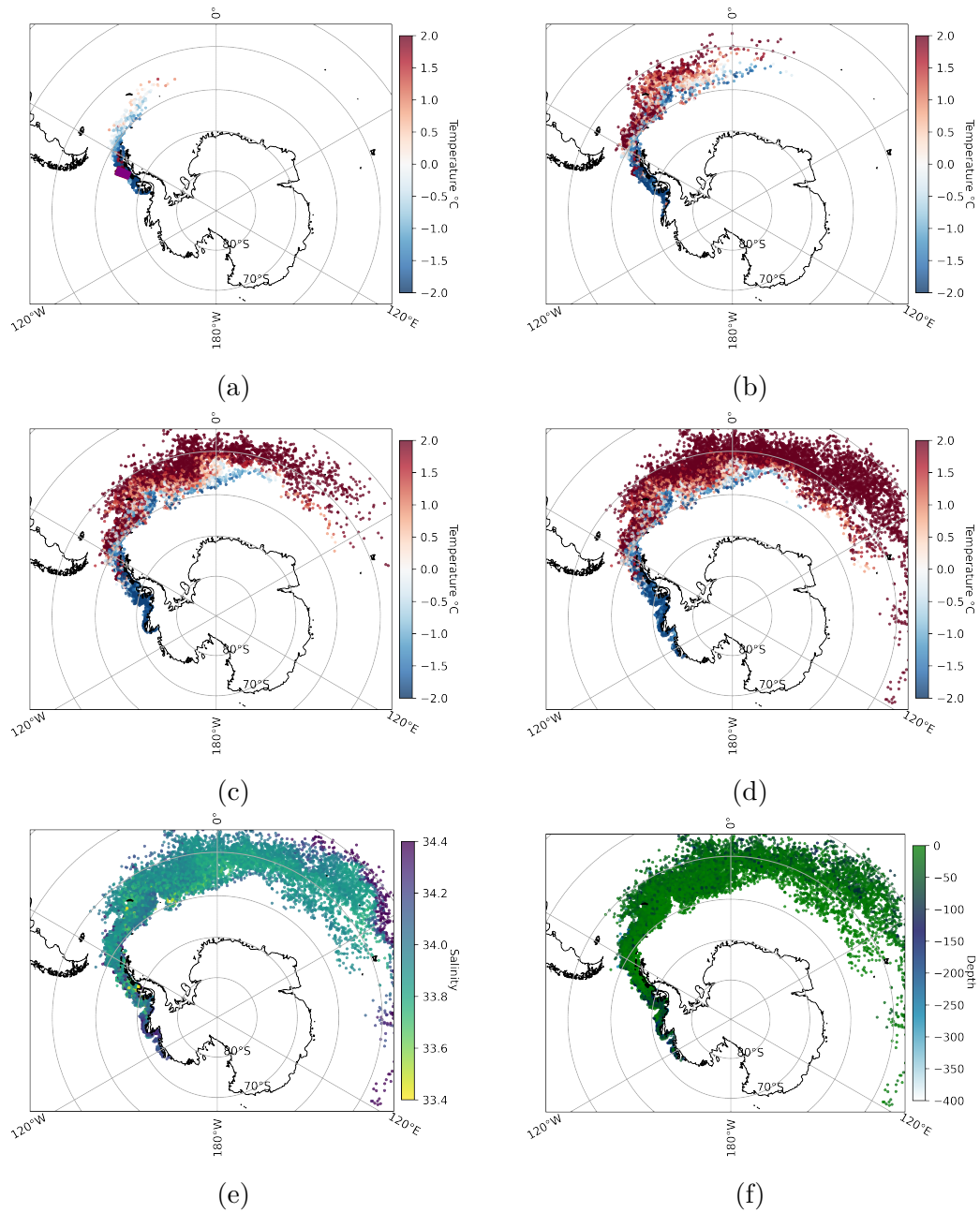


Figure 3.10: Temperature and position of particle released at the surface of the West Antarctic Peninsula (purple shaded area) during (a) month 12, (b) month 24, (c) month 36, (d) month 48. (e) Salinity during month 48, (f) depth during month 48.

it onto the Amundsen Sea continental shelf demonstrate relatively high salinity (Fig. 3.10e) and can be found in a variety of depths from the surface up to 400m (Fig. 3.10f), meaning that they are getting mixed with CDW. The time

taken for the particles to travel to the Amundsen Sea is consistent with the cold and fresh trend in different depths we see in the Amundsen Sea (Fig. 3.3b,c). Considering the high sea ice melt rates in West Antarctic Peninsula (Fig. 3.4b), and the pathway of the particles released there, fresh water anomalies could be transported from there to the Amundsen Sea (Flexas et al., 2022).

We have shown so far that the fresh and cold trend we see in the first 4 years in the Amundsen Sea (Fig. 3.2g; Fig. 3.3) cannot be explained by freshwater transported from the Weddell Sea, since it takes longer than that for the particles to arrive and there is not sea ice loss observed at that stage. However, the Weddell Sea sea ice has a downward trend from year 5 to 30 (Fig. 3.2a), and the westward volume transport in Drake Passage doubles in size (+20 Sv) during the same time (Fig. 3.2d), and could possibly be explained by the 20 Sv increase in northward volume transport in the Weddell Sea by the end of the run (Fig. 3.2c). While these changes in the Weddell Sea do not seem to initiate the changes we see in the West Antarctic continental shelf, we cannot exclude their contribution to the cold and fresh West Antarctic biases later on. For the purposes of this chapter we are interested in regions that undergo a large reduction in their sea ice, such as the Bellingshausen Sea (Fig. 3.4), and examining whether particles can be advected to the Amundsen Sea within the first years of the spin up run.

Next, particles are released at the surface of the Bellingshausen Sea. For the Bellingshausen Sea particle release (Fig. 3.11) we track particles for 12 months integrated forwards and backwards. The particles were released in the surface during the first month of the second year, and we show their location during the first month of the run (Fig. 3.11b) and month 24 (Fig. 3.11c,d). The hypothesis

we are testing here is that it roughly takes 12 months for the particles to advect from the Bellingshausen Sea to the Amundsen Sea, and that these particles were in the Bellingshausen Sea prior to that as well, meaning that they did not advect from another region.

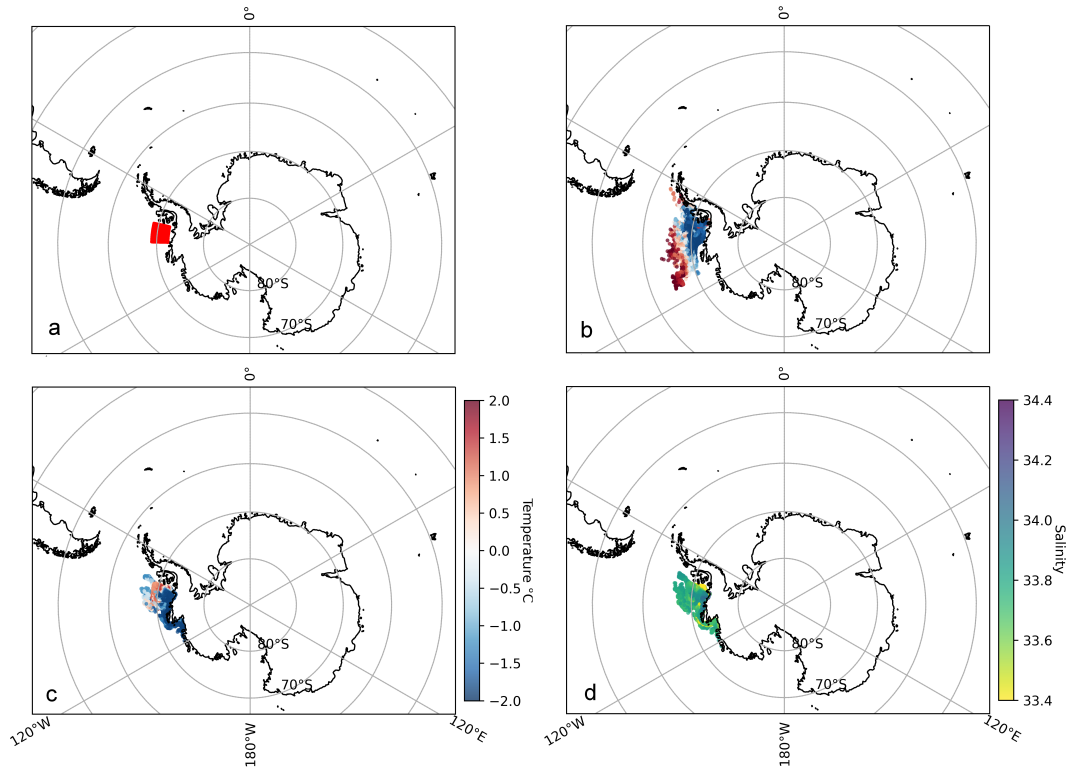


Figure 3.11: (a) Bellingshausen Sea particle release in location shaded red at the surface in month 12, (b) position and temperature of the particles in month 0, (c) position and temperature of the particles in month 24, (d) position and salinity of the particles in month 24.

The particles released in the Bellingshausen Sea (Fig. 3.11a) and tracked backwards are mostly local to the Bellingshausen Sea, while some of them are advected from further northwest, exhibiting warm temperatures above 2°C (Fig. 3.11b). While the majority of particles released near the West Antarctic Peninsula followed the coastal current from the Bellingshausen Sea to the Amundsen Sea conti-

mental shelf (Fig. 3.10), tracking the particles backwards from the Bellingshausen Sea revealed that the majority of them is either local or coming from a region where we have shown it has high sea ice melt rates (Fig. 3.4d). Tracking the particles forwards to month 24 (Fig. 3.11c,d), we see that cold and fresh particles are getting advected to the Amundsen Sea continental shelf. Within 12 months from their surface release, particles advected towards the west have reached the Amundsen Sea continental shelf, with salinity mostly below 33.8 and relatively cold temperatures. It takes roughly a maximum of 2 years for particles that are in the Bellingshausen Sea, a region with high rates of sea ice melt, to be advected onto the Amundsen Sea continental shelf (Fig. 3.11). This is consistent with the freshening trend we observe in the initial years of the run and the reduction in maximum temperature on the Amundsen Sea continental shelf. The time frame of these results agrees with the reversal and strengthening of the slope current that connects the Amundsen and Bellingshausen Sea (Fig. 3.5).

Next in this section we track particles backwards from 3 different 'boxes' in the Amundsen Sea, one in front of the Pine Island ice shelf, another near the shelf break and lastly one in the west Amundsen Sea, all released at 300m depth during month 48. We have already shown that in the Amundsen Sea the freshening trend is below 200m depth (Fig. 3.3c), rather than the surface, so we chose the 300 m release depth to ensure we capture the source of this. We have shown that particles from the Bellingshausen Sea and West Antarctic Peninsula can reach the Amundsen Sea within less than 4 years (Fig. 3.10; Fig.3.11). Tracking the particles backwards from the Amundsen Sea will allow us to demonstrate that there is no other potential fresh water source that is unaccounted for.

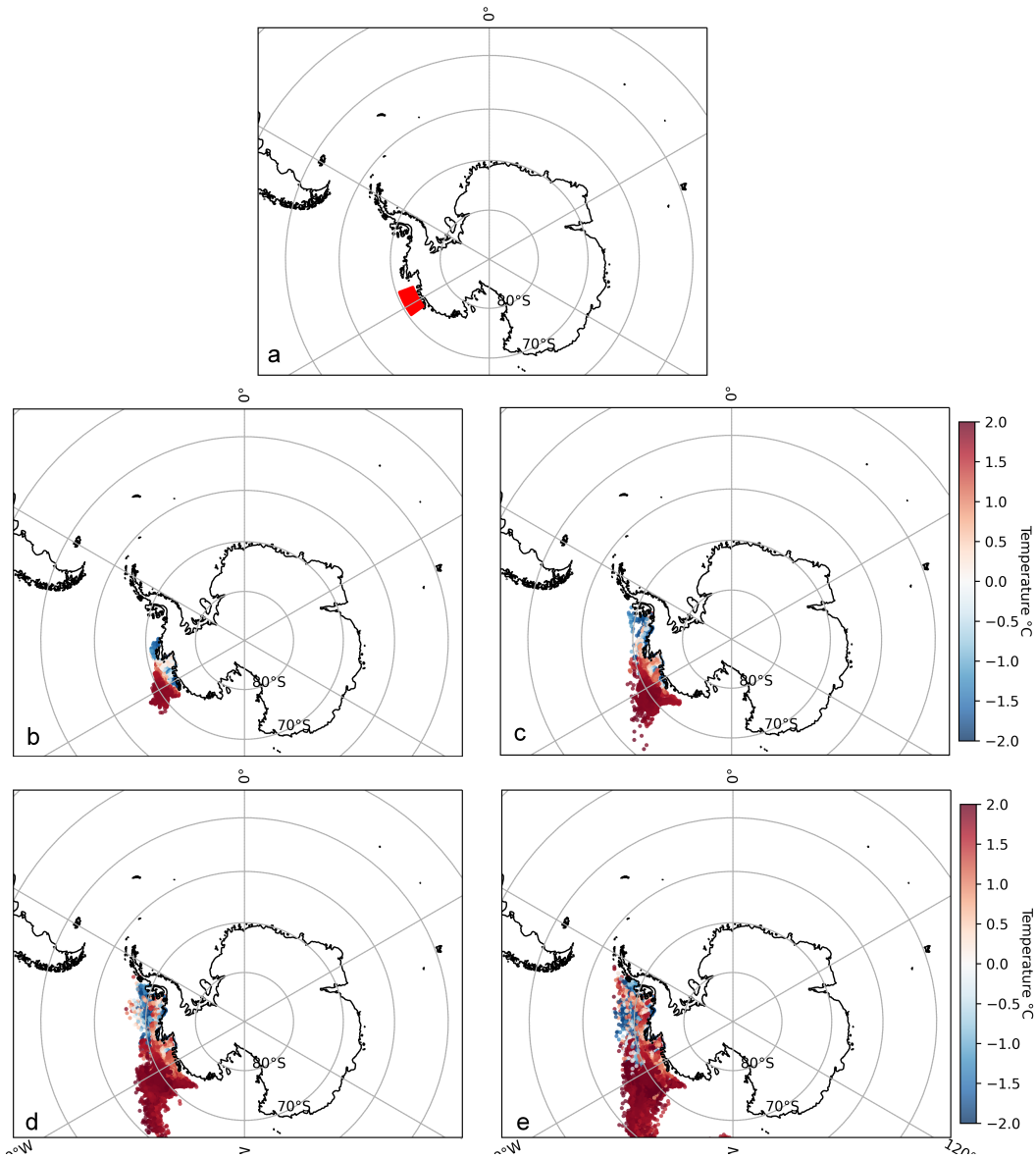


Figure 3.12: Amundsen Sea particle release in location shaded red at 300m depth (a) in month 48. Snapshots of position and temperature of the particles in (b) month 36, (c) month 24, (d) month 12, (e) month 0.

The temperature and position of the particles during month 36, a year back from their release in the west Amundsen Sea in month 48, demonstrate that there is warm water present near the continental shelf break, with temperature around 2°C, however on the continental shelf itself the temperature is less than 0.5°C

(Fig. 3.12b). Colder particles are advected from the Bellingshausen Sea, and by month 24, 2 years prior to the release, it is evident that particles with temperature below 0°C originate from the Bellingshausen Sea continental shelf (Fig. 3.12c). Tracking the particles backwards to year 1 and 2 of the run we observe that there are two distinct particle sources, the Bellingshausen Sea and the relatively warm CDW (Fig. 3.12d,e).

Particles released at 300m depth, in two different areas in the Amundsen Sea, were tracked backwards from month 48 (Fig. 3.13a,b; Fig. 3.14a,b). In both cases, the particles a year prior to their release (month 36) were on the Bellingshausen Sea continental shelf, concentrated near the coast and seemingly being advected by the coastal current, and on the slope of the Amundsen Sea continental shelf (Fig. 3.13c,d). There is a distinct temperature difference between the particles in the Bellingshausen Sea and the ones on the continental slope, the latter being warmer than 2°C . Despite the release in two different regions, one being in front of the Pine Island ice shelf and the other being near the shelf break in the east (Fig. 3.13a,b; Fig. 3.14a,b), the trajectories of the particles have a similar spatial and temporal pattern.

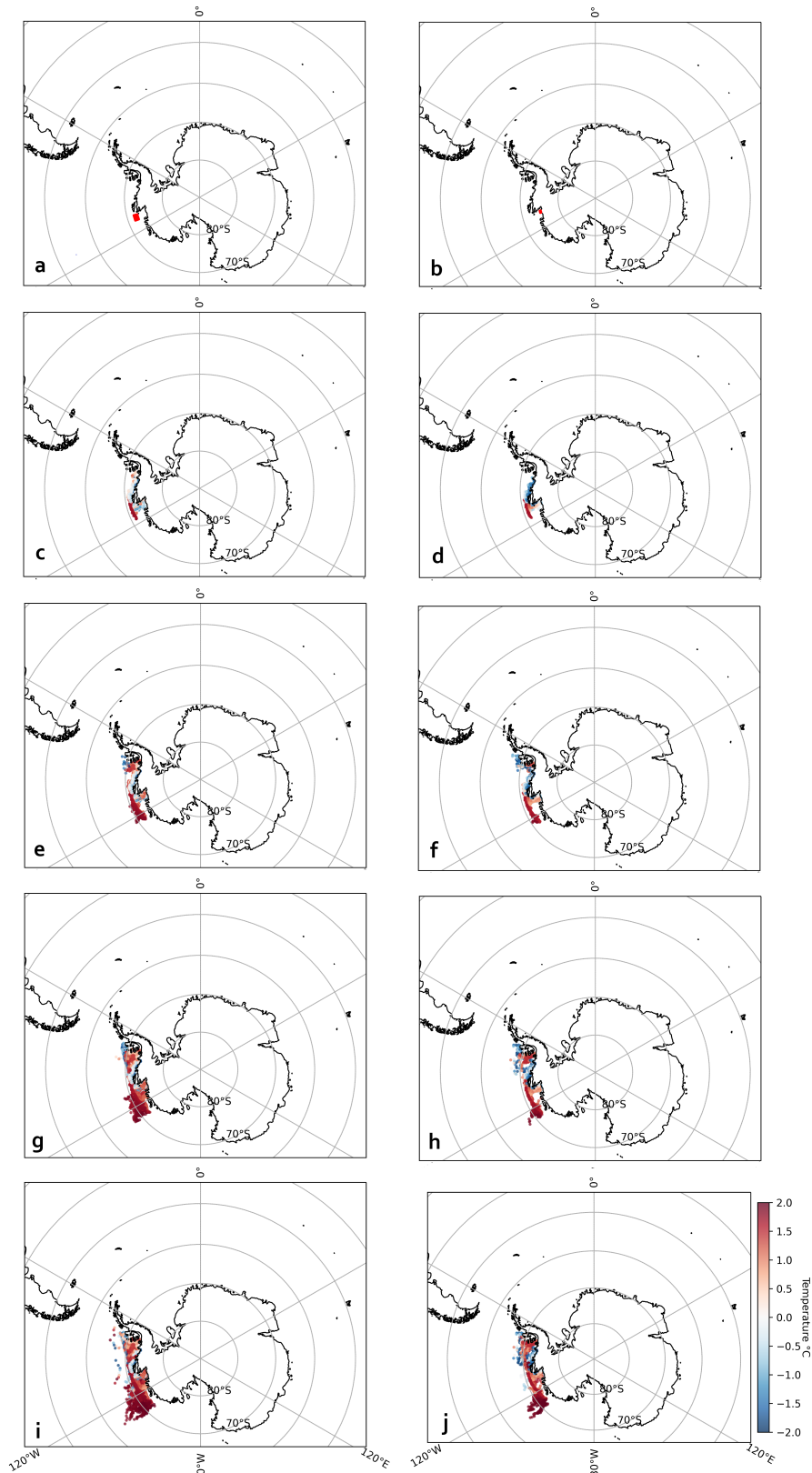


Figure 3.13: Amundsen Sea particle release in 2 location shaded in red at 300m depth (a), (b) in month 48 . Snapshots of position and temperature of the particles in (c), (d) month 36; (e), (f) month 24; (g), (h) month 12; (i), (j) month 0.

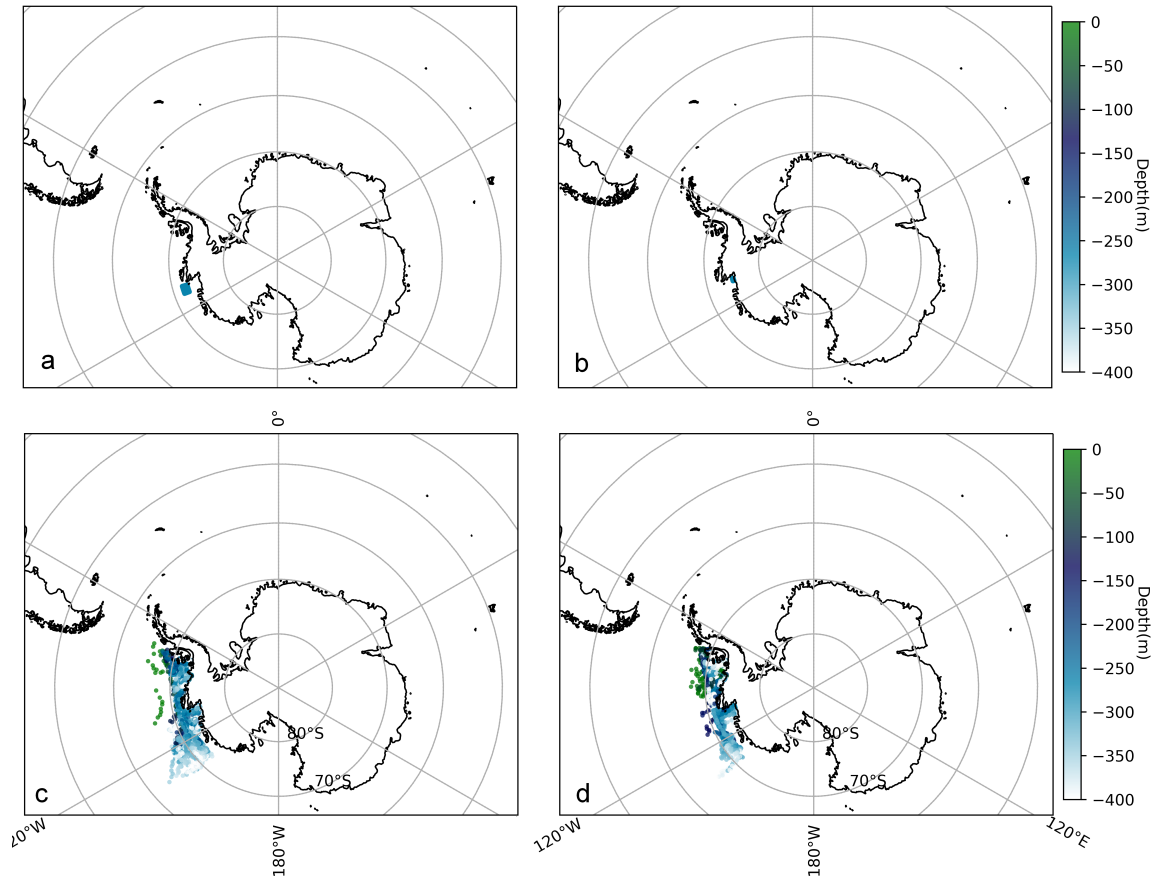


Figure 3.14: Amundsen Sea particle release in 2 location shaded in blue at 300m depth (a), (b) in month 48. Snapshots of position and depth of the particles in (c), (d) month 0.

Tracking the particles back to the beginning of the model run we can distinguish one source that is deep warm water from further north of the Amundsen Sea continental shelf and another source with a more mixed temperature profile, varying from cold to relatively warm water, in the Bellingshausen Sea (Fig. 3.13i,j). The water properties on the Amundsen Sea continental shelf are a result of mixing between water originating from the Bellingshausen Sea and CDW. The particles depth profile for the warm water source is deeper than 250m, which is consistent with the CDW depth range (Fig. 3.14c,d). Particles that advected from

the Bellingshausen Sea continental shelf were present at all ranges of depths (Fig. 3.14c,d). However, the particles that have been advected from further offshore in the Bellingshausen Sea are found exclusively at the surface.

3.5 Discussion and Conclusions

In this chapter we established the evolution of temperature, salinity, sea ice and transport biases in the spin up run of the medium resolution HadGEM3 model. Our main goal was to investigate further the origins of these biases, that we show more extensively in the previous chapter, by using data from the spin up run. We found that the time frame of the development of these biases indicates a relationship between excessive sea ice melt (Fig. 3.4) and rapid subsurface freshening on the West Antarctic continental shelf (Fig. 3.3). By the end of the spin up run, the West Antarctic continental shelf state has shifted into a cold and fresh regime (Fig. 3.1), with a westward slope current (Fig. 3.2f).

In Chapter 2 we showed that in the historical run of the medium resolution HadGEM3 the West Antarctic continental shelf is fresh and cold with a very strong westward slope current and that the Weddell Sea has warm SST biases (Fig. 2.2c,e) and virtually no sea ice (Fig. 2.1). Here we investigated whether the Weddell Sea biases could be responsible for the initiation of an extended westward slope current in the West Antarctic sector, transporting fresh water and shutting down the ACC supply of warm water on the continental shelf. We found that biases in sea ice, temperature, salinity and transport in West Antarctica are present early in the spin up run, before we observe any biases develop in the Weddell Sea (Fig. 3.1, 3.2). In addition to that, we tracked particles from the Weddell Sea and show that a minimum of 5 years is needed in order for some of them to reach the

Amundsen Sea continental shelf (Fig. 3.9), while large salinity and temperature biases are observed on the Amundsen Sea continental shelf by year 3 of the spin up run (Fig. 3.3).

The Weddell Sea does not play a role in the West Antarctic biases, at least not early on in the spin up run, but there is a fresh water source that is causing the freshening in West Antarctica. Here we propose that a strong positive trend of excessive sea ice melt, particularly in the Bellingshausen Sea and West Antarctic Peninsula (Fig. 3.4) is linked to the initiation of a strong westward slope current in West Antarctica, that prohibits warm water intrusion on the continental shelf.

Chapter 4

Future projections in West Antarctica using the high resolution model HadGEM-HH

4.1 Introduction

Antarctic continental shelf water changes can influence the Southern Ocean circulation ([Marshall and Speer, 2012](#)) and recent observations suggest that changes in shelf temperature and salinity can be attributed to increased melt water ([Bronse-laer et al., 2020](#)). Modelling studies that used freshwater forcing in low resolution models found an increase in sea ice and strong subsurface warming ([Beadling et al., 2022](#); [Richardson et al., 2005](#)). The Antarctic slope current cannot be resolved in low resolution models and it has been found that models that can resolve it realistically can have a fresher continental shelf ([Lockwood et al., 2021](#)). The

future response to increased freshwater in the Southern Ocean is uncertain, with low resolution models exhibiting deep warming, while higher resolution models respond to an increase in freshwater with deep cooling, so the future response to increased freshwater in the Southern Ocean remains uncertain (Beadling et al., 2022).

After careful evaluation of the 4 models in Chapter 2, we selected the high resolution HadGEM3 model as the best performing model and here we analyse its projected changes under the Shared Socioeconomic Pathway 5 scenario (SSP585) (Haarsma et al., 2016). The high resolution HadGEM3 has the best performance in the historical run and it can represent sea ice concentration, temperature, salinity and circulation realistically. Based on its performance in the historical run and its high horizontal resolution, this model's projected changes can add valuable information to the discussion about changes on the West Antarctic continental shelf under a changing climate.

In this chapter, we will focus on changes in deep salinity and temperature on the Amundsen Sea continental shelf under the SSP585 scenario. This is the only future scenario available to the high resolution HadGEM. The run starts at 2015 and stops at 2050, meaning that there is only a total of 35 years available. Nevertheless, we are expecting to see some changes even in this short amount of time, since the radiative forcing in this scenario is the highest among all the pathways, around 5 W/m^2 by 2050 (O'Neill et al., 2016). We hypothesise that due to increasing sea surface temperatures under this extreme scenario, the sea ice will decline rapidly. We have shown in Chapter 3 that changes in sea ice in higher than 1° horizontal resolution models can affect subsurface salinity and circulation. We will therefore investigate the implications of sea ice concentration changes in the Amundsen Sea,

Weddell Sea and Drake Passage circulation as well.

Lastly, we will briefly show future projections of temperature on the Amundsen Sea continental shelf under the SSP585 scenario from the rest of the models used in this thesis, UKESM1 and the low and medium resolution HadGEM, in order to compare them with the high resolution HadGEM. Output from 22 CMIP6 models and under the SSP585 scenario shows an average warming of continental shelf bottom water of 0.62°C by 2100, however the majority of the models considered in this study by [Purich and England \(2021\)](#) have a low horizontal resolution.

4.2 Changes on the West Antarctic continental shelf

During the first year of the SSP585 scenario run, the annual mean of maximum subsurface temperature on the Amundsen and Bellingshausen Sea continental shelf is around 1°C , while on the Weddell Sea continental shelf it is near -2°C (Fig. 4.1a). Half way through the run, the maximum subsurface temperature on the Amundsen Sea continental shelf increases slightly; however, we observe deep cooling on the Bellingshausen Sea continental shelf and no changes in deep temperature on the Weddell Sea continental shelf (Fig. 4.1b). The cooling on the Bellingshausen Sea continental shelf in the middle of the run is accompanied by freshening (Fig. 4.1e) and the complete disappearance of sea ice (Fig. 4.1h). Meanwhile, we observe significant sea ice loss in the Amundsen and Weddell Sea as well (Fig. 4.1h). During the last year of the run, the maximum subsurface temperature in the Amundsen Sea is near 0°C , while on the Bellingshausen and

Weddell Sea continental shelf it is below 0°C . By the end of the run, the maximum temperature off the Weddell Sea continental shelf is warmer than at the start of the run by almost 1°C (Fig. 4.1c), while the whole West Antarctic and Weddell Sea continental shelf is notably fresher (Fig. 4.1f), and the sea ice has almost vanished (Fig. 4.1i).

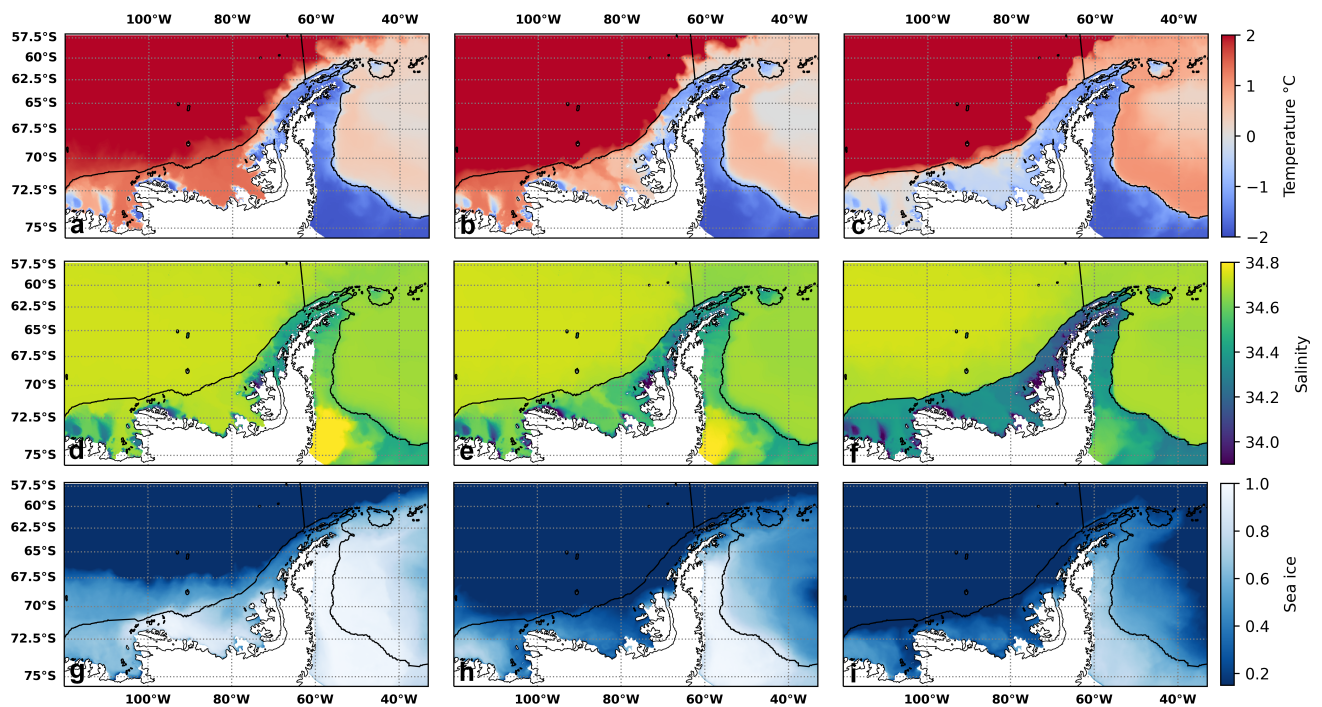


Figure 4.1: (a),(b),(c) Maximum subsurface temperature , (d),(e),(f) maximum subsurface salinity, (g),(h),(i) sea ice concentration ; black contours indicate the 1000 m isobath; annual mean of the (a),(d),(g) beginning of the spin run, (b),(e),(h) middle of the spin run, (c),(f),(i) end of the spin run.

We further examined the annual change of the water column temperature in three different grid points on the Amundsen Sea continental shelf (Fig. 4.2).

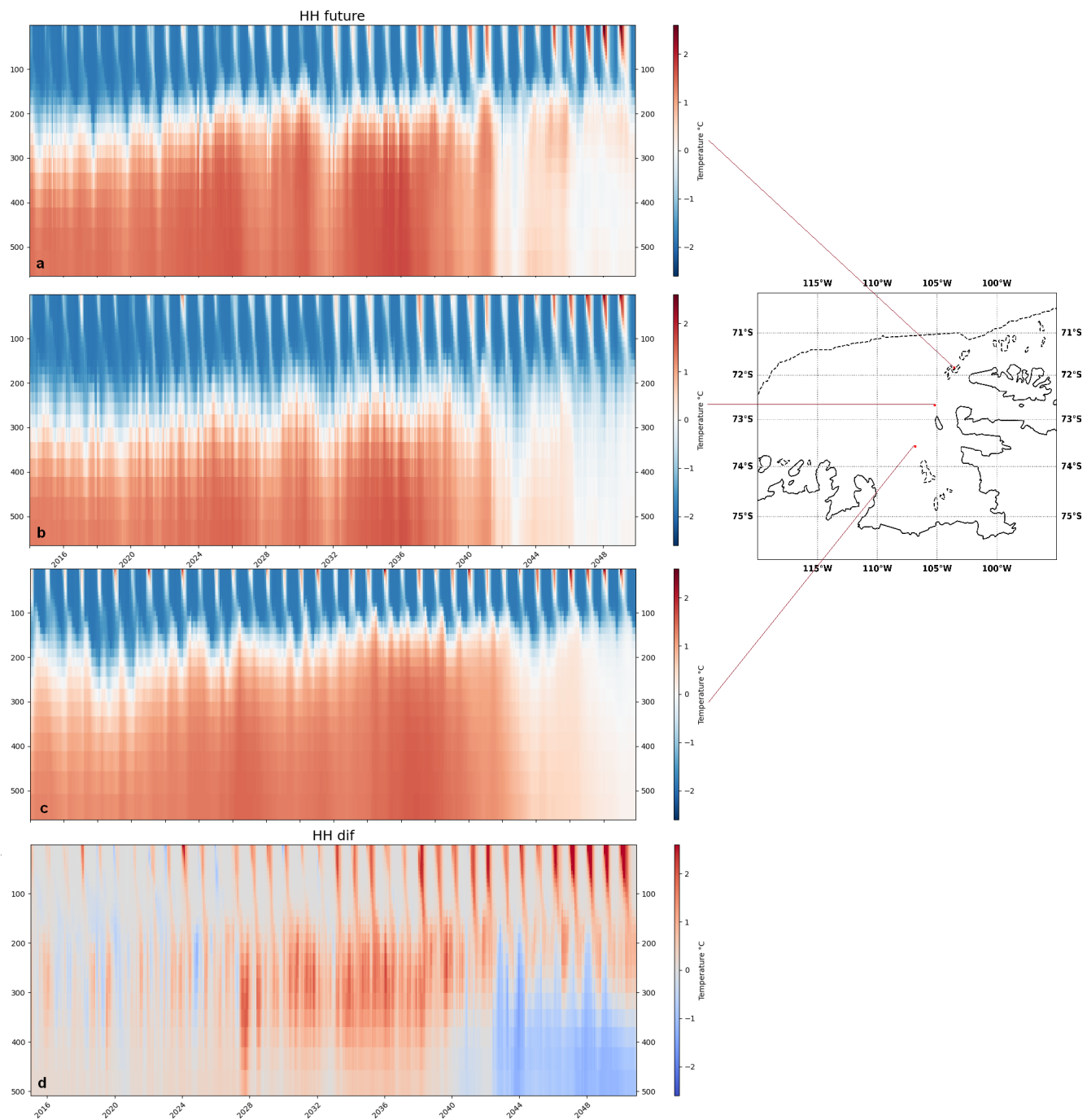


Figure 4.2: (a-c) Monthly mean temperature on the Amundsen Sea continental shelf under the SSP585 scenario; (d) difference of the central grid cell temperature between the SSP585 scenario and the equivalent years of the control run.

The grid points were chosen in a way that allows us to cover a variety of distances from the continental shelf break (Fig. 4.2a). While there is some inter-annual variability, it is clear that there is a period of deep warming preceding a period of deep cooling in all the selected grid points, regardless their distance from the continental shelf break (Fig. 4.2b,c,d). From year 2042 to year 2043, we observe the first major yearly change in deep temperature, after which the inter-annual variability seems stronger at the grid point closer to the continental shelf break where we observe what seems to be alternating pulses of warm and cold water. There is deep cooling during the last years of the run, but there is also substantial warming in the upper 100 m (Fig. 4.2b,c,d).

The surface, subsurface and deep salinity is decreasing throughout the model run (Fig. 4.3b). The surface and subsurface layers are fresher during the last years of the run compared to the initial years. This is consistent with the decrease in sea ice (Fig. 4.1 g,h,i). The surface temperature is increasing during the summer months throughout the run, and the warm temperatures are persistent for a longer period of time during the year (Fig. 4.3a) resulting in less sea ice formation and a fresher subsurface layer (Fig. 4.3b). Deep freshening is present during the last years of the run (Fig. 4.1d,e,f; Fig. 4.3b), however the changes in salinity are not as immense as the temperature changes. These changes (Fig. 4.3) are consistent with the development of the westward slope current in the Amundsen Sea (Fig. 4.4).

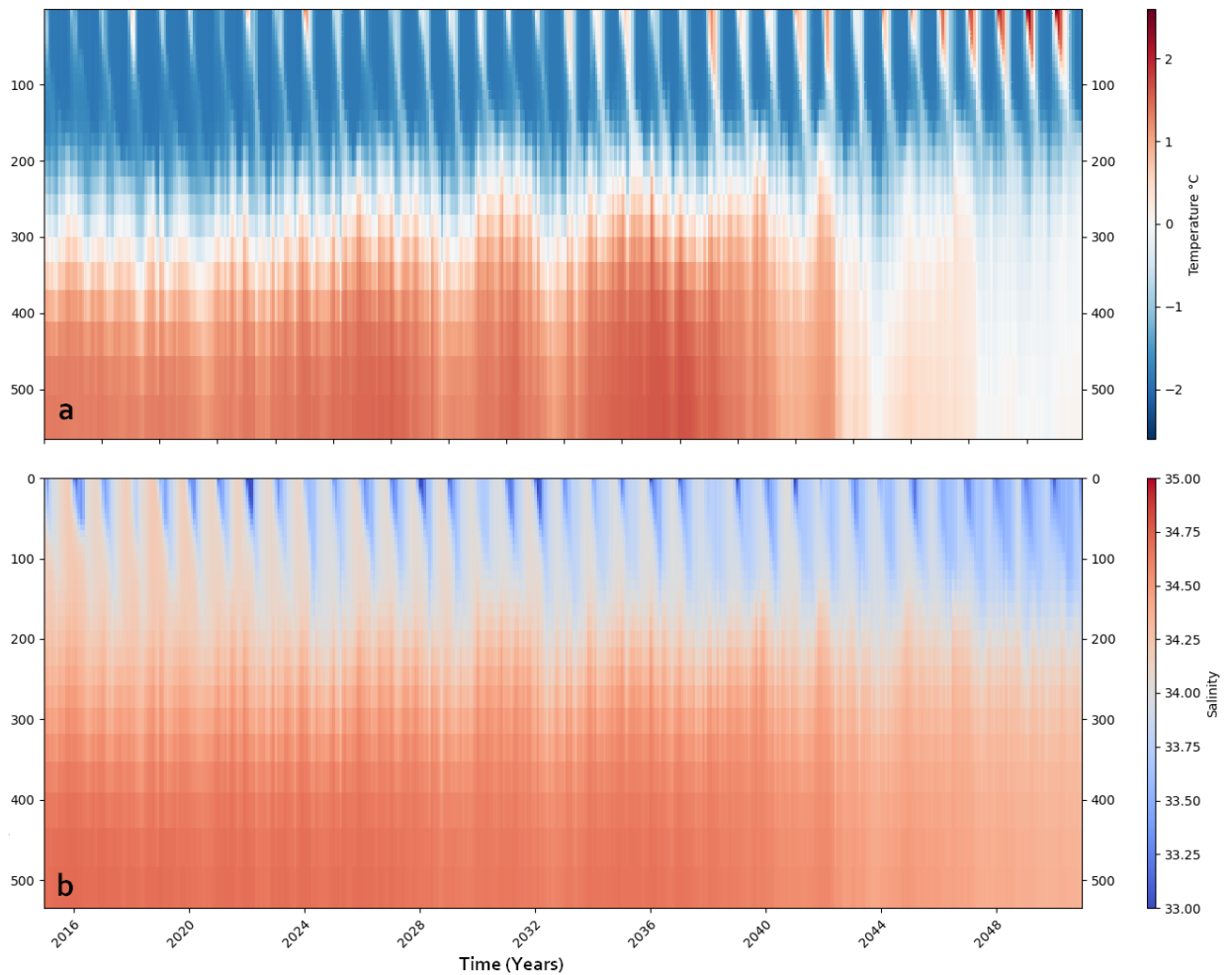


Figure 4.3: Monthly mean (a) temperature and (b) salinity on the Amundsen Sea continental shelf under the SSP585 scenario.

We have established in the two previous chapters a relationship between the strength and direction of the slope current and the temperature and salinity on the Amundsen Sea continental shelf. Similar to our previous results, that show a relationship between the freshening and deep cooling on the Amundsen Sea continental shelf and a westward slope current, we also found here the initiation of a westward slope current in the Amundsen Sea continental shelf slope (Fig.

4.4). While in the first years of the run the total volume transport is eastward, it reverses soon after and a strong westward slope current appears (Fig. 4.4a,b).

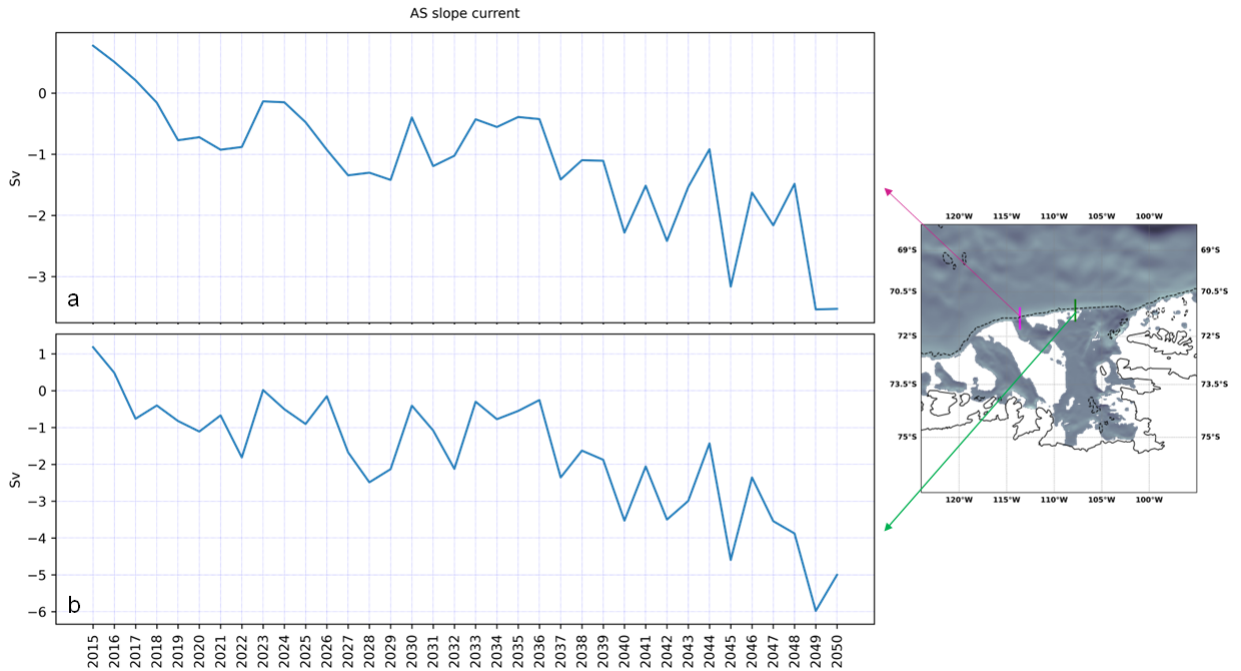


Figure 4.4: Timeseries of volume transport (Sv) in two cross sections on the Amundsen Sea continental slope.

The creation of a westward slope current and its front in the Amundsen Sea can tilt the isopycnals and inhibit warm water intrusion on the continental shelf and its creation is related to freshening throughout the whole West Antarctic continental shelf (Thompson et al., 2018). In the real world the Antarctic slope current is not present in the West Antarctic continental shelf, and does not continue past the tip of the Antarctic Peninsula. We hypothesise that changes in Drake Passage and the Weddell Sea such as sea ice reduction (Fig. 4.1 g,h,i), can influence the strength of the slope current locally and allow its continuation west of the Drake Passage and at the West Antarctic Peninsula. Another possible mechanism that could initiate a westward slope current in West Antarctica is strong freshening of the

West Antarctic continental shelf through local sources such as surface freshwater flux from extensive sea ice melt.

Here, the reversal and strength of the slope current in the Amundsen Sea continental shelf (Fig. 4.4) seems to be related to the strength of the Drake Passage total volume transport (Fig. 4.5a). There are big differences between the volume transport in Drake Passage during the first and the last year of the run (Fig. 4.5), and we found strong westward volume transports up to 10 Sv at the last year of the run (Fig. 4.5b). We hypothesise that these changes influence remotely the deep cooling and freshening on the Amundsen Sea continental shelf through a series of events. Half way through the run we observe deep freshening and cooling in the Bellingshausen Sea (Fig. 4.1b,e) as well as the disappearance of the sea ice there and extreme sea ice reduction in the Weddell Sea (Fig. 4.1h). At the same time in the run, a westward slope current has developed in the Amundsen Sea (Fig. 4.4), however on the Amundsen Sea continental shelf there is no deep cooling and freshening yet (Fig. 4.1b,e; Fig. 4.2). The evolution of the westward slope current in the Amundsen Sea (Fig. 4.4) is in agreement with the changes in the Drake Passage total volume transport (Fig. 4.5a). During the final years of the run we show major sea ice reduction in the Weddell Sea and West Antarctica (Fig. 4.1i), as well as strengthening of the westward velocities in Drake Passage (Fig. 4.5a) and the westward slope current in the Amundsen Sea (Fig. 4.4).

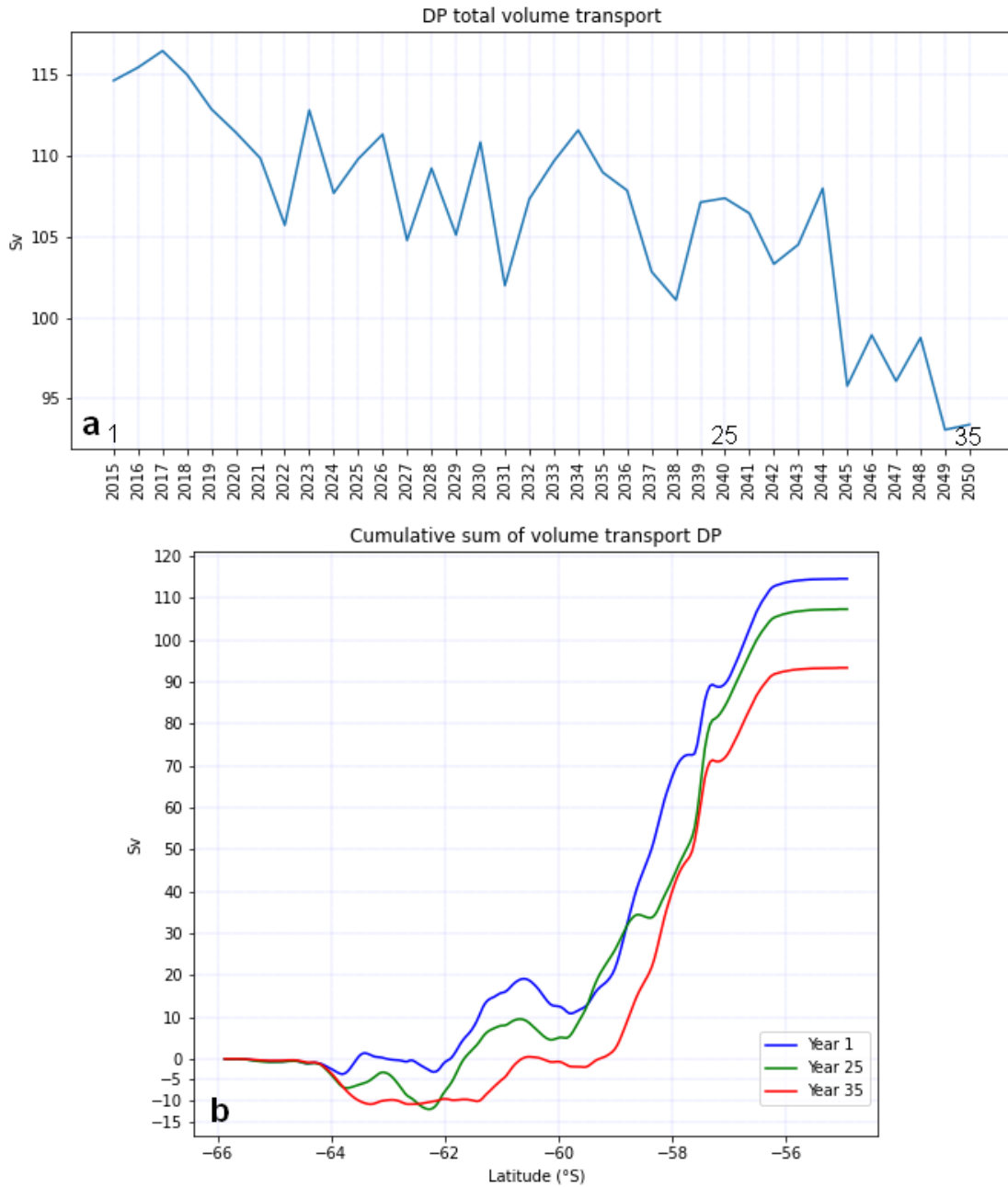


Figure 4.5: (a) Timeseries of annual mean total volume transport in Drake Passage (Sv), (b) Cumulative sum of total volume transport in Drake Passage (Sv), blue: year 1, green: year 25, red: year 35.

Most of the changes we show in this chapter seem to happen simultaneously; changes in the Amundsen Sea slope current, Drake Passage volume transport,

notable sea ice reduction in West Antarctica and the Weddell Sea and subsurface cooling and freshening in the Bellingshausen Sea. The relationship between the above-mentioned processes is not investigated in such detail as in the previous chapter, however, they are clearly related and responsible for the deep cooling and freshening we see on the Amundsen Sea continental shelf at the end of the run. We hypothesise that excess freshwater is initiating and strengthening the westward slope current in the Amundsen Sea, that in return is prohibiting warm water intrusion on the continental shelf. Lastly, a noteworthy result is that while the Bellingshausen Sea is showing deep freshening in the middle of the run (Fig. 4.1d,e), a westward slope current has been created in West Antarctica (Fig. 4.4), and the sea ice has been significantly reduced (Fig. 4.1h), the Amundsen Sea continental shelf is showing deep warming (Fig. 4.1a,b), before it enters its deep cooling state towards the end of the run (Fig. 4.1c).

4.3 Future projections from other UK climate models

Before we discuss the results of this chapter and make any conclusions, we will show the future projection of temperature on the Amundsen Sea continental shelf under the SSP858 scenario of the two low and the medium resolution HadGEM3 models. The horizontal resolution of these models allows them to run for a longer time, hence their projections are run up until the end of this century, 2100, instead of 2050 which is the end of the high resolution HadGEM3 SSP858 run. Our aim is to confirm that horizontal resolution differences between the models we use in our study have not only an impact on their present-day biases, but in their future

projections as well.

Both the low resolution models show surface and deep warming on the Amundsen Sea continental shelf by the end of the run (Fig. 4.6a,b). The low resolution HadGEM3 starts with less inter-annual variability than the UKESM model, and has a stronger deep warming trend, which is initiated earlier in the run (Fig. 4.6a,b). The results of these two models agree with the deep water warming trend that is usually present in low resolution CMIP6 models under climate change scenarios (Purich and England, 2021).

The Amundsen Sea continental shelf water is relatively cold in the medium resolution model (Fig. 4.6c), which is due to the biases discussed in Chapters 1 and 2. However, just a few years before the middle of the century, the deep water starts to get warmer and by the end of the run, the deep water state on the Amundsen Sea continental shelf has reversed into a warm one (Fig. 4.6c). This raises questions regarding the reversibility of a cold or warm deep water state on the Amundsen Sea continental shelf (Caillet et al., 2023).

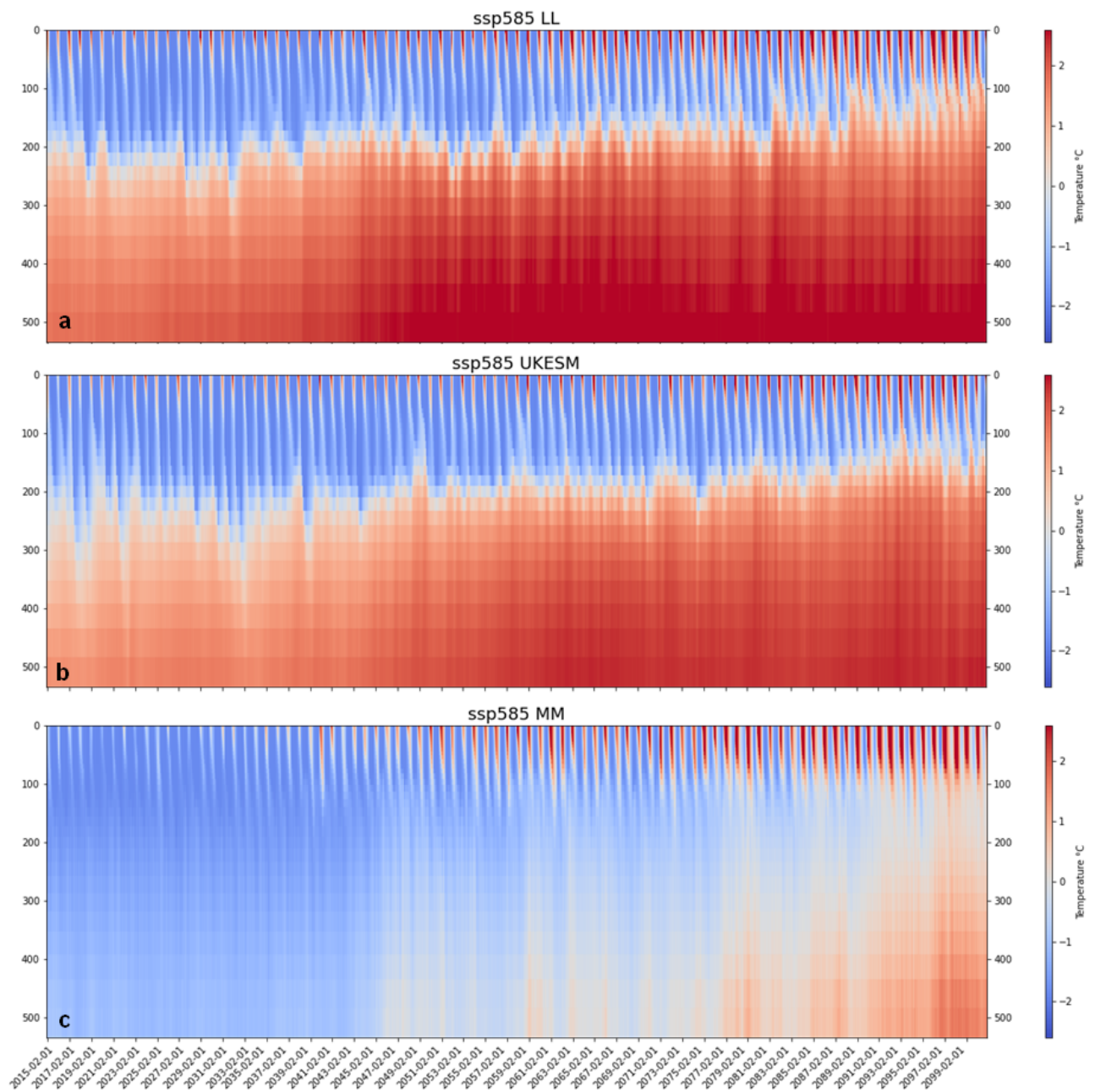


Figure 4.6: Future projection of temperature on the Amundsen Sea continental shelf under the SSP585 scenario, years 2015-2100 (a) HadGEM-LL, (b) UKESM1, (c) HadGEM-MM.

4.4 Conclusions and discussion

In Chapter 2, we showed that the high resolution HadGEM3 model performs the best among the selected 4 models in representing realistically present day temperature, salinity, volume transport and sea ice in the Southern Ocean. In this chapter we investigated future projections of deep temperature and salinity on the Amundsen Sea continental shelf under the SSP585 scenario of the high resolution HadGEM3 model. Even though the model has run for only 35 years under the SSP585 scenario, we found deep cooling on the West Antarctic continental shelf, the development of a westward slope current and disappearance of sea ice in the Weddell Sea and West Antarctica.

Our results are in disagreement with the projected bottom water warming under the SSP585 scenario across CMIP6 models ([Purich and England, 2021](#)). The majority of CMIP6 models used have a low horizontal ocean resolution of 1° , a warm bias in Antarctic shelf bottom water and sea ice biases. It has been suggested that eddy parameterisation versus eddy representation in a model can influence its response under future projections ([Hewitt et al., 2020](#)), so the differences between our results and previous studies that are using mainly low resolution models are not entirely unexpected. The other 3 models we show here, the two low resolution and the medium resolution HadGEM, led to different results. The two low resolution models revealed a subsurface warming trend, as expected and in agreement with [Purich and England \(2021\)](#).

The subsurface cooling trend we show in the high resolution HadGEM3 could be related to a deep freshening trend of the West Antarctic continental shelf and the creation of a westward slope current on the West Antarctic continental

shelf. The addition of freshwater in the Southern Ocean, its redistribution and the creation of an Antarctic slope current in West Antarctica have often created disagreement between studies that use low resolution models and the ones that use eddy permitting or eddy rich models. Enhanced freshwater in a low resolution model leads to strong stratification and subsurface warming (Bronseleer et al., 2018), while eddy permitting models tend to find subsurface cooling and consider the creation of a slope current a key contributor (Beadling et al., 2022).

Global climate models with 1 degree or higher horizontal resolution can simulate better the Antarctic Slope Current and Coastal Current and they respond with negative feedback to surface freshening and ice shelf melt (Thomas et al., 2023). Models with coarser resolution have a less well-defined Antarctic Slope Current and respond differently to freshwater perturbations, not capturing a colder state at the Amundsen Sea continental shelf (Beadling et al., 2022). The low horizontal resolution of the models is why the vast majority of CMIP models do not capture changes in the Antarctic Slope Current or projected cold states on the Amundsen Sea continental shelf. Changes in water masses in remote locations, such as the Weddell Sea, can also influence the temperature over the Amundsen Sea continental shelf (Morrison et al., 2023). Our results agree with all the above global or circumpolar models. However, some regional models, at a similarly high resolution, are projecting a warming Amundsen Sea continental shelf. Jourdain et al. (2022) uses a model domain with lateral boundaries derived by a CMIP5 multi-model mean under the RCP8.5 scenario. While the ice shelves are melting at a faster rate, half of the increase in melt rates is attributed to advection of warm water from the model's lateral boundaries (Jourdain et al., 2022). Similarly, Naughten et al. (2022) uses boundary conditions from the 1

degree horizontal resolution CESM1 and shows that the Amundsen Sea is rapidly warming. In addition to this, fixed boundary conditions are found to not have a strong effect in temperature changes (Naughten et al., 2022), while our results indicate the opposite.

A noteworthy finding was the response of the medium resolution model under the SSP858 scenario. We have shown extensively the biases in that model in Chapter 3 and the fact that it has a cool and fresh West Antarctic continental shelf. Here, however, the cold and fresh Amundsen Sea continental shelf in the medium resolution HadGEM3 is transitioning into a warm state. Caillet et al. (2023) suggest that a transition from a cold to warm continental shelf and vice versa in the Amundsen Sea is possible to be reversed.

The high resolution HadGEM3 has the highest ocean horizontal resolution among all other CMIP6 models and we have shown in Chapter 2 that it is the best performing model among the UK family of models, representing realistically the main Southern Ocean features. However, there is a number of limitations that cannot be ignored. There is currently only one SSP scenario available, the one we examined here, and its timescale is short, just 35 years. There is no way of knowing if by the end of the century the deep cooling trend would be reversed. Moreover, due to high costs, the spin up length of eddy-rich models is usually very short and that could influence model drift (Hewitt et al., 2020). On the other hand, the horizontal resolution of the HadGEM3-HH allows it to resolve the Antarctic slope current which plays a major role in understanding the impact of additional fresh water in the Southern Ocean under future scenarios.

Chapter 5

Discussion and conclusions

The aim of this thesis is to investigate how well global coupled climate models with different horizontal resolution represent the current state of the Southern Ocean, further explore their biases and understand their response to future changes. More specifically, we used output data from 4 models of the UK family, UKESM1, HadGEM3-GC3.1-HH, HadGEM3-GC3.1-MM and HadGEM3-GC3.1-LL. We are particularly interested in the representation of mechanisms that are driving or prohibiting warm water intrusion onto the West Antarctic continental shelf, such as deep freshening and the development of a westward slope current. The biases and response to future changes depends on the models resolution and their ability to resolve eddies in the ocean. Here we will discuss the results from the 3 preceding chapters and highlight their importance, limitations and potential future work that is needed.

5.1 Performance based evaluation and comparison of the 4 models

The models we used in this study have a range of different horizontal resolutions, from 1° to $1/12^\circ$. While the two lower resolution models are eddy parameterized, like the majority of CMIP6 models, the medium resolution ($1/4^\circ$) model is an eddy permitting model and the high resolution model ($1/12^\circ$) is eddy rich. A performance based evaluation of these 4 models revealed major differences among them, even though they all have the same atmospheric, ocean and sea ice components.

While the two low resolution models, UKESM1 (Sellar et al., 2019) and HadGEM3-GC3.1-LL (Roberts et al., 2019), have many similarities in the representation of historical surface properties such as temperature, salinity and sea ice in the Southern Ocean, the UKESM model has smaller biases in deep temperature and salinity and has overall more inter-annual variability. The better performance of the UKESM model could be attributed to its long 500-year spin up run, preceded by an ocean only 5000 years run, due to the fact that it is an earth system model and has the additional component of biochemistry in the ocean, land surface and atmosphere, which adds more complexity (Sellar et al., 2019). On the other hand, the low resolution HadGEM3 has a more affordable spin up run of only 30 years (Roberts et al., 2019). Despite the smaller biases in UKESM1 compared with the low resolution HadGEM3, neither of these models have the ability to accurately simulate important circulation features such as the Antarctic slope current, due to their coarse resolution, but they do have a more realistic ACC strength representation compared to the higher resolution models in our study.

The performance of the medium resolution HadGEM3 model in the historical run has large biases. A model that has a $1/4^\circ$ horizontal resolution is considered eddy permitting but has difficulties in simulating mesoscale eddies in high latitudes, however this resolution has been found to be promising (Held et al., 2019). Here we found that in the medium resolution model there is no warm water intrusion onto the Amundsen Sea continental shelf, where a strong westward slope current is present creating a front that steeply slopes the isopycnals and prohibits ACC water from reaching the continental shelf. In this model the Antarctic slope current has spun up all around Antarctica, continuing west along the Antarctic Peninsula and along the West Antarctic continental shelf slope. We found that deep freshening as a result of freshwater redistribution on the West Antarctic continental shelf is strongly related to the creation of the slope current, in medium and high resolution models. Another feature of the medium resolution HadGEM3 related to the above mentioned biases, is the lack of sea ice and the deep mixed layer in the Weddell Sea and the rest of East Antarctica.

The biases in the medium resolution model are unique in our study, meaning that no other model shows a cold and fresh West Antarctic continental shelf with a westward slope current that extends west from the Antarctic Peninsula in the historical run. However, these biases are not only present in the medium resolution HadGEM. The model CNRM-CM6-1-HR (Saint-Martin et al., 2021) has a $1/4^\circ$ horizontal resolution in the ocean and has similar biases in the historical run as the medium resolution HadGEM. A number of CMIP6 models with horizontal resolution $< 1/2^\circ$ exhibit westward velocities in Drake Passage, in contrast to models that have a coarser resolution, possibly because the circulation is better resolved in them (Beadling et al., 2020). Observations support that westward

circulation features exist in Drake Passage (Donohue et al., 2016), but not to the extent of the biases presented here. While some $1/4^\circ$ eddy permitting resolution models seem to exhibit a pattern of having large biases in sea ice, circulation and deep temperature and salinity, we consider their finer horizontal resolution a strength and a step towards the right direction if these biases improve in the next phase of CMIP models. In this case however, the medium resolution model is the worst performing model by far and its future projections will therefore be unreliable.

Regarding the high resolution model and its performance in the historical run, we concluded that it is the best performing model out of all the models considered in this study. The high resolution HadGEM3 model has the finest horizontal resolution of all the CMIP6 models and it is an eddy rich model. Overall, it realistically represents sea ice, salinity temperature and circulation in the Southern Ocean. However, it underestimates the ACC transport in Drake Passage and has some westward circulation flows slightly stronger than the estimates from observations in the region. These small circulation biases do not substantially influence any other Southern Ocean properties and the coastal current and warm water intrusion on the Amundsen Sea continental shelf are represented well.

5.2 Biases, future projections and the importance of freshwater redistribution in a changing climate

As the horizontal resolution has increased in CMIP6 models relative to previous phases, it is important to understand what that means in terms of the models' performance. In the case of our study, after evaluating the performance of 4 models in the Southern Ocean, we found very substantial biases in the $1/4^\circ$ resolution model, the most evident being a fresh and cold West Antarctic continental shelf with a strong westward slope current. In Chapter 3, we focused on investigating these biases and their origins. In the historical run the biases were already developed so we used data from the spin up run of the model to capture their initiation and time evolution. Our motivation is to gain a deeper understanding of the processes that led to an eddy permitting model having a cold and fresh West Antarctic continental shelf.

Sea ice representation in the Southern Ocean has not improved in CMIP6 models ([Beadling et al., 2020](#)), yet its representation is extremely important because freshwater from sea ice melt can transform water masses and lead to circulation changes ([Pellichero et al., 2018](#)). In the case of the biases in the medium resolution model here, in the historical run we found that the Weddell Sea and East Antarctic sector sea ice has disappeared, while in the West Antarctic sector the sea ice representation is relatively realistic. This raised questions regarding the relationship between biases in the Weddell Sea and the West Antarctic continental shelf. Can the biases in Weddell Sea remotely affect shelf waters in West Antarctica?

If yes, how long would it take for freshwater to be transported to the Amundsen Sea continental shelf? We found that a strong westward slope current in the Weddell Sea can transport salinity biases west of the Antarctic Peninsula, reaching the Amundsen Sea creating a slope front that prohibits warm water intrusion onto the West Antarctic continental shelf. However, our particle tracking analysis shows that this circulation anomaly takes a minimum of 5 years to develop. Instead, particles released in the surface of regions with strong positive anomalies of sea ice melt in West Antarctica, such as the Bellingshausen Sea and West Antarctic Peninsula, can reach the Amundsen Sea within 2 years. Therefore, we conclude that the biases in the Amundsen Sea are primarily driven by freshwater transported from the Bellingshausen Sea and West Antarctic Peninsula.

It is known that the medium resolution HadGEM3 model has warm SST biases in the Southern Ocean that are related to its reduced sea ice extent ([Andrews et al., 2020](#)). However, examining the biases from the moment of their development gives us the opportunity to gain a better understanding of how a declining sea ice trend affects freshwater advection in a model that can actually resolve a slope current. Since sea ice freeze and melt can transport freshwater to different latitudes ([Pellichero et al., 2018](#)), we tracked the progress of the models biases in order to study how freshwater can be redistributed in West Antarctica and determine what is the feedback from rapid freshening due to anomalous high sea ice melt rates on subsurface temperature and salinity.

Data output from the spin up of the medium resolution model show that while the first year of the model run was unbiased, salinity biases developed on the West Antarctic continental shelf during the first 3 years of the run. The freshening of the Amundsen Sea continental shelf was related to regions in West Antarctica,

such as the Bellingshausen Sea and West Antarctic Peninsula, that went through extensive surface and subsurface freshening due to very large amounts of sea ice melt. In some of these regions the freshwater release from sea ice melt increased by a factor of 4 within the first 3 years of the run. So here we established that high sea ice melt rates in West Antarctica can influence subsurface temperature and salinity and change the state of the Amundsen Sea continental shelf from warm to cool in an eddy permitting model.

Many studies use freshwater forcing near the Antarctic coast in order to simulate ice shelf melt water and to examine the response of subsurface temperature to freshwater input on the continental shelf. Published results so far give conflicting responses about changes in deep water temperature and salinity from increasing amounts of freshwater in West Antarctica. Until a few years ago the vast majority of studies argued that freshwater input stratifies the ocean and traps heat at depth ([Bintanja et al., 2013](#); [Bronseleer et al., 2018](#); [Ma and Wu, 2011](#)), however all of these studies utilize low resolution models that cannot simulate the Antarctic slope current. There is one study that found subsurface cooling and freshening in West Antarctica using a 1° resolution model as a result of additional fresh water under high emissions forcing ([Thomas et al., 2023](#)), and the rest of the studies with a deep freshening response on the West Antarctic continental shelf used exclusively ocean models with $1/4^\circ$ or higher resolution ([Beadling et al., 2022](#); [Moorman et al., 2020](#)). Our results are in agreement with these high resolution studies ([Beadling et al., 2022](#); [Moorman et al., 2020](#)), showing that excess fresh water reaching the West Antarctic continental shelf will result in deep freshening and cooling, initiating a westward slope current that can cut off warm water intrusion on the continental shelf.

Our motivation for performing a particle tracking analysis was to understand the pathway and distribution of freshwater from areas with high sea ice melt rates. Freshwater volume transport and sea ice melt and freeze play a big role in our freshwater budget calculations in West Antarctic regions. Particles tracked from the West Antarctic Peninsula, an area with very high sea ice melt rates, were transported to the Bellingshausen Sea within 1 year and the Amundsen Sea within 2-3 years. Similar to our findings, [Flexas et al. \(2022\)](#) found that fresh water anomalies were transported from the West Antarctic Peninsula to the Bellingshausen and Amundsen Sea within the same window of time, following a near-the-coast path.

Our conclusions regarding the biases in the medium resolution HadGEM3 are that high sea ice melt rates in the West Antarctic Peninsula and Bellingshausen Sea are causing excess fresh water to be redistributed in the West Antarctic continental shelf, creating deep cooling on the whole West Antarctic continental shelf, including the Amundsen Sea, and initiating a westward slope current. The freshwater volume transport from the Bellingshausen Sea to the Amundsen Sea continental shelf is doubled within the first 3-5 years in the model. Overall, the Amundsen Sea continental shelf is very sensitive to changes in the Bellingshausen Sea. Backward tracking of subsurface particles released near the continental shelf break and in front of the ice shelf in the Amundsen Sea, show that there are two distinctly different water masses intruding onto the continental shelf, one is warm and is coming from northwest and the other is cool and is advecting from the Bellingshausen Sea. Our hypothesis is that the fresh and cold water advection from the Bellingshausen Sea slopes the isopycnals and prohibits warm water intrusion on the continental shelf resulting in an increasingly fresh and cool shelf.

We used the high resolution HadGEM3 model in order to investigate future projections under the SSP585 scenario (Chapter 4) due to its very realistic, and best among the models analysed here, performance. There is notable sea ice reduction, first discernable in the Bellingshausen Sea and West Antarctic Peninsula, followed by the Weddell and Amundsen Sea. This is consistent with the average response of CMIP6 models where under strong forcing scenarios summer sea ice disappears, and winter sea ice is reduced by an average of 40% (Holmes et al., 2022). The ocean response to disappearing sea ice is similar to the response of the medium resolution model. The West Antarctic continental shelf becomes fresh and cool and there is a west slope current present in West Antarctica by the end of the run.

The above mentioned changes take more time to develop in the high resolution model in comparison to the biases in the medium resolution one, and we do see deep warming on the Amundsen Sea continental shelf before it cools down. While the sea ice has disappeared in the Bellingshausen Sea and significantly reduced in the Weddell Sea mid-run, the Amundsen Sea subsurface temperature is increased slightly. By tracking the progress of subsurface changes on the West Antarctic continental shelf and circulation we found that a decrease in Drake Passage volume transport is connected to the reversal of volume transport on the Amundsen Sea continental slope. The newly formed westward slope current gets stronger towards the last decade of the run, right before we observe deep cooling and freshening on the Amundsen Sea continental shelf. Even though the processes that lead to a cold and fresh West Antarctic continental shelf are similar between the two models, the high resolution model undergoes these changes under a strong forcing future projections scenario, after having realistically represented processes in the

Southern Ocean during the historical run.

Lastly, we briefly show future projections of temperature on the Amundsen Sea continental shelf under the SSP585 scenario from the rest of the models. As expected, the two low resolution models show increased deep temperatures on the Amundsen Sea continental shelf. However, the medium resolution model shows deep warming on the Amundsen Sea continental shelf after 3 decades. This raises the question of the reversibility of a continental shelf state from cold to warm. [Caillet et al. \(2023\)](#), using a $1/4^\circ$ model found that surface fluxes in the Amundsen Sea can alter its state from cold to warm and vice versa, by affecting the ocean stratification, and suggested that this process is reversible. Tipping points like this could also occur in the Weddell Sea, where the lack of sea ice can result in freshening of the continental shelf, facilitating warm water intrusion onto it and entering a self reinforced warm state ([Hellmer et al., 2017](#)). Freshening of the Weddell Sea continental shelf and warming of the Weddell Sea continental slope has been found to be connected to deep freshening on the West Antarctic continental shelf ([Li et al., 2023](#));([Thomas et al., 2023](#)).

5.3 Limitations and future work

CMIP6 models do not have an interactive ice shelf so basal melt rates are not changing in response to their surrounding ocean. This contributes to huge uncertainties about the relationship of basal melt and fresh water input ([Thomas et al., 2023](#)). We demonstrate here that increased freshwater input in the West Antarctic region, either initiated from high sea ice melt rates or freshwater advection from remote locations, can alter the state of deep salinity and temperature. However, while we are debating the subsurface response of the West Antarctic

continental shelf to a changing climate with increased freshwater, we are missing the very important component of fluctuating rates of ice shelf melt water.

Eddy permitting and eddy rich models often have different future climate responses and ocean mean state representation than their coarser resolution counterparts ([Hewitt et al., 2020](#)). A key Southern Ocean feature that has been found to play a huge role in deep changes on the West Antarctic continental shelf, the slope current, cannot be faithfully represented in low resolution models. An important improvement to our future predictions would be made by developing more models with increased horizontal resolution in the next phase of CMIP models. Warm water intrusion can be prohibited by the genesis of a strong Antarctic slope current so its evolution can influence the stability of the West Antarctic ice sheet ([Beadling et al., 2022](#)). Subsurface response to increased freshwater need to be studied to a greater extent. High resolution models with interactive ice sheets could improve future projections of subsurface temperature and salinity and by extension future projections of sea level rise ([Beadling et al., 2022](#)).

In this thesis we used HadGEM3 ensemble members that have an atmosphere horizontal resolution equivalent to their ocean horizontal resolution. However, different combinations exist and it would be interesting to see how the high resolution ocean model for example would perform in the historical run, and what the future projections of deep temperature would be, if the atmospheric resolution was coarser. Here we did not quantify changes in heat flux from the atmosphere and wind changes. Changes in wind stress under climate change can influence circulation in the Southern Ocean and so it should be explored further. The responses of surface Southern Ocean properties to changes in freshwater and wind stress are opposite to each other ([Beadling et al., 2022](#)). This is yet another reason

why using models with the ability to resolve a slope current is useful for this type of analysis.

While the Amundsen Sea continental shelf undergoes large changes in our analysis, they are driven by forcing outside of the Amundsen Sea. Large scale Southern Ocean circulation changes seem to be caused by excess fresh water and its redistribution. Particle tracking is a very useful tool to analyze the pathways of different water masses. Here we used it only to track the biases in the medium resolution model, but it could be used for tracing the redistribution of fresh water on the Antarctic continental shelf under future changes in high resolution models.

Lastly, eddy rich climate models usually have short spin up and future projections runs. The high resolution model which we analysed here has only one future projection run under a high emissions forcing scenario. The state of deep waters on the West Antarctic continental shelf shifted from warm to cool in less than 35 years. The run stops at 2050 and we cannot know if the changes we see are permanent or if they can be reversed by the end of the century, resulting in permanent warming under an extreme climate change scenario. With emerging model studies that find cooling responses to climate change, we need to further examine how robust these results are, but also if they are permanent or reversible.

5.4 Thesis summary

In this thesis we conducted a process based evaluation of 4 coupled climate models with different horizontal resolution. We found that biases in the historical run and changes in future projections are resolution dependent. The ability of a model to realistically represent the Antarctic slope current plays a major role

in its response to future changes. The two low resolution models show deep warming on the West Antarctic continental shelf under climate change. The medium resolution model does not have a realistic West Antarctic continental shelf due to warm SST biases, loss of sea ice and the initiation of a westward slope current. However, in the medium resolution model's future projections, by the end of the century, the Amundsen Sea continental shelf undergoes deep warming. The high resolution model does a good job in representing historical Southern Ocean properties, including a realistic slope current. However, under high future emissions forcing, the West Antarctic continental shelf shifts to a fresh and cool state, while the sea ice disappears almost in every region. Overall, changes in the Amundsen Sea subsurface temperature and salinity are linked to high sea ice melt rates in the Bellingshausen Sea and West Antarctic Peninsula and the development of a westward slope current. An increase in the Weddell Sea slope current and westward flow in Drake Passage could also play a role in the strengthening of the slope current in West Antarctica, but its initiation does not seem to be happening without extreme sea ice loss in West Antarctica. The disagreement in eddy resolving and eddy parameterised models regarding future projected changes on the West Antarctic continental shelf feeds into the uncertainty of future ice shelf melt rates and sea level rise. The usage of high resolution models in order to investigate the results of freshwater redistribution on the West Antarctic continental shelf is very promising and needs to be further explored.

Bibliography

- Adcroft, A., Anderson, W., Balaji, V., Blanton, C., Bushuk, M., Dufour, C. O., Dunne, J. P., Griffies, S. M., Hallberg, R., Harrison, M. J., et al. (2019). The gfdl global ocean and sea ice model om4. 0: Model description and simulation features. *Journal of Advances in Modeling Earth Systems*, 11(10):3167–3211.
- Anderson, J. B., Shipp, S. S., Lowe, A. L., Wellner, J. S., and Mosola, A. B. (2002). The antarctic ice sheet during the last glacial maximum and its subsequent retreat history: a review. *Quaternary Science Reviews*, 21(1-3):49–70.
- Andrews, M. B., Ridley, J. K., Wood, R. A., Andrews, T., Blockley, E. W., Booth, B., Burke, E., Dittus, A. J., Florek, P., Gray, L. J., et al. (2020). Historical simulations with hadgem3-gc3. 1 for CMIP6. *Journal of Advances in Modeling Earth Systems*, 12(6):e2019MS001995.
- Bamber, J. L., Riva, R. E., Vermeersen, B. L., and LeBrocq, A. M. (2009). Re-assessment of the potential sea-level rise from a collapse of the West Antarctic Ice Sheet. *science*, 324(5929):901–903.
- Barthélemy, A., Fichefet, T., Goosse, H., and Madec, G. (2015). Modeling the interplay between sea ice formation and the oceanic mixed layer: Limitations of simple brine rejection parameterizations. *Ocean Modelling*, 86:141–152.
- Beadling, R., Krasting, J., Griffies, S., Hurlin, W., Bronselaer, B., Russell, J., MacGilchrist, G., Tesdal, J.-E., and Winton, M. (2022). Importance of the antarctic slope current in the southern ocean response to ice sheet melt and wind stress change. *Journal of Geophysical Research: Oceans*, 127(5):e2021JC017608.
- Beadling, R., Russell, J., Stouffer, R., Goodman, P., and Mazloff, M. (2019). Assessing the quality of southern ocean circulation in cmip5 aogcm and earth system model simulations. *Journal of Climate*, 32(18):5915–5940.
- Beadling, R. L., Russell, J., Stouffer, R., Mazloff, M., Talley, L., Goodman, P., Sallée, J.-B., Hewitt, H., Hyder, P., and Pandde, A. (2020). Representation of southern ocean properties across coupled model intercomparison project generations: Cmp3 to CMIP6. *Journal of Climate*, 33(15):6555–6581.

- Bintanja, R., van Oldenborgh, G. J., Drijfhout, S., Wouters, B., and Katsman, C. (2013). Important role for ocean warming and increased ice-shelf melt in Antarctic sea-ice expansion. *Nature Geoscience*, 6(5):376–379.
- Bronselaer, B., Russell, J. L., Winton, M., Williams, N. L., Key, R. M., Dunne, J. P., Feely, R. A., Johnson, K. S., and Sarmiento, J. L. (2020). Importance of wind and meltwater for observed chemical and physical changes in the southern ocean. *Nature Geoscience*, 13(1):35–42.
- Bronselaer, B., Winton, M., Griffies, S. M., Hurlin, W. J., Rodgers, K. B., Sergienko, O. V., Stouffer, R. J., and Russell, J. L. (2018). Change in future climate due to Antarctic meltwater. *Nature*, 564(7734):53–58.
- Caillet, J., Jourdain, N. C., Mathiot, P., Hellmer, H. H., and Mouginot, J. (2023). Drivers and reversibility of abrupt ocean state transitions in the amundsen sea, antarctica. *Journal of Geophysical Research: Oceans*, 128(1):e2022JC018929.
- Chen, A., Barham, W., and Grooms, I. (2018). Comparing eddy-permitting ocean model parameterizations via lagrangian particle statistics in a quasigeostrophic setting. *Journal of Geophysical Research: Oceans*, 123(8):5637–5651.
- Church, J., Clark, P., Cazenave, A., Gregory, J., Jevrejeva, S., Levermann, A., Merrifield, M., Milne, G., Nerem, R., Nunn, P., Payne, A., Pfeffer, W., Stammer, D., and Unnikrishnan, A. (2013). *Sea Level Change*, book section 13, page 1137–1216. Cambridge University Press, Cambridge, United Kingdom and New York, NY, USA.
- DeConto, R. M. and Pollard, D. (2016). Contribution of antarctica to past and future sea-level rise. *Nature*, 531(7596):591–597.
- Dinniman, M. S., Asay-Davis, X. S., Galton-Fenzi, B. K., Holland, P. R., Jenkins, A., and Timmermann, R. (2016). Modeling ice shelf/ocean interaction in antarctica: A review. *Oceanography*, 29(4):144–153.
- Dinniman, M. S., Klinck, J. M., and Hofmann, E. E. (2012). Sensitivity of circumpolar deep water transport and ice shelf basal melt along the west antarctic peninsula to changes in the winds. *Journal of Climate*, 25(14):4799–4816.
- Donohue, K., Tracey, K., Watts, D., Chidichimo, M. P., and Chereskin, T. (2016). Mean antarctic circumpolar current transport measured in drake passage. *Geophysical Research Letters*, 43(22):11–760.
- Douglas, B. C. (1991). Global sea level rise. *Journal of Geophysical Research: Oceans*, 96(C4):6981–6992.
- Dutrieux, P., De Rydt, J., Jenkins, A., Holland, P. R., Ha, H. K., Lee, S. H., Steig,

- E. J., Ding, Q., Abrahamsen, E. P., and Schröder, M. (2014). Strong sensitivity of pine island ice-shelf melting to climatic variability. *Science*, 343(6167):174–178.
- Dutton, A. and Lambeck, K. (2012). Ice volume and sea level during the last interglacial. *science*, 337(6091):216–219.
- Eyring, V., Bony, S., Meehl, G., Senior, C., Stevens, B., Stouffer, R., and Taylor, K. (2015). Overview of the coupled model intercomparison project phase 6 (CMIP6) experimental design and organisation. *Geoscientific Model Development Discussions*, 8(12).
- Eyring, V., Bony, S., Meehl, G. A., Senior, C. A., Stevens, B., Stouffer, R. J., and Taylor, K. E. (2016). Overview of the coupled model intercomparison project phase 6 (cmip6) experimental design and organization. *Geoscientific Model Development*, 9(5):1937–1958.
- Feldmann, J. and Levermann, A. (2015). Collapse of the west antarctic ice sheet after local destabilization of the amundsen basin. *Proceedings of the National Academy of Sciences*, 112(46):14191–14196.
- Ferster, B. S., Subrahmanyam, B., and Macdonald, A. M. (2018). Confirmation of enso-southern ocean teleconnections using satellite-derived sst. *Remote Sensing*, 10(2):331.
- Firing, Y. L., Chereskin, T. K., and Mazloff, M. R. (2011). Vertical structure and transport of the antarctic circumpolar current in drake passage from direct velocity observations. *Journal of Geophysical Research: Oceans*, 116(C8).
- Flato, G., Marotzke, J., Abiodun, B., Braconnot, P., Chou, S. C., Collins, W., Cox, P., Driouech, F., Emori, S., Eyring, V., et al. (2014). Evaluation of climate models. In *Climate change 2013: the physical science basis. Contribution of Working Group I to the Fifth Assessment Report of the Intergovernmental Panel on Climate Change*, pages 741–866. Cambridge University Press.
- Flexas, M. M., Thompson, A. F., Schodlok, M. P., Zhang, H., and Speer, K. (2022). Antarctic peninsula warming triggers enhanced basal melt rates throughout west antarctica. *Science advances*, 8(31):eabj9134.
- Furtado, K. and Field, P. (2017). The role of ice microphysics parametrizations in determining the prevalence of supercooled liquid water in high-resolution simulations of a southern ocean midlatitude cyclone. *Journal of the Atmospheric Sciences*, 74(6):2001–2021.
- Gent, P. R. and Mewilliams, J. C. (1990). Isopycnal mixing in ocean circulation models. *Journal of Physical Oceanography*, 20(1):150–155.

- Goddard, P. B., Dufour, C. O., Yin, J., Griffies, S. M., and Winton, M. (2017). Co₂-induced ocean warming of the antarctic continental shelf in an eddying global climate model. *Journal of Geophysical Research: Oceans*, 122(10):8079–8101.
- Golledge, N. R., Kowalewski, D. E., Naish, T. R., Levy, R. H., Fogwill, C. J., and Gasson, E. G. (2015). The multi-millennial antarctic commitment to future sea-level rise. *Nature*, 526(7573):421–425.
- Good, S. A., Martin, M. J., and Rayner, N. A. (2013). En4: Quality controlled ocean temperature and salinity profiles and monthly objective analyses with uncertainty estimates. *Journal of Geophysical Research: Oceans*, 118(12):6704–6716.
- Haarsma, R. J., Roberts, M. J., Vidale, P. L., Senior, C. A., Bellucci, A., Bao, Q., Chang, P., Corti, S., Fučkar, N. S., Guemas, V., et al. (2016). High resolution model intercomparison project (highresmip v1. 0) for CMIP6. *Geoscientific Model Development*, 9(11):4185–4208.
- Hanna, E., Navarro, F. J., Pattyn, F., Domingues, C. M., Fettweis, X., Ivins, E. R., Nicholls, R. J., Ritz, C., Smith, B., Tulaczyk, S., et al. (2013). Ice-sheet mass balance and climate change. *Nature*, 498(7452):51–59.
- Hay, C. C., Morrow, E., Kopp, R. E., and Mitrovica, J. X. (2015). Probabilistic reanalysis of twentieth-century sea-level rise. *Nature*, 517(7535):481–484.
- Held, I., Guo, H., Adcroft, A., Dunne, J., Horowitz, L., Krasting, J., Shevliakova, E., Winton, M., Zhao, M., Bushuk, M., et al. (2019). Structure and performance of gfdl’s cm4. 0 climate model. *Journal of Advances in Modeling Earth Systems*, 11(11):3691–3727.
- Hellmer, H. H., Kauker, F., Timmermann, R., and Hattermann, T. (2017). The fate of the southern weddell sea continental shelf in a warming climate. *Journal of Climate*, 30(12):4337–4350.
- Heuzé, C., Heywood, K. J., Stevens, D. P., and Ridley, J. K. (2013). Southern ocean bottom water characteristics in cmip5 models. *Geophysical Research Letters*, 40(7):1409–1414.
- Hewitt, H. T., Roberts, M., Mathiot, P., Biastoch, A., Blockley, E., Chassignet, E. P., Fox-Kemper, B., Hyder, P., Marshall, D. P., Popova, E., et al. (2020). Resolving and parameterising the ocean mesoscale in earth system models. *Current Climate Change Reports*, 6:137–152.
- Heywood, K. J., Biddle, L. C., Boehme, L., Dutrieux, P., Fedak, M., Jenkins, A., Jones, R. W., Kaiser, J., Mallett, H., Garabato, A. C. N., et al. (2016). Between

- the devil and the deep blue sea: the role of the amundsen sea continental shelf in exchanges between ocean and ice shelves. *Oceanography*, 29(4):118–129.
- Holmes, C., Bracegirdle, T., and Holland, P. (2022). Antarctic sea ice projections constrained by historical ice cover and future global temperature change. *Geophysical Research Letters*, 49(10):e2021GL097413.
- Hughes, T. (1973). Is the West Antarctic ice sheet disintegrating? *Journal of Geophysical Research*, 78(33):7884–7910.
- Hyder, P., Edwards, J. M., Allan, R. P., Hewitt, H. T., Bracegirdle, T. J., Gregory, J. M., Wood, R. A., Meijers, A. J., Mulcahy, J., Field, P., et al. (2018). Critical southern ocean climate model biases traced to atmospheric model cloud errors. *Nature communications*, 9(1):3625.
- IPCC (2013). *Index*, book section Index, page 1523–1535. Cambridge University Press, Cambridge, United Kingdom and New York, NY, USA.
- IPCC (2021). *Climate Change 2021: The Physical Science Basis. Contribution of Working Group I to the Sixth Assessment Report of the Intergovernmental Panel on Climate Change*. Cambridge University Press, Cambridge, UK and New York, NY, USA.
- Jacobs, S. S. (1991). On the nature and significance of the antarctic slope front. *Marine Chemistry*, 35(1-4):9–24.
- Jacobs, S. S., Hellmer, H. H., and Jenkins, A. (1996). Antarctic ice sheet melting in the southeast pacific. *Geophysical Research Letters*, 23(9):957–960.
- Jenkins, A., Dutrieux, P., Jacobs, S. S., McPhail, S. D., Perrett, J. R., Webb, A. T., and White, D. (2010). Observations beneath pine island glacier in west antarctica and implications for its retreat. *Nature Geoscience*, 3(7):468–472.
- Joughin, I. and Alley, R. B. (2011). Stability of the West Antarctic ice sheet in a warming world. *Nature Geoscience*, 4(8):506–513.
- Jourdain, N. C., Mathiot, P., Burgard, C., Caillet, J., and Kittel, C. (2022). Ice shelf basal melt rates in the amundsen sea at the end of the 21st century. *Geophysical Research Letters*, 49(22):e2022GL100629.
- Kajtar, J. B., Santoso, A., Collins, M., Taschetto, A. S., England, M. H., and Frankcombe, L. M. (2021). Cmp5 intermodel relationships in the baseline southern ocean climate system and with future projections. *Earth's Future*, 9(6):e2020EF001873.
- Kuhlbrodt, T., Jones, C. G., Sellar, A., Storkey, D., Blockley, E., Stringer, M.,

- Hill, R., Graham, T., Ridley, J., Blaker, A., et al. (2018). The low-resolution version of hadgem3 gc3. 1: Development and evaluation for global climate. *Journal of advances in modeling earth systems*, 10(11):2865–2888.
- Li, Q., England, M. H., Hogg, A. M., Rintoul, S. R., and Morrison, A. K. (2023). Abyssal ocean overturning slowdown and warming driven by antarctic meltwater. *Nature*, 615(7954):841–847.
- Locarnini, M., Mishonov, A., Baranova, O., Boyer, T., Zweng, M., Garcia, H., Seidov, D., Weathers, K., Paver, C., Smolyar, I., et al. (2018). World ocean atlas 2018, volume 1: Temperature.
- Lockwood, J. W., Dufour, C. O., Griffies, S. M., and Winton, M. (2021). On the role of the antarctic slope front on the occurrence of the weddell sea polynya under climate change. *Journal of Climate*, 34(7):2529–2548.
- Luo, F., Ying, J., Liu, T., and Chen, D. (2023). Origins of southern ocean warm sea surface temperature bias in cmip6 models. *npj Climate and Atmospheric Science*, 6(1):127.
- Lythe, M. B. and Vaughan, D. G. (2001). Bedmap: A new ice thickness and subglacial topographic model of Antarctica. *Journal of Geophysical Research: Solid Earth*, 106(B6):11335–11351.
- Ma, H. and Wu, L. (2011). Global teleconnections in response to freshening over the antarctic ocean. *Journal of Climate*, 24(4):1071–1088.
- Mallett, H. K., Boehme, L., Fedak, M., Heywood, K. J., Stevens, D. P., and Roquet, F. (2018). Variation in the distribution and properties of circumpolar deep water in the eastern amundsen sea, on seasonal timescales, using seal-borne tags. *Geophysical Research Letters*, 45(10):4982–4990.
- Marshall, J. and Speer, K. (2012). Closure of the meridional overturning circulation through southern ocean upwelling. *Nature geoscience*, 5(3):171–180.
- Massom, R. A., Scambos, T. A., Bennetts, L. G., Reid, P., Squire, V. A., and Stammerjohn, S. E. (2018). Antarctic ice shelf disintegration triggered by sea ice loss and ocean swell. *Nature*, 558(7710):383–389.
- Mathiot, P., Gousse, H., Fichet, T., Barnier, B., and Gallée, H. (2011). Modelling the seasonal variability of the antarctic slope current. *Ocean Science*, 7(4):455–470.
- Mazloff, M. R., Heimbach, P., and Wunsch, C. (2010). An eddy-permitting southern ocean state estimate. *Journal of Physical Oceanography*, 40(5):880–899.

- Meijers, A. (2014). The southern ocean in the coupled model intercomparison project phase 5. *Philosophical Transactions of the Royal Society A: Mathematical, Physical and Engineering Sciences*, 372(2019):20130296.
- Meijers, A., Meredith, M., Abrahamsen, E., Morales Maqueda, M., Jones, D., and Naveira Garabato, A. (2016). Wind-driven export of Weddell sea slope water. *Journal of Geophysical Research: Oceans*, 121(10):7530–7546.
- Meijers, A. J., Shuckburgh, E., Bruneau, N., Sallée, J.-B., Bracegirdle, T. J., and Wang, Z. (2012). Representation of the antarctic circumpolar current in the cmip5 climate models and future changes under warming scenarios. *Journal of Geophysical Research: Oceans*, 117(C12).
- Mercer, J. H. (1968). Antarctic ice and eustatic sea level.
- Mercer, J. H. (1978). West Antarctic ice sheet and CO₂ greenhouse effect: a threat of disaster. *Nature*, 271(5643):321–325.
- Mercer, J. H. and Emiliani, C. (1970). Antarctic ice and interglacial high sea levels. *Science*, 168(3939):1605–1606.
- Meredith, M., Sommerkorn, M., Cassotta, S., Derksen, C., Ekaykin, A., Hollowed, A., Kofinas, G., Mackintosh, A., Melbourne-Thomas, J., Muelbert, M., et al. (2019). Polar regions. chapter 3, ipcc special report on the ocean and cryosphere in a changing climate.
- Moffat, C., Beardsley, R. C., Owens, B., and Van Lipzig, N. (2008). A first description of the antarctic peninsula coastal current. *Deep Sea Research Part II: Topical Studies in Oceanography*, 55(3-4):277–293.
- Moffat, C. and Meredith, M. (2018). Shelf–ocean exchange and hydrography west of the antarctic peninsula: a review. *Philosophical Transactions of the Royal Society A: Mathematical, Physical and Engineering Sciences*, 376(2122):20170164.
- Moorman, R., Morrison, A. K., and McC. Hogg, A. (2020). Thermal responses to Antarctic ice shelf melt in an eddy-rich global ocean–sea ice model. *Journal of Climate*, 33(15):6599–6620.
- Morrison, A. K., England, M. H., Hogg, A. M., and Kiss, A. E. (2023). Weddell sea control of ocean temperature variability on the western antarctic peninsula. *Geophysical Research Letters*, 50(15):e2023GL103018.
- Naughten, K. A., Holland, P. R., Dutrieux, P., Kimura, S., Bett, D. T., and Jenkins, A. (2022). Simulated twentieth-century ocean warming in the Amundsen Sea, West Antarctica. *Geophysical Research Letters*, 49(5):e2021GL094566.

- Nitsche, F., Jacobs, S., Larter, R., and Gohl, K. (2007). Bathymetry of the amundsen sea continental shelf: Implications for geology, oceanography, and glaciology. *Geochemistry, Geophysics, Geosystems*, 8(10).
- Núñez-Riboni, I. and Fahrback, E. (2009). Seasonal variability of the antarctic coastal current and its driving mechanisms in the weddell sea. *Deep Sea Research Part I: Oceanographic Research Papers*, 56(11):1927–1941.
- O’Neill, B. C., Tebaldi, C., van Vuuren, D. P., Eyring, V., Friedlingstein, P., Hurtt, G., Knutti, R., Kriegler, E., Lamarque, J.-F., Lowe, J., Meehl, G. A., Moss, R., Riahi, K., and Sanderson, B. M. (2016). The scenario model intercomparison project (scenariomip) for cmip6. *Geoscientific Model Development*, 9(9):3461–3482.
- Oppenheimer, M. (1998). Global warming and the stability of the west antarctic ice sheet. *Nature*, 393(6683):325–332.
- Paolo, F. S., Fricker, H. A., and Padman, L. (2015). Volume loss from antarctic ice shelves is accelerating. *Science*, 348(6232):327–331.
- Pattyn, F., Ritz, C., Hanna, E., Asay-Davis, X., DeConto, R., Durand, G., Favier, L., Fettweis, X., Goelzer, H., Golledge, N. R., et al. (2018). The greenland and antarctic ice sheets under 1.5 c global warming. *Nature climate change*, 8(12):1053–1061.
- Pellichero, V., Sallée, J.-B., Chapman, C. C., and Downes, S. M. (2018). The southern ocean meridional overturning in the sea-ice sector is driven by fresh-water fluxes. *Nature communications*, 9(1):1789.
- Pellichero, V., Sallée, J.-B., Schmidtko, S., Roquet, F., and Charrassin, J.-B. (2017). The ocean mixed layer under southern ocean sea-ice: Seasonal cycle and forcing. *Journal of Geophysical Research: Oceans*, 122(2):1608–1633.
- Petty, A. A., Holland, P. R., and Feltham, D. L. (2014). Sea ice and the ocean mixed layer over the antarctic shelf seas. *The Cryosphere*, 8(2):761–783.
- Poli, P., Hersbach, H., Dee, D. P., Berrisford, P., Simmons, A. J., Vitart, F., Laloyaux, P., Tan, D. G., Peubey, C., Thépaut, J.-N., et al. (2016). Era-20c: An atmospheric reanalysis of the twentieth century. *Journal of Climate*, 29(11):4083–4097.
- Pollard, D. and DeConto, R. M. (2009). Modelling West Antarctic ice sheet growth and collapse through the past five million years. *Nature*, 458(7236):329–332.
- Pritchard, H., Ligtenberg, S. R., Fricker, H. A., Vaughan, D. G., van den Broeke,

- M. R., and Padman, L. (2012). Antarctic ice-sheet loss driven by basal melting of ice shelves. *Nature*, 484(7395):502–505.
- Purich, A. and England, M. H. (2021). Historical and future projected warming of antarctic shelf bottom water in cmip6 models. *Geophysical Research Letters*, 48(10):e2021GL092752.
- Ren, L., Speer, K., and Chassignet, E. P. (2011). The mixed layer salinity budget and sea ice in the southern ocean. *Journal of Geophysical Research: Oceans*, 116(C8).
- Renner, A. H., Thorpe, S. E., Heywood, K. J., Murphy, E. J., Watkins, J. L., and Meredith, M. P. (2012). Advective pathways near the tip of the antarctic peninsula: Trends, variability and ecosystem implications. *Deep Sea Research Part I: Oceanographic Research Papers*, 63:91–101.
- Riahi, K., Van Vuuren, D. P., Kriegler, E., Edmonds, J., O’neill, B. C., Fujimori, S., Bauer, N., Calvin, K., Dellink, R., Fricko, O., et al. (2017). The shared socioeconomic pathways and their energy, land use, and greenhouse gas emissions implications: An overview. *Global environmental change*, 42:153–168.
- Ribeiro, N., Herraiz-Borreguero, L., Rintoul, S., McMahon, C., Hindell, M., Harcourt, R., and Williams, G. (2021). Warm modified circumpolar deep water intrusions drive ice shelf melt and inhibit dense shelf water formation in vincennes bay, east antarctica. *Journal of Geophysical Research: Oceans*, 126(8):e2020JC016998.
- Richardson, G., Wadley, M. R., Heywood, K. J., Stevens, D. P., and Banks, H. T. (2005). Short-term climate response to a freshwater pulse in the southern ocean. *Geophysical Research Letters*, 32(3).
- Rignot, E., Mouginot, J., Scheuchl, B., van den Broeke, M., van Wessem, M. J., and Morlighem, M. (2019). Four decades of antarctic ice sheet mass balance from 1979–2017. *Proceedings of the National Academy of Sciences*, 116(4):1095–1103.
- Roach, L. A., Dörr, J., Holmes, C. R., Massonnet, F., Blockley, E. W., Notz, D., Rackow, T., Raphael, M. N., O’Farrell, S. P., Bailey, D. A., et al. (2020). Antarctic sea ice area in CMIP6. *Geophysical Research Letters*, 47(9):e2019GL086729.
- Roberts, M. J., Baker, A., Blockley, E. W., Calvert, D., Coward, A., Hewitt, H. T., Jackson, L. C., Kuhlbrodt, T., Mathiot, P., Roberts, C. D., et al. (2019). Description of the resolution hierarchy of the global coupled hadgem3-gc3. 1 model as used in CMIP6 highresmip experiments. *Geoscientific Model Development*, 12(12):4999–5028.

- Russell, J. L., Kamenkovich, I., Bitz, C., Ferrari, R., Gille, S. T., Goodman, P. J., Hallberg, R., Johnson, K., Khazmutdinova, K., Marinov, I., et al. (2018). Metrics for the evaluation of the southern ocean in coupled climate models and earth system models. *Journal of Geophysical Research: Oceans*, 123(5):3120–3143.
- Saint-Martin, D., Geoffroy, O., Voldoire, A., Cattiaux, J., Brient, F., Chauvin, F., Chevallier, M., Colin, J., Decharme, B., Delire, C., et al. (2021). Tracking changes in climate sensitivity in cnrm climate models. *Journal of Advances in Modeling Earth Systems*, 13(6):e2020MS002190.
- Sallée, J.-B., Shuckburgh, E., Bruneau, N., Meijers, A. J., Bracegirdle, T. J., Wang, Z., and Roy, T. (2013). Assessment of southern ocean water mass circulation and characteristics in cmip5 models: Historical bias and forcing response. *Journal of Geophysical Research: Oceans*, 118(4):1830–1844.
- Scherer, R. P. (1991). Quaternary and tertiary microfossils from beneath ice stream b: evidence for a dynamic West Antarctic Ice Sheet history. *Global and Planetary Change*, 4(4):395–412.
- Schodlok, M. P., Menemenlis, D., Rignot, E., and Studinger, M. (2012). Sensitivity of the ice-shelf/ocean system to the sub-ice-shelf cavity shape measured by nasa icebridge in pine island glacier, west antarctica. *Annals of Glaciology*, 53(60):156–162.
- Schoof, C. (2007). Ice sheet grounding line dynamics: Steady states, stability, and hysteresis. *Journal of Geophysical Research: Earth Surface*, 112(F3).
- Sellar, A. A., Jones, C. G., Mulcahy, J. P., Tang, Y., Yool, A., Wiltshire, A., O’connor, F. M., Stringer, M., Hill, R., Palmieri, J., et al. (2019). Ukesm1: Description and evaluation of the uk earth system model. *Journal of Advances in Modeling Earth Systems*, 11(12):4513–4558.
- Shu, Q., Wang, Q., Song, Z., Qiao, F., Zhao, J., Chu, M., and Li, X. (2020). Assessment of sea ice extent in CMIP6 with comparison to observations and cmip5. *Geophysical Research Letters*, 47(9):e2020GL087965.
- Spence, P., Griffies, S. M., England, M. H., Hogg, A. M., Saenko, O. A., and Jourdain, N. C. (2014). Rapid subsurface warming and circulation changes of antarctic coastal waters by poleward shifting winds. *Geophysical Research Letters*, 41(13):4601–4610.
- Stewart, A. L., Klocker, A., and Menemenlis, D. (2019). Acceleration and overturning of the antarctic slope current by winds, eddies, and tides. *Journal of Physical Oceanography*, 49(8):2043–2074.

- Sutter, J., Gierz, P., Grosfeld, K., Thoma, M., and Lohmann, G. (2016). Ocean temperature thresholds for last interglacial west antarctic ice sheet collapse. *Geophysical Research Letters*, 43(6):2675–2682.
- Thoma, M., Jenkins, A., Holland, D., and Jacobs, S. (2008). Modelling circumpolar deep water intrusions on the amundsen sea continental shelf, antarctica. *Geophysical Research Letters*, 35(18).
- Thomas, M., Ridley, J. K., Smith, I. J., Stevens, D. P., Holland, P. R., and Mackie, S. (2023). Future response of Antarctic Continental Shelf temperatures to ice shelf basal melting and calving. *Geophysical Research Letters*, 50(18):e2022GL102101.
- Thompson, A. F., Speer, K. G., and Schulze Chretien, L. M. (2020). Genesis of the antarctic slope current in west antarctica. *Geophysical Research Letters*, 47(16):e2020GL087802.
- Thompson, A. F., Stewart, A. L., Spence, P., and Heywood, K. J. (2018). The antarctic slope current in a changing climate. *Reviews of Geophysics*, 56(4):741–770.
- Turner, J., Orr, A., Gudmundsson, G. H., Jenkins, A., Bingham, R. G., Hillenbrand, C.-D., and Bracegirdle, T. J. (2017). Atmosphere-ocean-ice interactions in the amundsen sea embayment, west antarctica. *Reviews of Geophysics*, 55(1):235–276.
- Wählin, A., Yuan, X., Björk, G., and Nohr, C. (2010). Inflow of warm circumpolar deep water in the central amundsen shelf. *Journal of physical oceanography*, 40(6):1427–1434.
- Walker, D. P., Jenkins, A., Assmann, K. M., Shoosmith, D. R., and Brandon, M. A. (2013). Oceanographic observations at the shelf break of the amundsen sea, antarctica. *Journal of Geophysical Research: Oceans*, 118(6):2906–2918.
- Wang, C., Zhang, L., Lee, S.-K., Wu, L., and Mechoso, C. R. (2014). A global perspective on cmip5 climate model biases. *Nature Climate Change*, 4(3):201–205.
- Wang, Y., Zhou, M., Zhang, Z., and Dinniman, M. S. (2023). Seasonal variations in circumpolar deep water intrusions into the ross sea continental shelf. *Frontiers in Marine Science*, 10:1020791.
- Webber, B. G., Heywood, K. J., Stevens, D. P., and Assmann, K. M. (2019). The impact of overturning and horizontal circulation in pine island trough on ice shelf melt in the eastern amundsen sea. *Journal of Physical Oceanography*, 49(1):63–83.

- Webber, B. G., Heywood, K. J., Stevens, D. P., Dutrieux, P., Abrahamson, E. P., Jenkins, A., Jacobs, S. S., Ha, H. K., Lee, S. H., and Kim, T. W. (2017). Mechanisms driving variability in the ocean forcing of pine island glacier. *Nature communications*, 8(1):14507.
- Williams, K., Copsey, D., Blockley, E., Bodas-Salcedo, A., Calvert, D., Comer, R., Davis, P., Graham, T., Hewitt, H., Hill, R., et al. (2018). The met office global coupled model 3.0 and 3.1 (gc3. 0 and gc3. 1) configurations. *Journal of Advances in Modeling Earth Systems*, 10(2):357–380.
- Wunsch, C. and Heimbach, P. (2007). Practical global oceanic state estimation. *Physica D: Nonlinear Phenomena*, 230(1-2):197–208.
- Zhang, X., Thompson, A. F., Flexas, M. M., Roquet, F., and Bornemann, H. (2016). Circulation and meltwater distribution in the bellingshausen sea: From shelf break to coast. *Geophysical Research Letters*, 43(12):6402–6409.